Binary population biofilms
by Maarten Alexander Siebel

A thesis submitted in partial fulfillment of the requirements for the degree of Doctor of Philosophy in Civil Engineering
Montana State University

Abstract:
Biofilm research has been restricted to studies of undefined mixed microbial populations and to investigations of (defined) mono microbial populations. In the first case, the organisms are considered as a homogeneous mass, biomass, ignoring the properties of individual species, the sum of which determines the observed phenomena. The second case concentrates on the properties and processes of one microbial species ignoring the influence of the broader environment, eg. other microbial species, on this species.

Goal of this research was to study a defined mixed microbial biofilm and to determine possible interactive effects between the species comprising the biofilm. Biofilm experiments were conducted with mono populations of Klebsiella pneumoniae and Pseudomonas aeruginosa and with binary populations of K. pneumoniae and P aeruginosa . Process rates and stoichiometric coefficients, determined for the mono population biofilms were compared with those found in the binary population biofilm.

Results indicate that the specific cellular product formation rate of K. pneumoniae or P. aeruginosa in the binary biofilm is not affected by the presence of the other species. Similarly, the glucose-oxygen stoichiometric ratio of K. pneumoniae or P. aeruginosa in the binary biofilm is not affected by the presence of the other species. Many processes at the cellular level are performed faster by K. pneumoniae than by P. aeruginosa: eg. biofilm specific product formation rate and the maximum specific growth rate of K. pneumoniae are 5 times that rate of P. aeruginosa. Nevertheless, K. pneumoniae cell mass does not dominate the biofilm, possibly because of its non-motility and its product formation properties.

BINARY POPULATION BIOFILMS

by

Maarten Alexander Siebel

A thesis submitted in partial fulfillment
of the requirements for the degree of

Doctor of Philosophy
in
Civil Engineering

MONTANA STATE UNIVERSITY
Bozeman, Montana
September 1987

APPROVAL

of a thesis submitted by

Maarten Alexander Siebel

This thesis has been read by each member of the thesis committee and been found to be satisfactory regarding content, English usage, format, citations, bibliographic style and consistency and is ready for submission to the College of Graduate Studies.

Sept 18, 1987 — Date

W. Schmaltz — Chairperson, Graduate Committee

Approved for Major Department

18 Sept 87 — Date

Theodore E. Lang — Head, Major Department

Approved for College of Graduate Studies

9-24-87 — Date

Graduate Dean

STATEMENT OF PERMISSION TO USE

In presenting this thesis in partial fulfillment of the requirements for a doctoral degree at Montana State University, I agree that the Library shall make it available to borrowers under rules of the Library. I further agree that copying of this thesis is allowable only for scholarly purposes, consistent with the "fair use" as prescribed in the U.S. Copyright Law. Requests for extensive copying or production of this thesis should be referred to University Microfilms International, 300 North Zeeb Road, Ann Arbor, Michigan 48106, to whom I have granted "the exclusive right to reproduce and distribute copies of the dissertation in and from microfilm and the right to reproduce and distribute by abstract in any format".

Signature 

Date Sept. 18, 1987

ACKNOWLEDGEMENT

Completion of this study would have been impossible without the help, encouragement and love of numerous people. Realizing that completeness is impossible I like to mention the following:

My friends at I.P.A. - Diane, Wendy, Pam, Shari, Kelly, Anne, Rob, Andy, Rich, Mukesh, Nick, Rune, Zbigniew, Bjørn, Ewout, Dick, Al, Bob, Laura, Frank, Whon Chee, Joe, Kim, Jan, Brent, Dave, Dave, Chris; a group of people that provided the most stimulating environment one could wish to work in.

My thesis committee - Keith Cooksey, Gordon McFeters, Hayden Ferguson, Karel Luyben, Al Cunningham.

Those people who provided technical and analytical support - Gordon Williams, John Rompel, Stuart Aasgaard, Andy Blixt.

The staff in Civil Engineering, Computing Services, Library, Montana Hall for patiently answering my questions.

The staff of International Education for helping me with more than just the legal part of my stay.

Niek Luijtjes for financial and 'computational' support and Vicky Thompson for proofreading the manuscript.

Last but certainly not least those who supported and encouraged me on a day to day basis:

The Characklii for giving me this 'Bozeman experience'. Your encouragement and stimulating excitement will guide me for many years to come.

Gerrie and Edwin for your love and patience. Your invaluable moral and practical support was a necessary ingredient to complete this job.

Financial support is acknowledged from the Office of Naval Research, National Science Foundation, Montana State University Experiment Station and the I.P.A. Associates Program.

TABLE OF CONTENTS

LIST OF TABLES

LIST OF FIGURES

ABSTRACT

Biofilm research has been restricted to studies of undefined mixed microbial populations and to investigations of (defined) mono microbial populations. In the first case, the organisms are considered as a homogeneous mass, biomass, ignoring the properties of individual species, the sum of which determines the observed phenomena. The second case concentrates on the properties and processes of one microbial species ignoring the influence of the broader environment, eg. other microbial species, on this species.

Goal of this research was to study a defined mixed microbial biofilm and to determine possible interactive effects between the species comprising the biofilm. Biofilm experiments were conducted with mono populations of Klebsiella pneumoniae and Pseudomonas aeruginosa and with binary populations of K. pneumoniae and P. aeruginosa. Process rates and stoichiometric coefficients, determined for the mono population biofilms were compared with those found in the binary population biofilm.

Results indicate that the specific cellular product formation rate of K. pneumoniae or P. aeruginosa in the binary biofilm is not affected by the presence of the other species. Similarly, the glucose-oxygen stoichiometric ratio of K. pneumoniae or P. aeruginosa in the binary biofilm is not affected by the presence of the other species. Many processes at the cellular level are performed faster by K. pneumoniae than by P. aeruginosa: eg. biofilm specific product formation rate and the maximum specific growth rate of K. pneumoniae are 5 times that rate of P. aeruginosa. Nevertheless, K. pneumoniae cell mass does not dominate the biofilm, possibly because of its non-motility and its product formation properties.

INTRODUCTION

A biofilm is a layer of microbial cells and inorganic debris held together in a polymeric matrix and firmly attached to a substratum. Accumulation of biofilm is encountered in many natural environments. Natural purification of surface waters depends to a large extent on the activity of adsorbed microorganisms to remove pollutants from the bulk liquid. In certain engineered environments, adsorption of organisms is fundamental to the processes anticipated eg., fixed-film biological wastewater treatment. In other environments, adsorption of microorganisms is considered a nuisance resulting in energy losses, sudden deterioration of water quality and possible destruction of long-term exposed surfaces.

A major dilemma in the study of biofilm processes is the extreme complexity of natural biofilms which makes distinguishing individual processes and obtaining process oriented information virtually impossible. This is in contrast with study of biofilms of one single microbial species, mono population biofilms. As far as we know, however, these films do not exist in natural systems and information exposed serves mainly to improve theoretical understanding.

The focus of this research is accumulation of binary population biofilms, biofilms resulting from accumulation of two identified microbial species. The behaviors of different microbial species respiring in close proximity does not necessarily equal the sum of the behavior of the individual microbial species. Different interactions between organisms have been distinguished. However, most studies in this area have been conducted in suspended growth systems and results may not be directly applicable to systems with attached microbial growth. The scope of

this study was to elucidate processes describing accumulation of a binary population biofilm by comparison with processes describing accumulation of mono population biofilms.

Goal and Objective

The goal of this research was to determine the effect of a mixed microbial population on biofilm accumulation processes and biofilm properties.

The objective was to describe biofilm accumulation of a binary population of Klebsiella pneumoniae and Pseudomonas aeruginosa in terms of the accumulation of the mono population biofilms of K. pneumoniae and P. aeruginosa. Process variables were monitored to determine the process kinetics and stoichiometry for mono population biofilms of each species and for the two species combined.

LITERATURE REVIEW

Biofilm Processes

Biofilm accumulation is the result of microbial, chemical and physical processes occurring in the liquid phase, both within the biofilm and at the substratum:

Transport and adsorption of organic macromolecules and nutrients from the liquid phase to the substratum: Research indicates that adsorbed macromolecules may both enhance and inhibit microbial adsorption. Characklis and Cooksey (1983) conclude that the role of conditioning film in microbial adsorption to surfaces is not yet clear.

Transport and adsorption of microorganisms from the liquid phase to the substratum: Microbial cells (0.5-10 μm effective diameter) can be transported from the bulk fluid to the wetted substratum by (Brownian) diffusion, gravity, thermophoresis, taxis and fluid dynamic forces like inertia, lift, drag, drainage and downsweep. The relative contribution of each of those forces depends on the size of the organism, its density, etc. Motility can contribute significantly to the rate of transport of a microbial cell to the substratum. Adsorption of microorganisms may be reversible or irreversible, closely related to the bonding energy between the substratum and the macromolecular conditioning film (Mitchell and Kirchman, 1981). Irreversible adsorption occurs following the production of extracellular fibers that allow the bacteria to overcome repulsive forces (Marshall et al. 1971).

Reactions within the biofilm: Once organisms are adsorbed energy is expended for growth or replication, for the formation of extracellular products (eg. polysaccharides, proteins, small molecules, peptides,

antimicrobial agents), for cell maintenance, and for death or lysis of the cell.

Detachment of biofilm and associated products: Parts of the biofilm may separate from the biofilm and become reentrained in the bulk liquid. Erosion occurs when detachment concerns individual cells. Detachment generally refers to separation of pieces of biofilm (cells and products). Desorption refers to the reentrainment of cells from the substratum.

Reactions between the biofilm and the substratum: Reactions may occur between microbial products and the substratum and reactions may occur between locations of the substratum, covered with biofilm and locations not covered. The adsorbed cells grow and reproduce forming colonies which constitute physical anomalies on a surface. Nonuniform or "patchy" colonization by microorganisms results in the formation of differential aeration cells where areas under respiring colonies are depleted of oxygen relative to surrounding, non-colonized areas, forming differential surface chemistries.

Biofilm Properties

Biofilm properties can be distinguished in physical, chemical and biological properties. Relevant thermodynamic properties are volume (thickness seldom over 1000 μm) and mass (dry mass density varies from 10 - 50 $kg.m^{-3}$ in fluid flow systems) (Characklis and Cooksey, 1983). Both values are highly dependent on hydraulic conditions and on the chemical regime to which the film is exposed. Transport properties of biofilms determine mass, heat and momentum transfer. Diffusion coefficients in biofilms are most probably related to biofilm density (Characklis and Cooksey, 1983); thermal conductivity is not significantly

different from that of water (Characklis et al., 1981).

Chemical properties of the biofilm vary with the chemical composition of the bulk liquid and probably affect the physical and biological structure of the film, eg., interspecies bonding strength is probably affected by calcium (Turakhia, 1986). In addition, inert suspended solids and corrosion products, when substratum is ferro-metallic, may accumulate in the biofilm matrix.

Organic composition of biofilms is closely related to the energy, carbon and nutrient sources available for metabolism. For example, nitrogen limitation can result in a relatively large amount of carbon being devoted to production of extracellular microbial polysaccharide (EPS). In terms of macromolecular composition, Bryers (1979) has measured protein-to-polysaccharide mass ratios from 0 - 10 (the former in terms of casein equivalents, the latter in terms of glucose equivalents). In addition, the physiological state of organisms is of importance in determining the composition of a biofilm: stationary phase cells are generally EPS producers rather than log phase cells (Characklis and Cooksey, 1983).

Biological properties of a biofilm strongly depend on the species colonizing the substratum in addition to the physical and chemical properties of the environment in which the biofilm accumulates. Initial microbial activity on the substratum results in small colonies of cells distributed randomly. In time, colonies may grow together forming a relatively smooth biofilm or grow as isolated colonies with bare substratum in between, forming a patchy biofilm.

Viable cell numbers are relatively low in relation to the biofilm volume ($10^{10} - 10^{14}.m^{-3}$), occupying only from 1 to 10% of the biofilm volume in dilute nutrient solutions (Characklis, 1980; Trulear, 1983). Cell densities are in

the order of 10^{10}-10^{13} cells.m^{-2}.

Microbial Species

Klebsiella pneumoniae

K. pneumoniae, also described as Klebsiella type I (Erbing et al., 1976), is an organism in the coliform group. It is commonly found in soil and water and is present in 30 - 40 % of all warm-blooded animals, including humans. Individual densities range up to 10^8.(gram of feces)$^{-1}$. K. pneumoniae is frequently implicated in hospital infections. Approximately 60 - 85% of all Klebsiella from feces and clinical specimens are K. pneumoniae. Strains that are positive by the fecal coliform test (ferment lactose with gas production at 44.5°C) are considered K. pneumoniae (Geldreich and Rice, 1987). This organism is the rare cause of pneumonia in humans (Brock, 1979). Several investigations (Knittel, 1975; Brown and Seidler, 1973) suggest that the origin of K. pneumoniae in surface waters could be human, animal or mixed sources (Campbell et al., 1976). When growing anaerobically, Klebsiella strains fix N_2, a property not found among other enteric bacteria (Brock, 1979). K. pneumoniae is generally a non-motile, gram negative, rod shaped bacterium. Relevant characteristics of K. pneumoniae are summarized in Table 1.

NB. K. pneumoniae appears to be referred to by a variety of names including, Aerobacter aerogenes, Klebsiella aerogenes, K. eduardii, and K. oxytocum (Brown and Seidler, 1973).

Pseudomonas aeruginosa

P. aeruginosa is a polymer-forming bacterium, ubiquitous in nature and the cause of many infections and disease. The primary mode of growth is in polymer-enclosed

microcolonies (Buchanan and Gibbons, 1977), attached to a wide variety of substrata. The polymer capsule is assumed to act as a protective layer. This polymer layer is relatively diffuse, and is easily dispersed in the liquid phase.

P. aeruginosa has been studied extensively in both suspension and in biofilms (Trulear, 1983; Mian et al, 1978; Robinson et al., 1984; Bakke et al., 1984; Turakhia, 1986). Kinetic and stoichiometric coefficients for this organisms have been determined. Relevant characteristics of P. aeruginosa are summarized in Table 1.

Table 1. Relevant characteristics of K. pneumoniae and P. aeruginosa.

	K. pneumoniae	P. aeruginosa
shape	rod shaped [1]	rod shaped [1]
breadth (μm)	0.3 - 1.5 [1]	0.5 - 0.8 [1]
length (μm)	0.6 - 6.0 [1]	1.5 - 4.0 [1]
EPS formation	+	+
EPS composition	glucose, fucose, glucuronic acid, and pyruvic acid [4]	primarily mannuronic and guluronic acid [5]
motility	non motile	polar flagella [1]
respiration	facultative anaerobic [3]	obligate aerobe except when nitrate present [3]
denitrification	+ [3]	
metabolism	chemoorganotroph [2]	chemoorganotroph
gram stain	negative [1]	negative [1]
optimal temperature	35-37°C [1]	35-37°C [3]
optimal pH	7.2 [1]	6.8 [3]

[1] (Holt, 1977)
[2] (Sutherland, 1977)
[3] (Buchanan and Gibbons, 1974)
[4] (Erbing et al., 1976)
[5] (Mian et al., 1978)

Extracellular Products

Extracellular Polymeric Substances (EPS) are by-products of microbial metabolism produced mostly in the cytoplasm and transported through the cell wall. These, generally large chain macromolecules may either take the form of a discrete capsule located around the cell perimeter or may be present as extracellular slime apparently unattached to the bacterial surface, depending on the species (Sutherland, 1977). Capsules are generally quite stable but stability depends on cell age, chemical composition of surrounding liquid, etc. Consequently, capsule layer thickness will vary from hardly discernible to extending 0.1 to 10 μm beyond the exterior of the cell wall (Sutherland, 1977). It should be noted that observations of capsular material very much depend on the sample preparation procedure. Several methods and resulting observations on K. pneumoniae, discussed by Roth (1977), show that capsule appearance can range from a clearly visible, layered structure with a well-defined edge to not visible.

Cell growth rate and the nature of the compound limiting cell growth rate, eg. nitrogen or carbon, strongly influence the rate of product formation and the product yield. Under nitrogen limitation in chemostat growth, specific polysaccharide synthesis by P. aeruginosa increased from 0.27 g.(g of cell.h)$^{-1}$ at a dilution rate of 0.05.h^{-1} to 0.44 g.(g of cell.h)$^{-1}$ at a dilution rate of 0.1.h^{-1}. Polysaccharide yields, based on glucose used, ranged from 56 to 64% (Mian, 1978).

Polysaccharides were also produced under carbon limitation at a rate of 0.19 g.(g of cell.h)$^{-1}$ at D=0.05.h^{-1} at a yield of 19%. (Mian et al., 1978). Similar results were obtained with Klebsiella aerogenes. Product formation

increased with nitrogen relative to carbon as limiting nutrient (Sutherland, 1977). It was even observed that Klebsiella continued to produce considerable amounts of polysaccharide after cessation of cell growth despite the presence of residual carbohydrate in the growth medium (Dudman, 1960). Neijssel and Tempest (1975), however, report that K. aerogenes, growing at very high substrate concentrations going into the chemostat (10 g $C.l^{-1}$ when carbon limited, 30 g $C.l^{-1}$ when nitrogen, phosphate or sulphate limited) and at low dilution rate, 0.17.h^{-1}, did not produce any polysaccharide or other metabolic products when growing under carbon limitations. In that case, cell yields were reportedly 0.45 (g cell-C.(g glucose-C)$^{-1}$) for growth on glucose carbon; glucose-oxygen stoichiometric ratio was 2.83 (g O_2.(g glucose-C)$^{-1}$).

Oxygen has also been implicated in production of polymeric material. Dudman (1960) found that increased aeration led to decreased product yields in a variety of microorganisms but resulted in an increased polysaccharide production in E. coli and Klebsiella species. It seems possible that in bacteria, which are facultative anaerobes utilizing the Embden-Meyerhof pathway, optimal conditions of polysaccharide production include aeration, whereas in obligate aerobes this leads to reduced yield of extracellular polysaccharide (Sutherland, 1977).

Microbial Interactions

Many examples of microbial interactions are described in the context of biodegradation, microbial communities degrading compounds. Slater and Lovatt (1984) give an overview of the significance of microbial communities in biodegradation and discuss why techniques for the isolation of strains might fail to reveal community interactions.

Batch culturing of an originally adsorbed community, plating and nutrient excess are examples of conditions that are liable to disturb and not reveal species interactions.

Traditionally microbial interaction studies have been conducted in laboratory type chemostats (Frederickson, 1977) which allow the definition of the various types of interactions between microbial organisms. Generally interaction has a strong tendency to result in exclusion of one of the competitors. But often mitigating circumstances are present, resulting in 'balanced coexistence' (Van Gemerden, 1974).

Extrapolation of results from suspended growth interaction studies to attached growth cultures is virtually impossible. Homogeneity of chemostat conditions is not available in the attached growth system while characteristic aspects of the latter (transport through laminar sublayer, adsorption, growth on substratum, shear force, gliding, desorption, detachment) are not accounted for in the suspended growth system. Interestingly, discrepancy between the mathematical description of a predator - prey relation and observations could be removed by addition of a wall growth term in the equation, and Frederickson (1977) concludes that 'variation of the ratio of chemostat wetted surface area to culture volume should be an important part of future studies on microbial predator - prey relations'.

If interorganism distance is a variable of importance in microbial interaction (Crisp, 1981), attached growth seems more liable to result in interaction than suspended growth. Based on data from biofilm experiments in Rototorque reactors (Trulear, 1983), cell density is approximately 4 orders of magnitude higher in biofilms than in suspension (cell number per volume of biofilm or volume of suspension).

Interactions between algal and bacterial species in a variety of environments have been documented (Schiefer and Caldwell, 1982; Haack and McFeters, 1982; Escher and Characklis, 1982; Sandbeck and Ward, 1981). Few have been described to occur on solid substrata. Holmes (1986) studied the colonization of vinyl by 2 algal species on open air swimming pool walls. Rate and extent of algal colonization drastically increased in the presence of bacteria. Bacterial extracellular products (EPS) seemed to play a role in initial bacterial and in subsequent algal colonization. In a laboratory assembled (no growth took place during biofilm formation) algal bacterial biofilm (Murray et al., 1986), it was shown that algal exudates served as a sole carbon source for attached bacteria.

Microbial interaction is mathematically approached by Wanner and Gujer (1985-a) describing biofilm formation by a heterotrophic and autotrophic bacteria. Frederickson (1977) is the first to denote a microbial system consisting of 2 identified species by a binary population.

MATHEMATICAL DESCRIPTION

Microbial conversion of substrate into cell mass can be mathematically described using a mass balance approach. The equation describing a mass balance is of the following general form:

net rate of accumulation	=	net rate of transport	+	net rate of transformation

Mass accumulation equals the sum of rates of mass transformation and rates of mass flow in or out of a control volume.
For two microbial species in the system, the following sequence of events is considered:

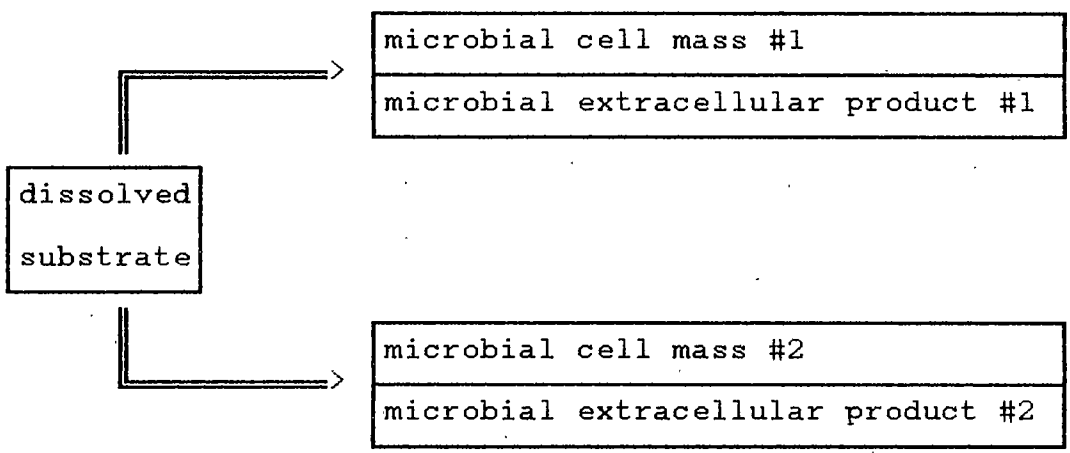

Substrate carbon is used to provide microbial cell carbon and extracellular product carbon. CO_2 is produced as a respiration product. Thus, microbial cell carbon is used for cell synthesis (cell mass) and respiration (energy).

Mass Balance Equations for the Biofilm Reactor

Liquid phase substrate carbon (1):

$$\frac{dS_{Sl}}{dt} = D(S_{Si}-S_{Sl}) - X_{Mf}.\frac{A}{V}.r_S - X_{Ml}.\left[\frac{\mu}{Y_{MS}} + \frac{r_{Pl}}{Y_{PS}}\right]$$

net rate of substrate accumulation = net rate of substrate inflow − rate of substrate uptake by biofilm − rate of substrate uptake in liquid phase

where:

S_{Sl} = substrate carbon concentration in liquid phase $[M_S L^{-3}]$

t = time $[t]$

D = dilution rate $[t^{-1}]$ (= flow rate into divided by volume of reactor)

S_{Si} = substrate carbon concentration in influent $[M_S L^{-3}]$

X_{Mf} = cell carbon concentration in biofilm $[M_M L^{-2}]$

A = substratum area $[L^{-2}]$

V = reactor volume $[L^{-3}]$

r_S = biofilm specific substrate uptake rate $[M_S M_M^{-1} t^{-1}]$

X_{Ml} = cell carbon concentration in liquid phase $[M_M L^{-3}]$

μ = specific cellular growth rate $[t^{-1}]$

Y_{MS} = yield of cell carbon from substrate carbon $[M_M M_S^{-1}]$

r_{Pl} = specific product formation rate in liquid phase $[M_P M_M^{-1} t^{-1}]$

Y_{PS} = yield of product carbon from substrate carbon $[M_P M_S^{-1}]$

Liquid phase cell carbon (2):

$$\frac{dX_{Ml}}{dt} = D(X_{Mi}-X_{Ml}) + X_{Mf}.\frac{A}{V}.r_{Md} + X_{Ml}.\mu$$

net rate of cell mass accumulation = net rate of cell mass inflow + rate of cell mass detachment + rate of cell growth in liquid phase

where:

X_{Mi} = cell carbon concentration in influent $[M_M L^{-3}]$

r_{Md} = specific cell detachment rate $[t^{-1}]$

Liquid phase product carbon (3):

$$\frac{dS_{Pl}}{dt} = D(S_{Pi}-S_{Pl}) + S_{Pf}.\frac{A}{V}.r_{Pd} + XM_l.r_{Pl}$$

net rate of product accumulation = net rate of product inflow + rate of product detachment + rate of product formation in liquid phase

where:

S_{Pl} = product carbon concentration in liquid phase $[M_P L^{-3}]$

S_{Pi} = product carbon concentration in influent $[M_P L^{-3}]$

S_{Pf} = product carbon concentration in biofilm $[M_P L^{-2}]$

r_{Pd} = specific rate of product detachment $[t^{-1}]$

Biofilm substrate carbon (4):

$$\frac{dS_{Sf}}{dt} = X_{Mf}.r_S - X_{Mf}.f_D.\left[\frac{\mu}{Y_{MS}} + \frac{r_{Pl}}{Y_{PS}}\right]$$

net rate of substrate accumulation = net rate of substrate uptake − rate of substrate consumption for cell growth − rate of substrate consumption for product formation

where:

S_{Sf} = substrate carbon concentration in biofilm $[M_S L^{-3}]$

f_D = effectiveness factor for substrate diffusion [-]

Biofilm cell carbon (5):

$$\frac{dX_{Mf}}{dt} = - X_{Mf}.r_{Md} + X_{Mf}.f_D.\mu$$

net rate of cell mass accumulation = net rate of cell mass detachment + rate of cellular growth

Biofilm product carbon (6):

$$\frac{dS_{Pf}}{dt} = - S_{Pf}.r_{Pd} + X_{Mf}.r_{Pf}$$

net rate of product accumulation = net rate of product detachment + rate of product formation

where:

r_{Pf} = specific rate of product formation in biofilm $[M_P M_M^{-1} t^{-1}]$

Oxygen (7):

$$\frac{dS_{Ol}}{dt} = D(S_{Os}-S_{Ol}) + N_O.\frac{A}{V} +$$

net rate of oxygen accumulation = net rate of oxygen inflow in dilution water + rate of oxygen inflow by diffusion

$$- X_{Mf}.f_D.\left[\frac{\mu}{Y_{MO}} + \frac{r_P}{Y_{PO}}\right].\frac{A}{V} - X_{Ml}\left[\frac{\mu}{Y_{MO}} + \frac{r_P}{Y_{PO}}\right]$$

- rate of oxygen uptake for cell growth and product formation in biofilm
- rate of oxygen uptake for cell growth and product formation in liquid phase

where:

S_{Ol} = concentration of oxygen in liquid phase $[M_O L^{-3}]$

S_{Os} = oxygen saturation concentration in influent $[M_O L^{-3}]$

N_O = flux of dissolved oxygen into reactor system $[M_O L^{-2} t^{-1}]$

Y_{MO} = yield of cell carbon from oxygen $[M_M M_O^{-1}]$

Y_{PO} = yield of product carbon from oxygen $[M_P M_O^{-1}]$

The following simplifying assumptions are made:

1. With long biofilm detention times, biofilm substrate concentration (S_{Sf}) is zero.
2. Glucose is the only carbon and energy source in the influent.
3. Specific product formation rate is (Luedeking & Piret, 1959) growth associated and non-growth associated:

$$r_{Pl} = k_{Pg}.\mu + k_{Pn} \qquad (8)$$

where:

k_{Pg} = growth associated product formation coefficient $[M_P M_M^{-1}]$

k_{Pn} = non-growth associated product formation coefficient $[M_P M_M^{-1} t^{-1}]$

4. Specific microbial growth rate is dependent on substrate concentration according to Monod (1949):

$$\mu = \frac{\mu_m . S_{Sl}}{K_S + S_{Sl}} \qquad (9)$$

where:

μ_m = maximum specific cellular growth rate $[t^{-1}]$

K_S = half saturation concentration $[M_S L^{-3}]$

5. The flux of oxygen into the reactor can be estimated as (Appendix A):

$$N_O = k_c.(S_{Os}-S_{Ol}).\frac{V}{A} \qquad (A\text{-}2)$$

where:

k_c = dissolved oxygen specific mass transfer rate $[t^{-1}]$

With dilution water at saturation concentration, the oxygen diffusion component in Eq. 17 can be substituted by an expression similar to transport of oxygen by dilution water:

$$N_O.\frac{V}{A} = k_c.(C_{Os}-C_{Ol}) \qquad (10)$$

Mass Balance Equations for the Chemostat

Liquid phase substrate carbon (11):

$$\frac{dS_{Sl}}{dt} = D(S_{Si}-S_{Sl}) - X_{Ml}\cdot\left[\frac{\mu}{Y_{MS}} + \frac{r_P}{Y_{PS}}\right]$$

net rate of substrate accumulation = net rate of substrate inflow − rate of substrate uptake in liquid phase

Liquid phase cell carbon (12):

$$\frac{dX_{Ml}}{dt} = D(X_{Mi}-X_{Ml}) + X_{Ml}.\mu$$

net rate of cellular accumulation = net rate of cellular inflow + rate of cell growth in liquid phase

Liquid phase product carbon (13):

$$\frac{dS_{Pl}}{dt} = D(S_{Pi}-S_{Pl}) + XM_l.r_{Pl}$$

net rate of product accumulation = net rate of product inflow + rate of product formation in liquid phase

Mass Balance Equations for the Batch Reactor

Liquid phase substrate carbon (14):

$$\frac{dS_{S1}}{dt} = - X_{M1} \cdot \left[\frac{\mu}{Y_{MS}} + \frac{r_P}{Y_{PS}} \right]$$

net rate of substrate accumulation = rate of substrate uptake

Liquid phase cell carbon (15):

$$\frac{dX_{M1}}{dt} = X_{M1} \cdot \mu$$

net rate of cell mass accumulation = rate of cell growth

Liquid phase product carbon (16):

$$\frac{dS_{P1}}{dt} = XM_1 \cdot r_{P1}$$

net rate of product accumulation = rate of product formation

Oxygen (17):

$$\frac{dS_{O1}}{dt} = - X_{M1} \left[\frac{\mu}{Y_{MO}} + \frac{r_P}{Y_{PO}} \right] + R_O$$

net rate of oxygen accumulation = − rate of oxygen uptake for cell growth and product formation + rate of oxygen generation

EXPERIMENTAL APPROACH

The experimental work can be divided in three parts according to the reactor used. Experiments conducted in the Rototorque resulted in stoichiometric and kinetic coefficients for biofilm processes for both the mono and binary populations. Chemostat experiments provided kinetic and stoichiometric coefficients for mono population processes in suspension. Batch experiments provided stoichiometric data on the consumption of oxygen.

Rototorque

The Rototorque, essentially a Couette vessel, consists of two concentric cylinders, a stationary outer cylinder and a rotating inner cylinder (Figure 1). Removable slides (4-12) which form an integral part of the inside wall of the outer cylinder permit sampling of the biofilm so that thickness, mass, and/or biofilm chemical composition can be determined. The reactor liquid phase is completely mixed by virtue of draft tubes bored through the solid inner cylinder (Figure 1). The draft tubes are positioned at angles so that the rotation of the inner cylinder pumps the fluid through the tubes. By virtue of the complete mixing, effluent liquid samples represent the reactor liquid composition.

The Rototorque is a continuous flow stirred tank reactor (CFSTR), an open reactor (i.e., there are flows in and out) in which concentration gradients within the liquid volume are minimized. The CFSTR provides significant advantages for observing, separating and evaluating the kinetics and stoichiometry of each biofilm process:

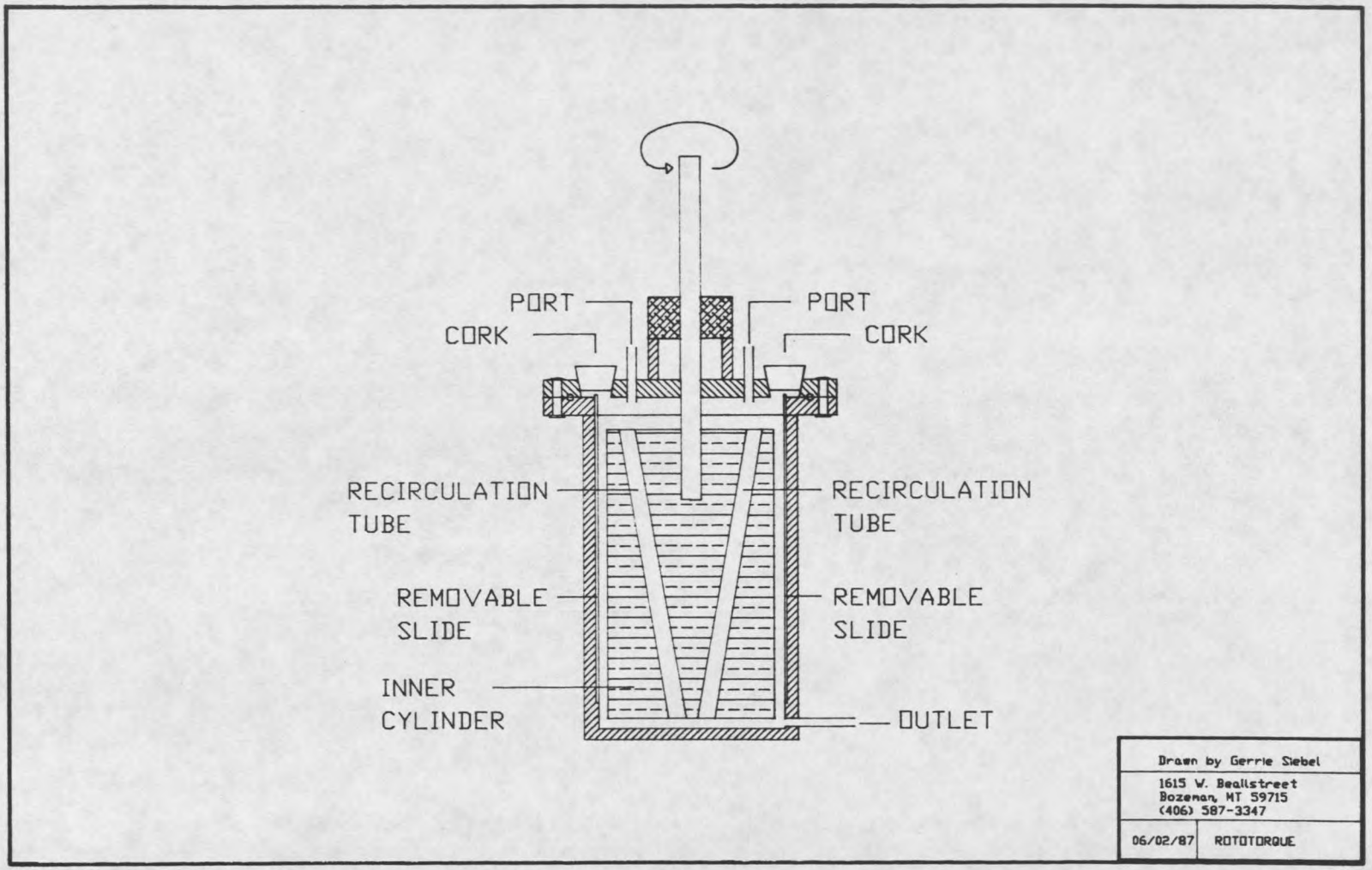

Figure 1. Schematic of a Rototorque reactor.

1. The liquid phase is homogeneous which simplifies sampling, chemical analysis, and mathematical modelling.
2. The mass transfer rate and shear stress in the annular geometry at different rotational speeds has been described mathematically (Mizushina, 1971).
3. The annular geometry has been used in numerous experimental observations related to biofilm processes (Trulear & Characklis, 1982; Bakke et al. 1984; Turakhia, 1986).

Material balance calculations for carbon permit a measure of biofilm activity. Oxygen balances can also be performed. Fluid shear stress at the wall is a function of rotational speed. Mean liquid residence time depends on dilution flow rate through the reactor. Thus fluid shear stress and residence time can be varied independently. Reactor residence time was maintained at approximately 10 minutes so that suspended growth was negligible and all reactor activity can be attributed to the biofilm. The reactor has a high surface area-to-volume ratio and most of its surface area is exposed to a uniform shear stress. A summary of characteristics and dimensions of the Rototorque is presented in Appendix B.

Preparation of Rototorque

Biofilm experiments were prepared by initiating the standard cleaning procedure for reactor and tubing components. This consisted of brushing all reactor components in a solution of 2% active chlorine followed by rinsing with distilled water. After drying, the slides were inserted and the intake ports on top of the reactor were filled with loosely packed cotton plugs. The air vent was attached, the effluent line connected and closed with a

screw clamp. Parts of the slide were provided with a thin layer of resin for the preparation of biofilm Transmission Electron Micrographs (TEM). The entire assembly was then autoclaved for 15 minutes at 121°C.
Tubing and flow meters between feed stock solutions and the reactor were flushed with distilled water and tube ends were sealed with aluminum foil and clamped. Tubing was autoclaved for 15 minutes at 121°C.

Preparation of Chemostat

A 500 ml solution of nutrient medium was made up, added to the clean chemostat and autoclaved for 15 minutes at 121°C. After cooling to room temperature, the chemostat was inoculated with 1 ml of the appropriate microbial suspension, previously grown in batch culture. The chemostat was operated in batch mode for 12 to 16 hours to obtain a cell density between 10^{12} and $10^{13}.m^{-3}$. Then a continuous flow of nutrients and substrate (40 g $C.m^{-3}$) was started. Steady state conditions were assumed to have been reached after 6 residence times.

Start-up and Operating Conditions

The Rototorque setup was assembled. The reactor was then filled with dilution water and continuous flows started (dilution water $3.6*10^{-3}$ $m^3.h^{-1}$) giving final concentrations of calcium 25 g $Ca.m^{-3}$, buffer 1.5 mMol of mono- and dibasic phosphate and substrate 8 or 20 g $C.m^{-3}$. The rotational speed was set at 200 rpm. After a minimum of 15 minutes, the Rototorques were inoculated by starting a flow of microorganisms ($0.06*10^{-3}$ $m^3.h^{-1}$, cell density 10^{12}-$10^{14}.m^{-3}$) from the chemostat at time zero. The inoculation period was 12 hours.
A schematic of the Rototorque experimental setup is presented in Figure 2.

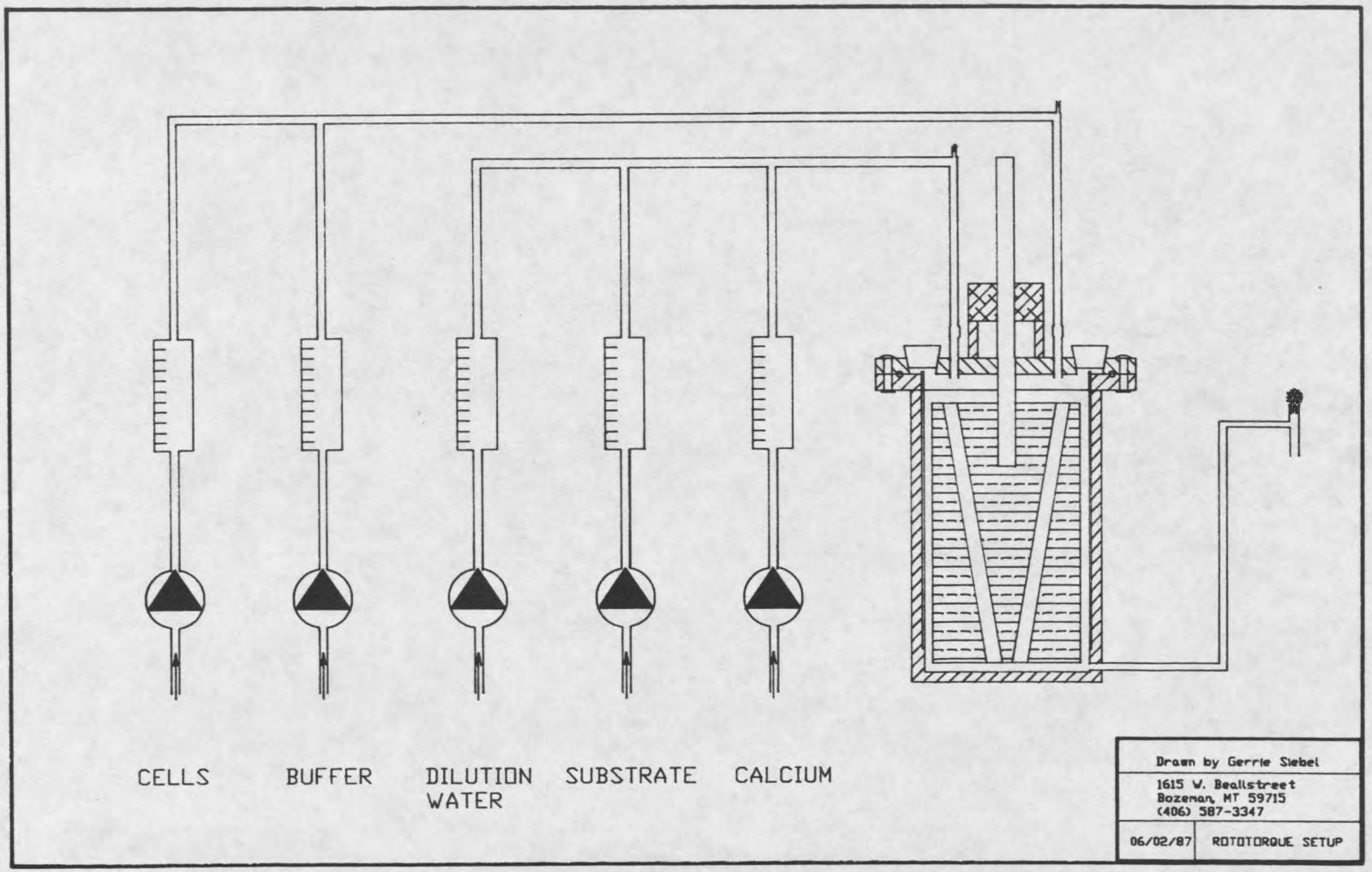

Figure 2. Schematic of a Rototorque experimental setup.

Dilution Water

The source of dilution water was Bozeman city tap water which was pretreated by fine sand filtration, activated carbon filtration, ion exchange and reverse osmosis. The product was stored in a flow-through tank. Additional micro-filtration, before entering the Rototorques, was provided by a 0.45 μm and a 0.2 μm high volume filter in series (Gelman Sciences Acroflow II) and a 0.2 μm mini capsule filter (Gelman Sciences) (Figure 3).

Sampling

Samples were collected:

1) once or twice daily from the influent line directly before flows enter the Rototorque, representing the influent solution,
2) once or twice daily from the effluent line, representing the liquid phase of the biofilm reactor, and
3) once a day or once every other day from the slides, representing the biofilm phase.

Influent samples: 20 ml of influent sample was collected in a test tube, that had been heated previously to 500°C to remove residual carbon, and samples were taken for

Total organic carbon (TOC): 4 samples of 2 ml each were pipetted into TOC ampules. Ampules were sealed immediately (Oceanography International Corp., College Station, TX).

Glucose: 2 samples of 1 ml each were pipetted into test tubes, previously heated to 500°C, sealed with parafilm and frozen.

Effluent samples: 80 ml of effluent sample was homogenized (DuPont Instruments, Sorvall Omni Mixer) for 1 minute at 60% speed and the following volumes taken for:

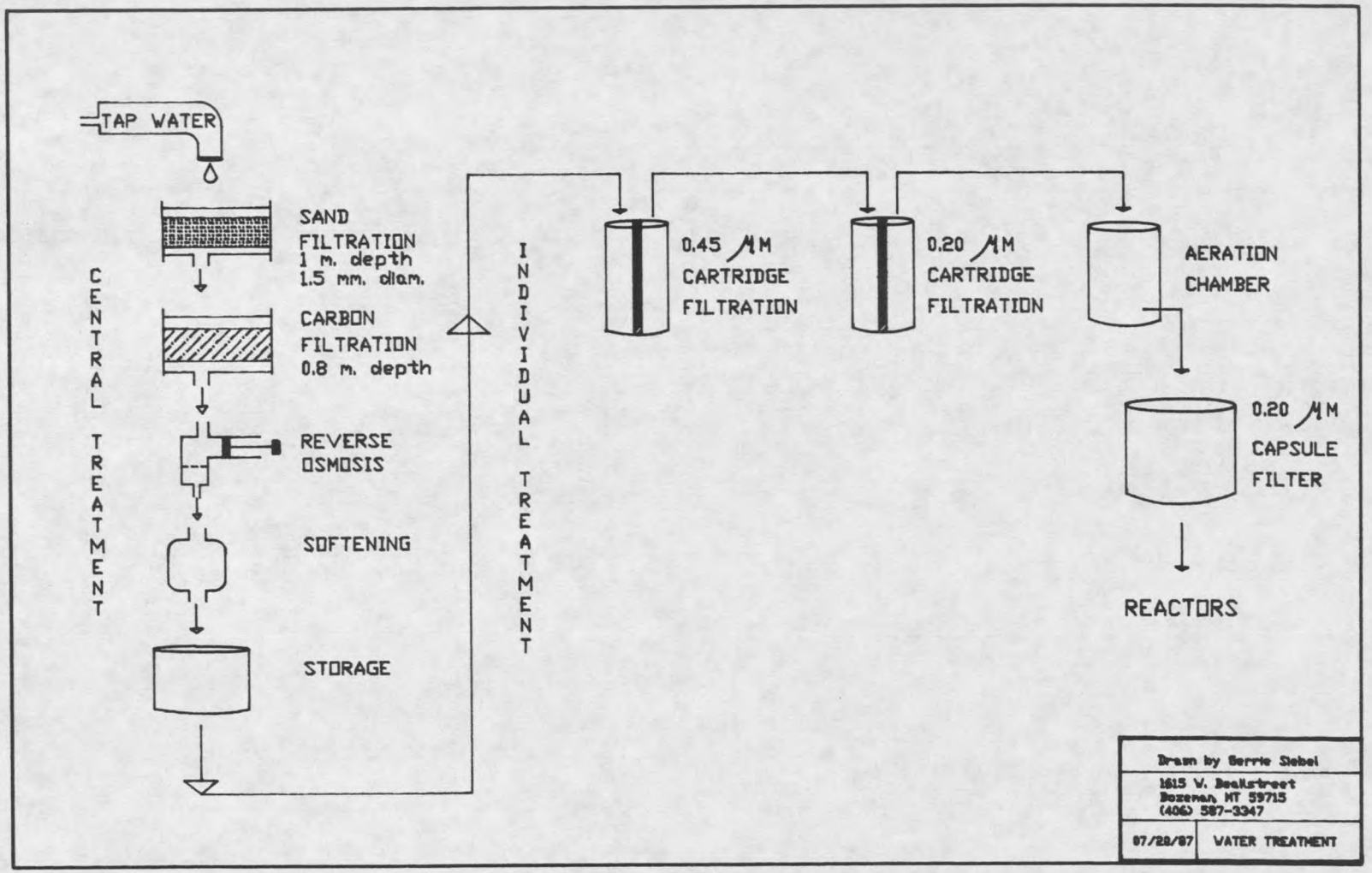

Figure 3. Overview of dilution water treatment.

Total organic carbon (TOC): 4 samples of 2 ml each were pipetted into TOC ampules. Ampules were sealed immediately (Oceanography International Corp., College Station, TX).

Acridine orange direct count (AODC): 4 ml sample was pipetted into 4 ml 4% sterile formaldehyde solution and stored.

Plate count: 1 ml of sample was added to a sterile test tube filled with 9 ml of sterile water and mixed thoroughly. 1 ml was then transferred into a second sterile test tube filled with 9 ml of sterile water and again thoroughly mixed. Additional dilutions were added as appropriate to obtain a countable cell density on the plate. After mixing, 0.1 ml of sample from the 3 most appropriate dilutions was added to agar plates, spread, incubated for 24 hours or less if necessary and counted.

Suspended mass: 50 ml of sample was filtered through a 0.42 μm Nuclepore filter, that had been dried previously at 103°C for 1 hour and preweighed. Filters were dried at 103°C for 1 hour and reweighed. Difference between mass before and after weighing is mass per sample volume.

Filtrate of suspended solids measurement was collected for the following determinations:

Soluble organic carbon (SOC): 4 samples of 2 ml of filtrate were pipetted into TOC ampules. Ampules were sealed immediately (Oceanography International Corp., College Station, TX).

Glucose: 2 samples of 1 ml of filtrate were pipetted into test tubes, previously heated to 500°C, sealed with parafilm and frozen.

Dissolved oxygen (DO): 200 ml of effluent was collected in an Erlenmeyer flask and DO was determined with a DO-probe (model 54, Yellow Springs Instruments, Co. Inc.), that was previously standardized in oxygen saturated water.

Biofilm samples: A slide was removed from the reactor and immediately immersed in a measuring glass filled with reactor effluent.

Biofilm thickness: Thickness was measured by light microscopy, noting stage micrometer setting, by focussing on the biofilm surface and on the biofilm-substratum interface (Trulear and Characklis, 1982).

Biofilm was removed from a known surface area of the slide with a razor blade and added to 50 ml of autoclaved, filtered, carbon free water. The sample was homogenized for 1 minute at 60% speed and samples were taken:

Total organic carbon (TOC): 4 samples of 2 ml each were pipetted into TOC ampules. Ampules were sealed immediately (Oceanography International Corp., College Station, TX).

Acridine orange direct count (AODC): 4 ml sample was pipetted into 4 ml 4% sterile formaldehyde solution and stored.

Plate count: 1 ml of sample was added to a sterile test tube filled with 9 ml of sterile water and mixed thoroughly. 1 ml was then transferred into a second sterile test tube filled with 9 ml of sterile water and again thoroughly mixed. Additional dilutions were added as appropriate to obtain a countable cell density on the plate. After mixing, 0.1 ml of sample from the 3 most appropriate dilutions was added to agar plates, spread, incubated for 24 hours or less if necessary and counted.

Adsorbed mass: 25 ml was filtered through a 0.42 μm Nuclepore filter, previously dried at 103°C for 1 hour and preweighed. Filter was dried again at 103°C for 1 hour and reweighed. Difference between mass before and after weighing is mass per sample volume.

In addition, the following observations were made:

Transmission electron micrographs (TEM): Parts of the slide with the adsorbed biofilm sample were immersed in a solution of 2.5% glutaraldehyde in phosphate buffer for a minimum period of 6 to 14 hours, then stored in buffer solution until TEM sample preparation.

Optical photomicrographs (OPM): The biofilm slide was air dried and stored in a closed container for microscopic examination.

Chemostat

The chemostat was used for the determination of kinetic and stoichiometric coefficients. The chemostat is a constant volume, continuous flow stirred tank reactor (CFSTR) used for growth of microbial cells. It consists of a Pyrex beaker ($0.45*10^{-3}$ m^{-3} volume) with side arm and rubber stopper. The chemostat was continuously stirred so as to maintain homogeneous conditions throughout the liquid and contained a device for scraping the reactor walls to minimize biofilm accumulation (Figure 4).

Preparation and Start-up

A 450 ml solution of nutrients and substrate (40 g glucose-C.m^{-3}) was prepared and added to the chemostat.

Figure 4. Schematic of a chemostat.

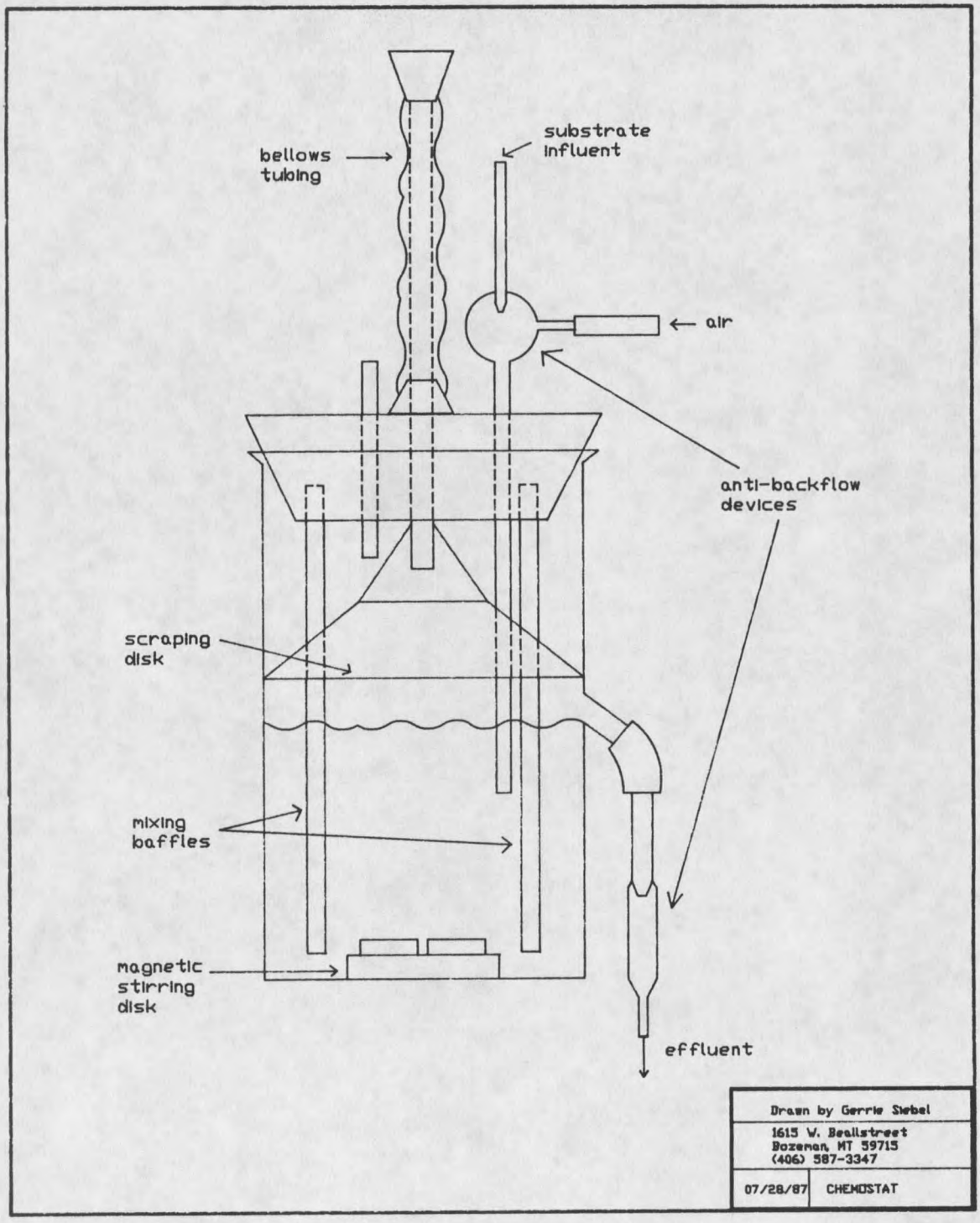

Chemostat tubing was flushed, ends were sealed with aluminum foil and clamped, and the entire assembly was autoclaved for 15 minutes at 121°C. After cooling, the chemostat was inoculated with 1 ml of the appropriate inoculum, previously cultured in a batch reactor. The chemostat was operated in batch mode for 12 hours to obtain a cell density of between 10^{12} to 10^{14} cells.m^{-3}. Then a continuous flow of nutrients was started. Initial flow rate was set at 0.12 $l.h^{-1}$ (dilution rate 0.27 h^{-1}).

Operation and Sampling

Steady state conditions were assumed to have been reached 6 residence times (24 hours) after starting up the continuous nutrient flow. Samples were taken by homogenizing 80 ml of effluent (DuPont Instruments, Sorvall Omni Mixer) for 1 minute at 60 % speed for the following analyses:

Total organic carbon (TOC): 4 samples of 2 ml each were pipetted into TOC ampules. Ampules were sealed immediately (Oceanography International Corp., College Station, TX).

Acridine orange direct count (AODC): 4 ml sample was pipetted into 4 ml 4% sterile formaldehyde solution and stored.

Suspended mass: 50 ml was filtered through a 0.42 μm Nuclepore filter, previously dried at 103°C for 1 hour and preweighed. Filter was dried again at 103°C for 1 hour and reweighed. Difference between mass before and after weighing is mass per sample volume.

The filtrate of suspended mass measurement was collected for the following determinations.

Soluble organic carbon (SOC): 4 samples of 2 ml of filtrate were pipetted into TOC ampules. Ampules were sealed

immediately (Oceanography International Corp., College Station, TX).

Glucose: 2 samples of 1 ml of filtrate were pipetted into test tubes, previously heated at 500°C, sealed with parafilm and frozen.

The chemostat was operated at the following dilution rates: 0.10, 0.13, 0.40, 0.50, 0.56, 0.67, 0.80, 1.07, 1.60 and 1.87 h^{-1}. After each change in dilution rate, a period of 6 residence times elapsed before samples were taken.

Batch Reactor

Principles of Operation

The batch reactor used is a respirometer (Oceanography International Corp., College Station, TX) designed to continuously monitor and replace oxygen consumed as a result of microbial activity.

It consists of a sample bottle with a manometer and an electrolysis cell (Figure 5). When oxygen is consumed, the oxygen partial pressure decreases, raising the electrolyte level on the inside of the manometer and, consequently, lowering it on the outside. This breaks an electrical circuit through a switch electrode and initiates oxygen production on the DO-electrode simultaneously producing hydrogen on the H_2-electrode. The hydrogen is allowed to leave instantaneously while the oxygen pressure reduces the electrolyte level in the inside and raises it on the outside of the manometer. Oxygen is produced until the outside electrolyte level in the manometer touches the switch electrode. CO_2 produced as a result of microbial activity is removed from the air space by KOH pellets.

The time that oxygen is generated is monitored and as

Figure 5. Schematic of a batch reactor.

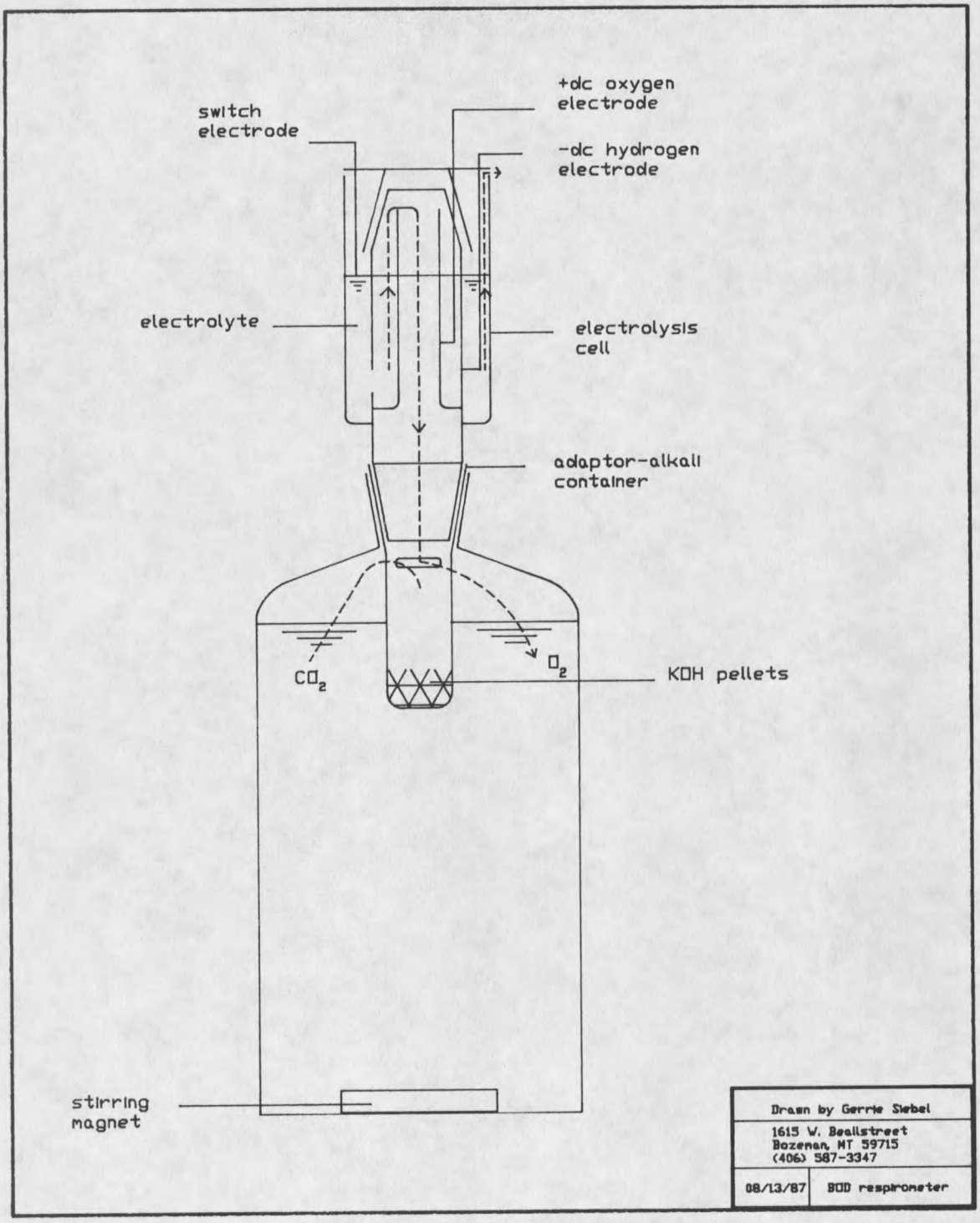

oxygen production is proportional to the current flowing through the electrolysis cell, DO-production can be determined as a function of time.

Monitoring, Operation and Sampling

The amount of oxygen produced and, hence, of oxygen consumed is registered automatically as a function of time. When oxygen consumption (temporary) stalls, a plateau has been reached and liquid samples were taken by homogenizing 80 ml of suspension (DuPont Instruments, Sorvall Omni Mixer) for 1 minute at 60% speed for the following analyses:

Total organic carbon (TOC): 4 samples of 2 ml each were pipetted into TOC ampules. Ampules were sealed immediately (Oceanography International Corp., College Station, TX).

Acridine orange direct count (AODC): 4 ml sample was pipetted into 4 ml 4% sterile formaldehyde solution and stored.

Suspended mass: 25 ml was filtered through a 0.42 μm Nuclepore filter, previously dried at 103°C for 1 hour and preweighed. Filter was dried again at 103°C for 1 hour and reweighed. Difference between mass before and after weighing is mass per sample volume.

Filtrate of suspended mass measurement was collected for the following determinations:

Soluble organic carbon (SOC): 4 samples of 2 ml of filtrate were pipetted into TOC ampules. Ampules were sealed immediately (Oceanography International Corp., College Station, TX).

Glucose: 2 ml samples of 1 ml of filtrate was pipetted into test tubes, previously heated to 500°C, sealed with parafilm and frozen.

Nutrient Medium

Nutrient Solution

The composition of the influent nutrient solution (Table 2) is identical to the one discussed by Turakhia (1986) with the exception that the calcium concentration is maintained at 25 g $Ca.m^{-3}$.

Table 2. Composition of nutrient solution.

	batch reactor	chemo-stat	annular reactor	units
glucose-Carbon	40.0	40.0	8.0	$g.m^{-3}$
NH_4CL	36.0	36.0	7.2	$g.m^{-3}$
$MgSO_4.7H_2O$	10.0	10.0	2.0	$g.m^{-3}$
$(NH_4)6Mo_7O_{24}.4H_2O$	.005	.005	.001	$g.m^{-3}$
$ZnSO_4.7H_2O$	.5	.5	.1	$g.m^{-3}$
$MnSO_4.H_2O$	.040	.040	.008	$g.m^{-3}$
$CuSO_4.5H_2O$	.010	.010	.002	$g.m^{-3}$
$Na_2B_4O_7.10H_2O$	.005	.005	.001	$g.m^{-3}$
$FeSO_4.7H_2O$	.560	.560	.112	$g.m^{-3}$
$(HOCOCH_2)_3N$	2.0	2.0	.4	$g.m^{-3}$
$CaCO_3$-Ca	-	-	25.0	$g.m^{-3}$
(Na_2HPO_4)	4.0	4.0	1.5	mmol
Na_2HPO_4	568.0	568.0	213.0	$g.m^{-3}$
(KH_2PO_4)	4.0	4.0	1.5	mmol)
KH_2PO_4	544.0	544.0	204.0	$g.m^{-3}$
final pH	6.8	6.8	6.8	-

Preparation of Plates

Agar plates of 2 different media composition were used, depending on the bacterial strain to be counted. Pseudomonas aeruginosa plates were prepared by adding 12 grams of Tryptone Glucose Extract Agar (Difco Laboratories, Detroit, MI) to 500 ml of distilled water. The solution was heated to dissolve the medium, autoclaved for 15 minutes at 121°C, allowed to cool and poured into plates.

Klebsiella pneumoniae plates were prepared by adding 24 grams of Bacto Agar (Difco Laboratories, Detroit, MI) and 7.5 grams of m Endo Broth MF (Difco Laboratories, Detroit, MI) to 500 ml of distilled water. Mixture was heated. 10 ml of absolute ethanol was added just before boiling and the mixture was allowed to cool and poured into plates.

Microbial Species

Klebsiella pneumoniae

The K. pneumoniae strain used in this study was originally isolated in the water distribution system of New Haven, CT. and was obtained from Anne Kamper, Dept. of Microbiology, Montana State University, Bozeman, MT.

Pseudomonas aeruginosa

The P. aeruginosa strain used for this study was obtained from the American Type Culture Collection, Denver, CO.

Analytical Methods

An overview of analytical procedures and their interrelations is shown in Figure 6.

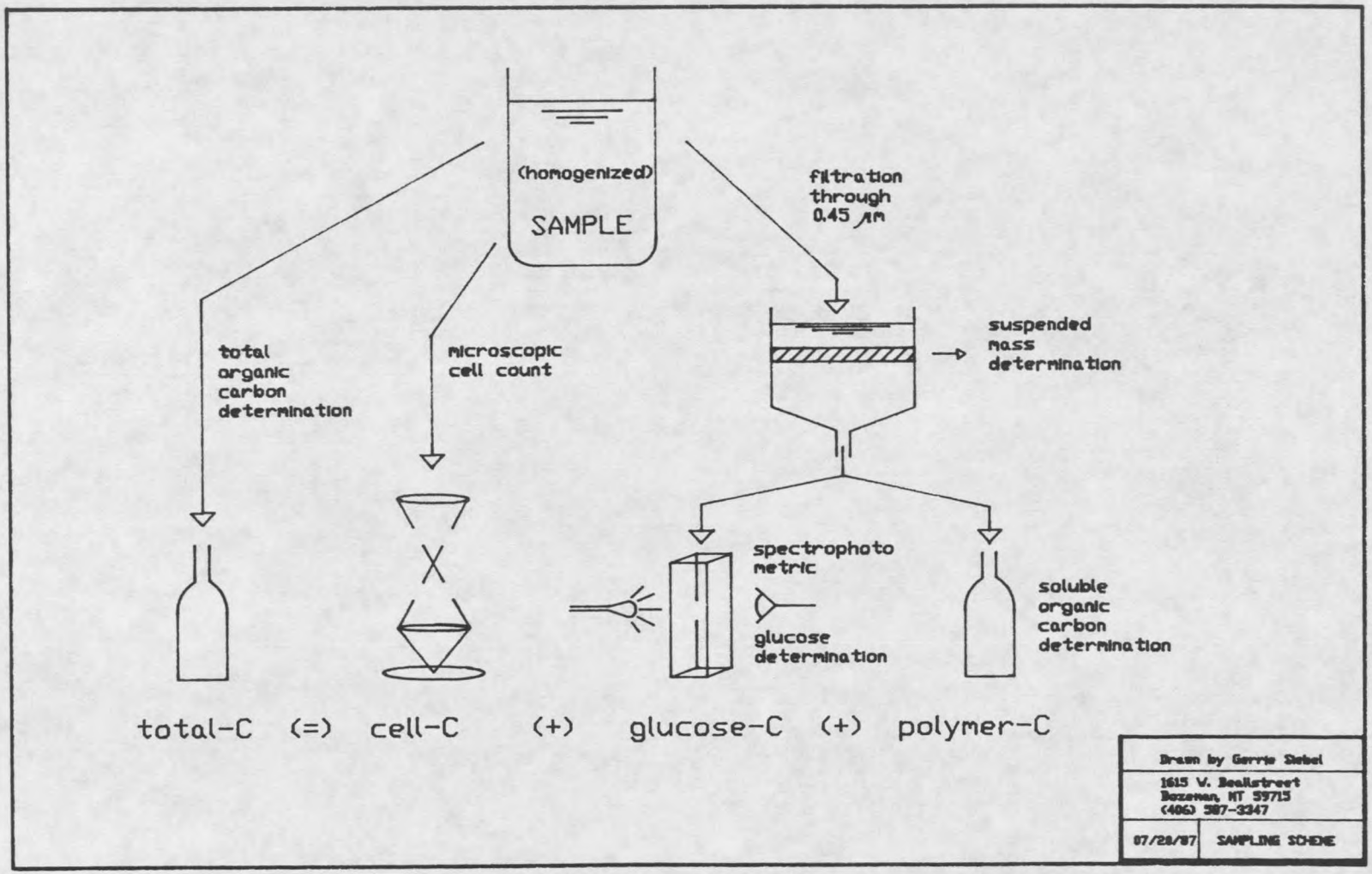

Figure 6. Overview of the sampling scheme and analytical procedures.

Acridine orange direct count: Total number of cells in effluent and resuspended biofilm samples were determined after staining with acridine orange according to Hobbie et al. (1977).

Plate count: Cell density in liquid phase was determined by multiplying the cell number counted per plate by the dilution factor and dividing by the volume of diluted sample applied per plate.

Cell density in the biofilm was determined by multiplying the cell number counted per plate by the dilution factor, dividing by the volume of diluted sample applied per plate, dividing by the liquid volume into which the biofilm sample was suspended and dividing by the surface area of the biofilm removed.

Mass: Mass in effluent and resuspended biofilm samples was determined as described in sections on Sampling.

Glucose carbon: Glucose carbon (S_{Sl}) was determined using the procedure of the enzymatic Glucose Analysis Procedure Sigma 510 (Sigma Chemical Co., St. Louis, MO) and modified by Trulear (1983).

Carbon: Carbon was determined with the ampule analysis module of the Oceanography International Carbon Analyzer (Oceanography International Corp., College Station, TX).

Cell carbon: Cell carbon in liquid phase (X_{Ml}) and in the biofilm (X_{Mf}) was determined by multiplying the cell number obtained with the Acridine Orange Direct Count by, successively, 1) cell volume, 2) cell density ($1.07*10^{6}$ g cell.m^{-3}, Doetsch et al., 1973; Bakken and Olsen, 1983), 3) dry cell mass to wet cell mass ratio (0.22 dry cell mass.(wet cell mass)$^{-1}$, Bakken and Olsen, 1983) and 4) ratio of carbon mass to dry cell mass (0.5 g cell carbon.(g

cell dry mass)$^{-1}$, Doetsch et al., 1973).

Liquid phase product carbon: Mass of product carbon in the liquid phase (S_{Pl}) was determined by subtracting the mass of liquid phase glucose (S_{Sl}) and cell carbon (X_{Ml}) from the liquid phase total organic carbon mass:

$$S_{Pl} = S_{TOCl} - S_{Sl} - X_{Ml} \quad (18)$$

Biofilm product carbon: Mass of product carbon in the biofilm (S_{Pf}) was determined by subtracting the mass of biofilm cell carbon (X_{Mf}) from the biofilm total organic carbon:

$$S_{Pf} = S_{TOCf} - X_{Mf} \quad (19)$$

Liquid phase adsorbed product carbon: Mass of liquid phase product carbon adsorbed to the cell was determined by subtracting glucose carbon, soluble organic carbon and cell carbon from total organic carbon:

$$S_{Pla} = S_{TOCl} - S_{Sl} - S_{SOCl} - X_{Ml} \quad (20)$$

Dissolved oxygen: Dissolved oxygen was determined with a DO-probe (model 54, Yellow Springs Instruments, Co. Inc.).

Biofilm thickness: Biofilm thickness was measured according to Trulear (1983) and calculated according to Bakke and Ollson (1986). Biofilm thickness data are the mean of 8 observations along premarked points on the center line of the slide.

Transmission electron micrographs (TEM): Samples stored in buffer solution were prepared for electron microscopy according Appendix F.

Optical photo micrographs (OPM): Nomarsky microscopy on the air dried biofilm slides was used to follow progression of biofilm formation processes.

Statistical Methods

Time progression of biofilm variables can generally be represented by a sigmoidally shaped curve, either starting from zero at time zero and increasing in magnitude to reach a steady state value or starting at a certain value at time zero and decreasing in magnitude to a steady state value. The sigmoidal shape can mathematically be represented by the logistical equation. Measured variables were fit to the logistic equation using the statistical package Logit (LOGIT, 1986). The logistic function is presented in the following version:

$$Y = \frac{A + A_s(X-X_o) + A_q(X-X_o)^2}{1+e^{\left[\frac{(X-X_o)}{2D_o}\left[1+e^{Q(X-X_o)}\right]\right]}} + \frac{B + B_s(X-X_o) + B_q(X-X_o)^2}{1+e^{-\left[\frac{(X-X_o)}{2D_o}\left[1+e^{Q(X-X_o)}\right]\right]}}$$

$\underbrace{\qquad\qquad A \qquad\qquad}$ $\underbrace{\qquad\qquad B \qquad\qquad}$

With X being the independent variable, in this case, time, Y is some form of system response in time. The model consists of 3 regions. The first part of the equation (A) relates to the pretransition region of the model for which the intercept (A), the slope (A_s) and a quadratic term (A_q) define the pretransition asymptote. Similarly, the second part of the equation (B) relates to the posttransition region of the model for which the intercept (B), the slope (B_s) and a quadratic term (B_q) define the posttransition asymptote. The transition region of the model is described by the transition region width parameter (D_o), the position of the transition region (X_o) and the asymmetry parameter (Q) which allows the curvature in the pre- and post

transition ends of the transition region to vary.

Asymptotes for both pre- and posttransition region were assumed to be described by the intercept terms only (A_s, A_q, B_s and B_q were made zero). As a result, the model is described by the intercept parameters A and B, the position parameter X_o and width parameter D_o of transition region and the asymmetry parameter Q. Determination of parameter values allowed analysis of experimental results by means of the model generated.

Nonlinear regression using the saturation model was used to correlate TOC standards to TOC readings, and to correlate dilution rate to substrate effluent concentration in the chemostat experiments (BMDP, 1983). Linear regression was used to correlate glucose standards to glucose readings and to determine product formation coefficients (MSUSTAT, 1986).

RESULTS

Batch reactor and chemostat experiments using Klebsiella pneumoniae were conducted for the determination of stoichiometric coefficients and coefficients describing the growth and product formation kinetics. Raw data from the batch experiments are listed in Appendix C, from the chemostat experiments in Appendix D.

Rototorque experiments were conducted with Pseudomonas aeruginosa and Klebsiella pneumoniae, both in mono and in binary population experiments. Objectives were to determine the biofilm formation properties of K. pneumoniae, to compare them with those of P. aeruginosa and to study those properties when both organisms form the biofilm. Raw data and parameter estimates from the Rototorque experiments are listed in Appendix G (K. pneumoniae), H (P. aeruginosa) and I (binary population).

Throughout this thesis cell mass, product mass and substrate mass data are reported as carbon equivalents. Glucose was used as the sole source of carbon and energy at concentrations of 40 g $C.m^{-3}$ for the batch and chemostat experiments and at 10 g $C.m^{-3}$ for the Rototorque experiments. In two binary population experiments the influent substrate concentration was 20 g $C.m^{-3}$.
When applicable, results are expressed in terms of mean ± standard error. K. pneumoniae, P. aeruginosa and binary populations are, when space required, referred to by KP, PA and BP.

Batch Experiments

Batch experiments were conducted to determine the oxygen consumption by *K. pneumoniae* (see Figure 7). Experimental results are presented in Appendix C, a summary is presented in Table 3.

Table 3. Summary of batch reactor experimental results.

Reactor #	Product soluble S_{Pl}	Cell mass X_{Ml}	Product adsorbed S_{Pla}	Product total S_{Plt}	Glucose oxygen ratio Y_{SO}
	..... ($g\ C.m^{-3}$)				($gC.gO^{-1}$)
I	10.7	7.1	3.7	14.4	0.90
II	11.3	7.6	4.7	16.0	0.91
III	9.0	8.0	4.4	13.4	0.90
MEAN	10.3	7.6	4.3	14.6	0.90
STDEV	1.2	.9	2.0	2.3	0.01

Yield Coefficients

Yield coefficients can be calculated from the results of the batch reactor experiments:

Table 4. Means and standard deviations of yield coefficients in batch reactor experiments.

Y_{MS}	$= 0.20 \pm 0.02\ g_C.g_{C-1}^{-1}$
Y_{SO} [1]	$= 0.90 \pm 0.01\ g_C.g_{O-1}$
Y_{PSl} [2]	$= 0.27 \pm 0.03\ g_C.g_{C-1}$
Y_{PSt}	$= 0.38 \pm 0.06\ g_C.g_C$

[1] Yield of soluble product carbon from substrate carbon.

[2] Yield of total product carbon from substrate carbon.

Figure 7 Typical progression of oxygen consumption by K. pneumoniae in a batch reactor.

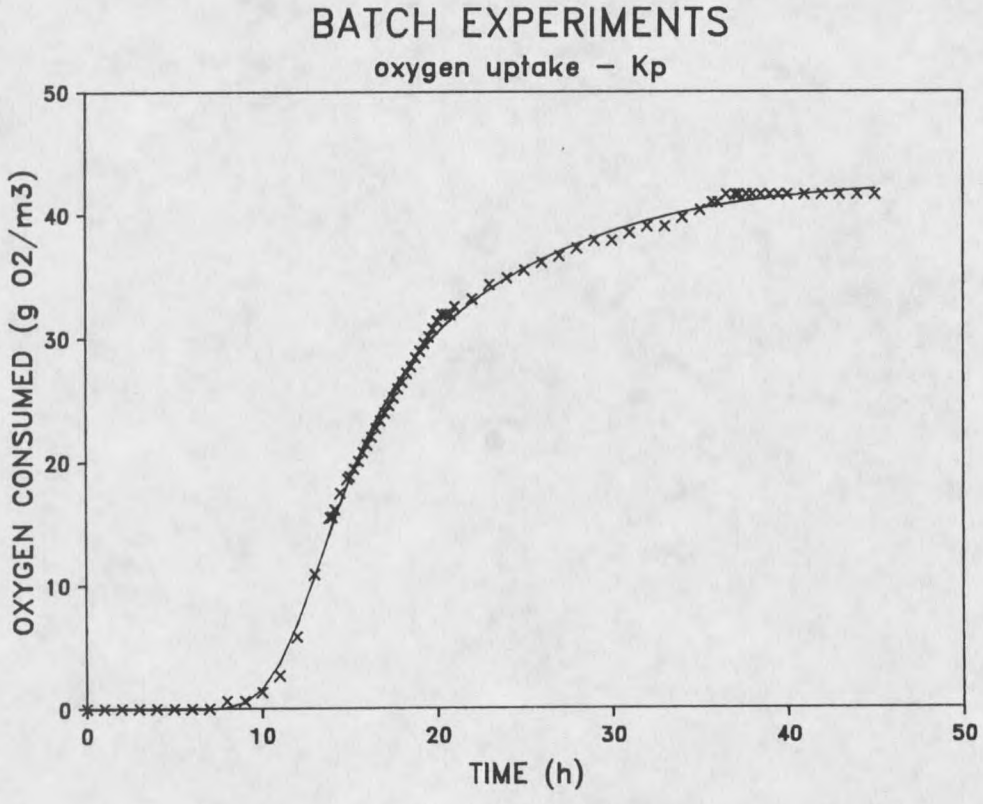

Chemostat Experiments

Relevant kinetic and stoichiometric information for *K. pneumoniae* was obtained by conducting a series of chemostat experiments and determining, for various dilution rates, steady state values of

- cell carbon concentration, X_{M1},
- product carbon concentration, S_{P1},
- substrate carbon concentration in influent, S_{Si}, and in effluent, S_{S1}, and
- biomass carbon concentration, X_{X1}.

Results are presented in Appendix D, a summary is presented in Table 5.

Table 5. Summary of chemostat experimental results for *K. pneumoniae*.

Dilution rate (h^{-1})	S_{Si}	S_{S1}	X_{X1}	X_{M1}	S_{P1}	S_{P1a}	S_{P1t}
	.....		.....	($g\ C.m^{-3}$)	.....		.....
.00	36.4	.0	.0	.0	.0	.0	.0
.10	37.4	.3	8.1	5.7	9.1	2.3	11.4
.13	37.3	.3	10.0	7.8	9.6	2.2	11.9
.27	37.1	.7	13.8	7.4	8.5	6.4	14.9
.27	37.1	.4	13.4	6.1	8.6	7.4	16.0
.40	37.0	.6	14.0	7.2	8.9	6.8	15.7
.40	37.0	.2	14.3	8.1	9.3	6.2	15.5
.50	36.5	.5	13.0	5.8	10.3	7.1	17.5
.50	36.5	1.3	12.2	7.2	11.0	5.0	16.0
.56	35.4	.2	12.6	6.3	11.4	6.3	17.7
.56	35.4	.6	12.7	11.0	11.3	1.7	13.0
.67	34.5	.2	14.8	6.2	11.2	8.6	19.8
.67	34.5	.0	12.6	8.4	11.2	4.3	15.5
.80	35.9	.4	14.5	4.2	10.1	10.3	20.4
.80	35.9	.4	12.1	7.3	9.6	4.8	14.4
1.07	37.1	.8	11.1	6.6	10.1	4.5	14.6
1.07	37.1	1.0	12.9	7.7	9.0	5.2	14.1
1.60	36.7	6.0	11.5	4.3	8.4	7.1	15.5
1.87	36.7	17.8	10.2	1.2	3.5	9.0	12.6

The effect of dilution rate on effluent concentration of substrate (stars), product (crosses) and cell carbon (triangles) is demonstrated in Figure 8. Also indicated is the influent substrate concentration (squares). Cell carbon concentration, rather stable over the range of dilution rates from 0.13 to 1.3 h^{-1}, decreases beyond this value and reaches zero around 2 h^{-1}. Product carbon behaves very similar to cell carbon and appears to indicate that product concentration is a function of growth rate. Simultaneously, glucose carbon concentration in the effluent is almost zero below dilution rates of 1 h^{-1}, but increases rapidly hereafter.

Growth Kinetic Coefficients

A material balance on cell carbon in the chemostat is described by:

$$\frac{dX_{M1}}{dt} = D(X_{Mi}-X_{M1}) + X_{M1}.\mu \qquad (12)$$

With data collection in the chemostat experiment taking place in steady state conditions and no cell carbon entering the chemostat, Eq. 12 can be rewritten as:

$0 = - D.X_{M1} + X_{ML}.\mu$ (21) or after dividing by X_{M1},

$D = \mu$ (22)

indicating that at steady state, the dilution rate equals the specific cellular growth rate. As microbial growth rate is dependent upon substrate concentration (Monod, 1949), Eq. 22 can be written as

$$D = \mu = \frac{\mu_m.S_{S1}}{K_S+S_{S1}}. \qquad (22)$$

Figure 8. Change in chemostat carbon concentrations with varying dilution rate (squares = influent glucose carbon, crosses = product carbon, triangles = cell carbon and stars = glucose carbon in effluent).

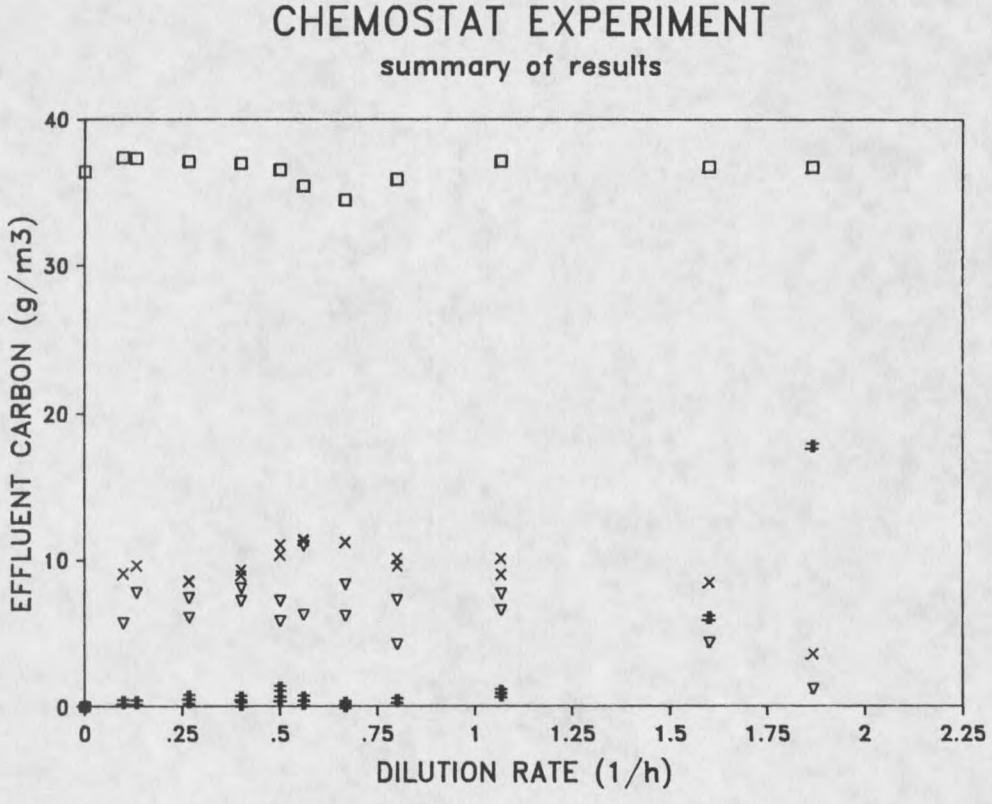

Substrate concentration in the effluent vs. dilution rate (Figure 9) was modelled according to Monod kinetics for determination of μ_m and K_S, using non-linear regression (BMDP, 1983). Parameter values are:

$\mu_m = 2.00 \pm 0.29\ h^{-1}$ and

$K_S = 1.43 \pm 0.53\ g\ C.m^{-3}$.

Product Formation Kinetic Coefficients

A material balance for product formation in the chemostat is given by Eq. 13:

$$\frac{dS_{Pl}}{dt} = D(S_{Pi}-S_{Pl}) + XM_l.r_{Pl} \qquad (13)$$

Product growth and non-growth associated kinetic coefficients (Luedeking and Piret, 1959) can be determined by rearranging Eq. 13. Assuming steady state conditions, no product material in the chemostat influent, substituting Eq. 8 for the specific product formation rate, assuming that the specific cellular growth rate equals the dilution rate and dividing by the cell carbon concentration, the following expression arises:

$$\frac{D.S_{Pl}}{X_{Ml}} = k_{Pg}.D + k_{Pn} \qquad (23)$$

representing a linear equation for which the intercept equals the non-growth associated product formation coefficient (k_{Pn}) and the slope equals the growth associated product formation coefficient (k_{Pg}). Using linear regression (MSUSTAT, 1986), parameter values were

Figure 9. Change in chemostat effluent glucose carbon concentration with varying dilution rate.

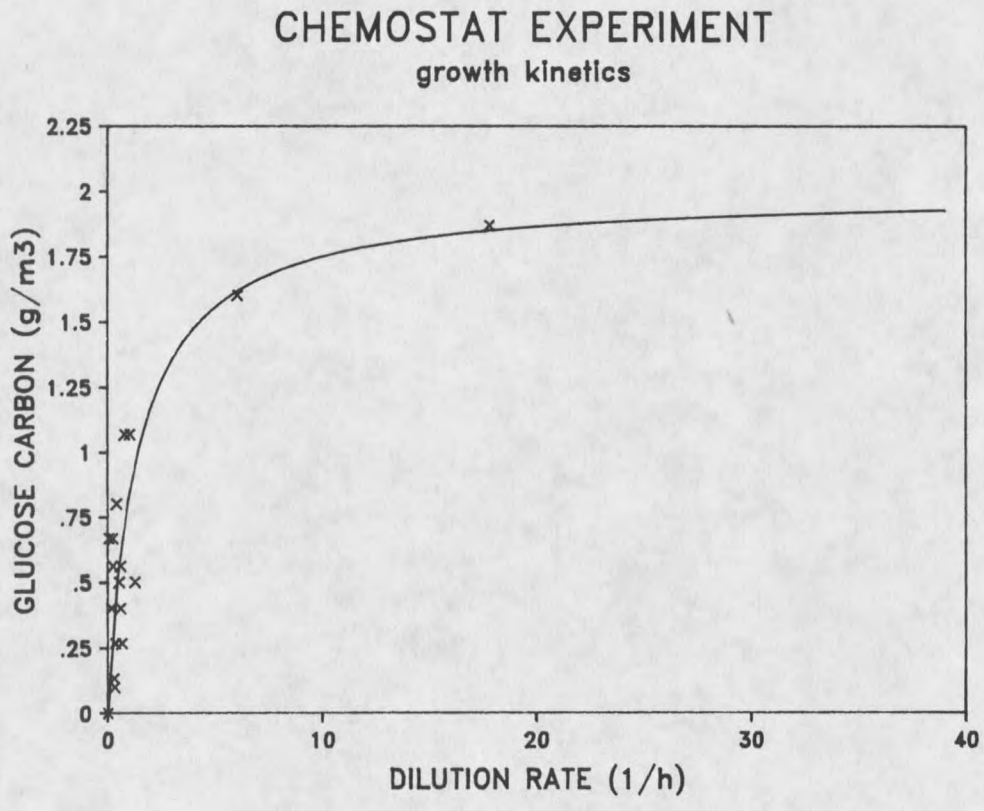

obtained for formation of unadsorbed product (calculated as the difference between S_{SOC1} and S_{S1}) and for formation of total product (unadsorbed + adsorbed product; the last calculated as the difference between $S_{TOC1} - S_{SOC1} - X_{M1}$).

Table 6. Specific growth- and non-growth associated product formation coefficients for K. pneumoniae in the chemostat.

		soluble	total [1]
kPg	($g.g^{-1}$)	1.45 ± 0.13	2.33 ± 0.35
kPn	($g.g^{-1}h^{-1}$)	-.01 ± 0.06	-.02 ± 0.20

[1] sum of soluble product and product adsorbed to cell mass.

Values for the intercept were not different from zero at the 5% level of significance. A plot of dilution rate vs. specific (unadsorbed and total) product formation rate is shown in Figure 10 together with the lines describing the linear models. Under the conditions of this chemostat experiment, almost two-thirds of the product formed appears unadsorbed while the remainder is adsorbed to the cell.

Cell and Product Yield Coefficients

When accepting a saturation model for the relation between effluent substrate concentration and dilution rate, it seems reasonable to assume that, considering the relation between substrate consumed and biomass produced, cell mass and product mass will follow a model that is related to the saturation model. Therefore, mass of cell carbon and product carbon were fitted to an inverse and displaced saturation model described by the following equation:

Figure 10. Specific product formation rate vs. dilution rate for chemostat growth of K. pneumoniae. Models for soluble (triangles, R^2=0.95) and total product (crosses, R^2=0.86) are represented by continuous lines.

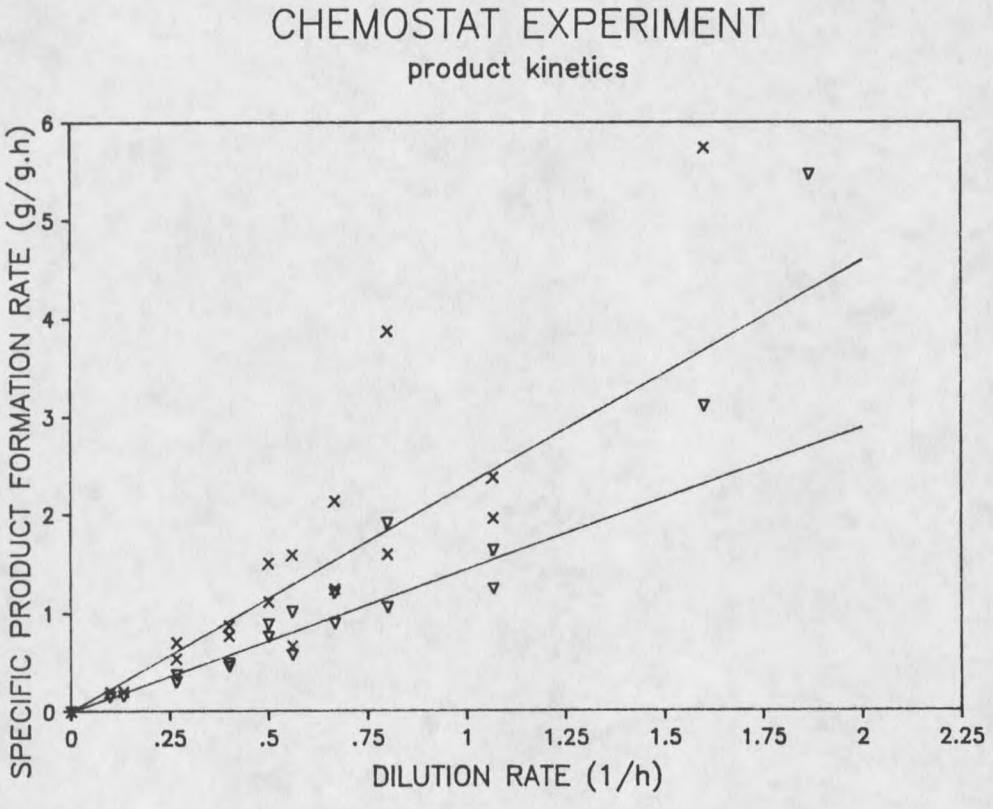

$$Y = \frac{-A * (X - C)}{B - (X - C)}$$

where Y = response (eg. product carbon in effluent),

X = dilution rate D,

A = parameter describing maximum value of concentration,

B = parameter comparable to K_S in the saturation equation, and

C = parameter describing model displacement, comparable with μ_m in the saturation equation.

The dilution rate at which no substrate is consumed can neither support growth of microbial cells nor can product be formed. Consequently, the parameter for the model displacement, C, does necessarily assume the value of dilution rate at which the effluent glucose concentration equals the influent glucose concentration.

Mass of cell carbon and product carbon vs. dilution rate were fitted to an inverse and displaced saturation model. The models are graphically shown in Figure 11 together with the raw data. Also shown is the model curve for effluent substrate concentration.

Yield coefficients for the conversion of substrate to cell mass and product mass appear not necessarily constant over the whole range of dilution rates (Figure 12). Mean values and standard deviations for the yield coefficients are summarized below.

Figure 11. Change in chemostat carbon concentrations with dilution rate (squares = influent glucose carbon, crosses = product carbon, triangles = cell carbon and stars = glucose carbon in effluent). Continuous lines represent models describing the change in carbon concentration with dilution rate.

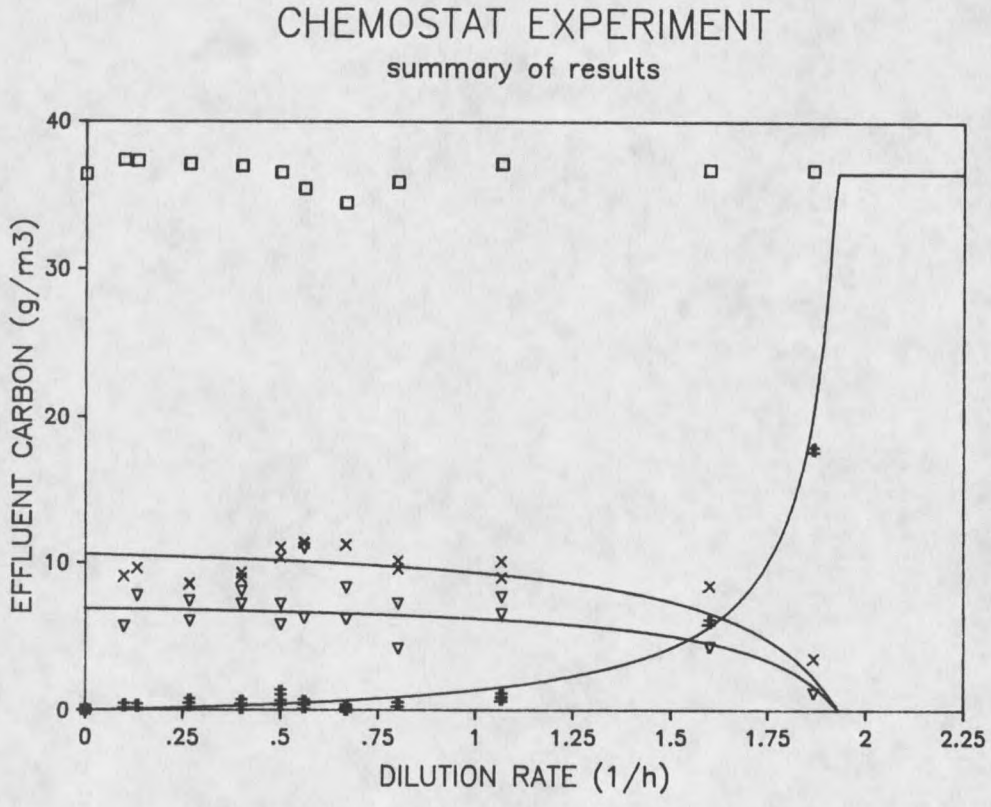

Figure 12. Variation in yield coefficients with dilution rate (triangles = yield of product carbon, crosses = yield of cell carbon).

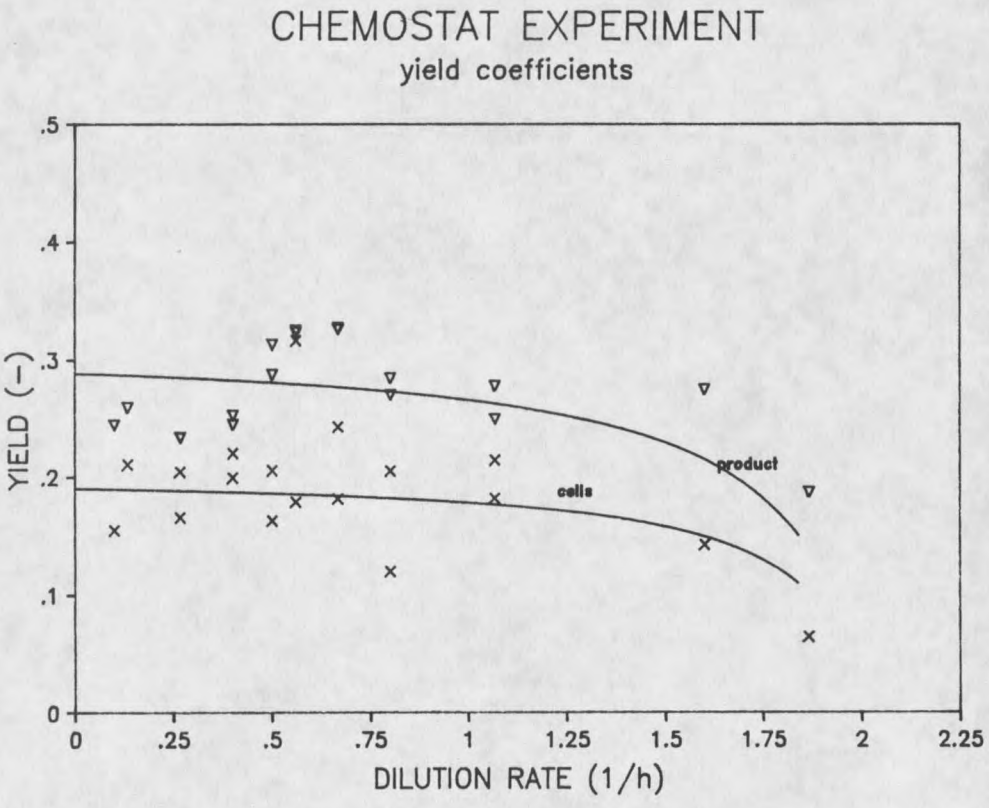

Table 7. Yield coefficients for K. pneumoniae chemostat experiments.

Y_{MS}	$= 0.19 \pm 0.05\ g_C.g_C^{-1}$
Y_{PSl}[1]	$= 0.27 \pm 0.04\ g_C.g_C^{-1}$
Y_{PSt}[2]	$= 0.45 \pm 0.09\ g_C.g_C^{-1}$

[1] Yield of soluble product carbon from substrate carbon.

[2] Yield of total product carbon from substrate carbon.

Cell Dimensions as Function of Dilution Rate

Cell dimensions were measured during the cell count procedure using Image Analysis Microscopy. Cell length increases rapidly with increasing dilution rate until a dilution rate of approximately 0.6 to 0.7 h^{-1} after which it decreases. Cell length at maximum dilution rate is very similar to cell length at low dilution rate. In contrast, cell breadth remains almost constant over the range of dilution rates (Figure 13).

Figure 13. Variation in cell length and breadth with dilution rate. Length of bars is two times the standard error.

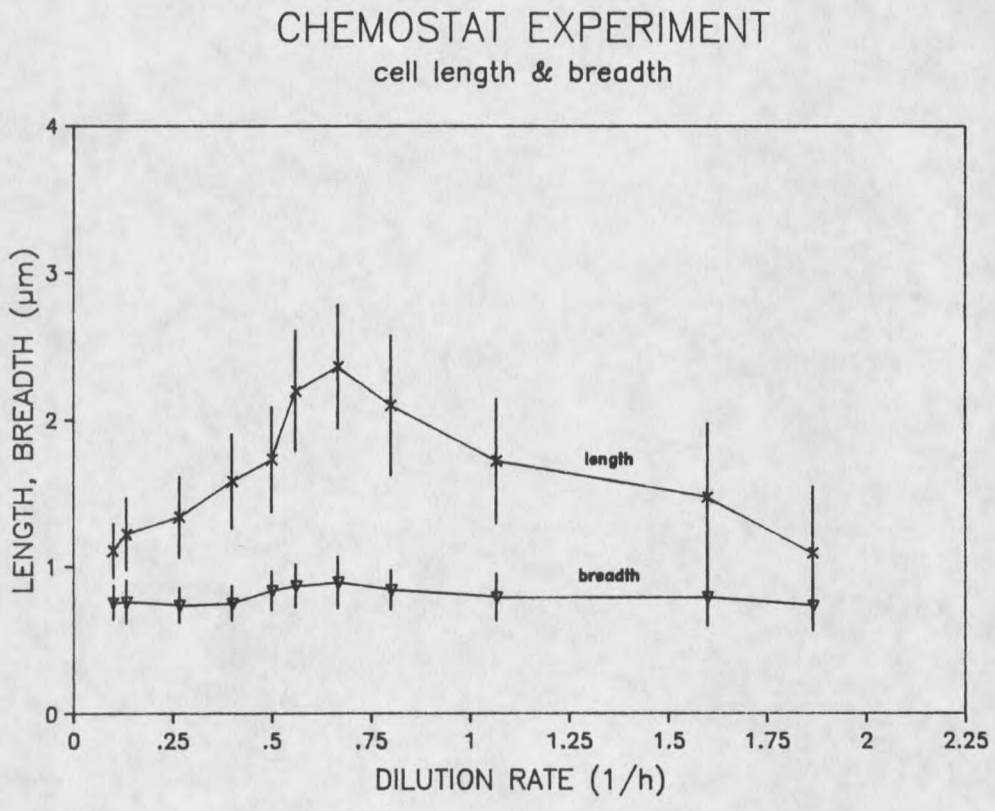

Biofilm Experiments

Biofilm experiments included 3 sets of 4 experiments conducted in the Rototorque. The first set featured K. pneumoniae, the second set featured P. aeruginosa, both as mono populations. The last set of experiments was conducted with both organisms in a binary population. Initial conditions in all experiments were the same (S_{Si} = 10 g C.m^{-3}) except for 2 binary population experiments (S_{Si} = 20 g C.m^{-3}). As a result, the only variable in these experiments is the microbial inoculum. The following parameters were determined:

In influent: - Glucose, S_{Si}
- Dissolved Oxygen, S_{Oi}

In effluent: - Cell mass, X_{Ml}
- Product mass, S_{Pl}
- Glucose, S_{Sl}
- Dissolved Oxygen S_{Ol}

In biofilm : - Cell mass, X_{Mf}
- Product mass, S_{Pf}
- Biofilm thickness, δ_f.

Results are presented for K. pneumoniae, for P. aeruginosa and for the binary population experiments. Raw data and parameter estimates for the biofilm experiments are summarized in Appendix G (K. pneumoniae), H (P. aeruginosa) and I (binary population).

Progression of Biofilm Carbon Components

In a typical progression, the mass of biofilm cell carbon in a K. pneumoniae experiment (Figure 14) is one tenth of that in a P. aeruginosa experiment (Figure 15). However, the product mass is almost the same for both organisms, indicating a relatively high specific product formation rate for K. pneumoniae. By comparison, the combined mass of biofilm cell carbon in the binary population biofilm is a little higher than for the P. aeruginosa biofilm, and the mass of product carbon is about twice as great (Figure 16). Biofilm composition in terms of carbon for K. pneumoniae, P. aeruginosa and the binary populations (with low, 10 g $C.m^{-3}$ and high, 20 g $C.m^{-3}$ substrate influent concentration) is shown for steady state conditions in Figure 17.

Specific Rates

Information on biofilm specific rates may give an indication of biofilm activity and as such is a useful tool in the evaluation of biofilm performance.

Figure 14. Typical progression of organic carbon in a K. pneumoniae biofilm. Length of bars is two times the standard error.

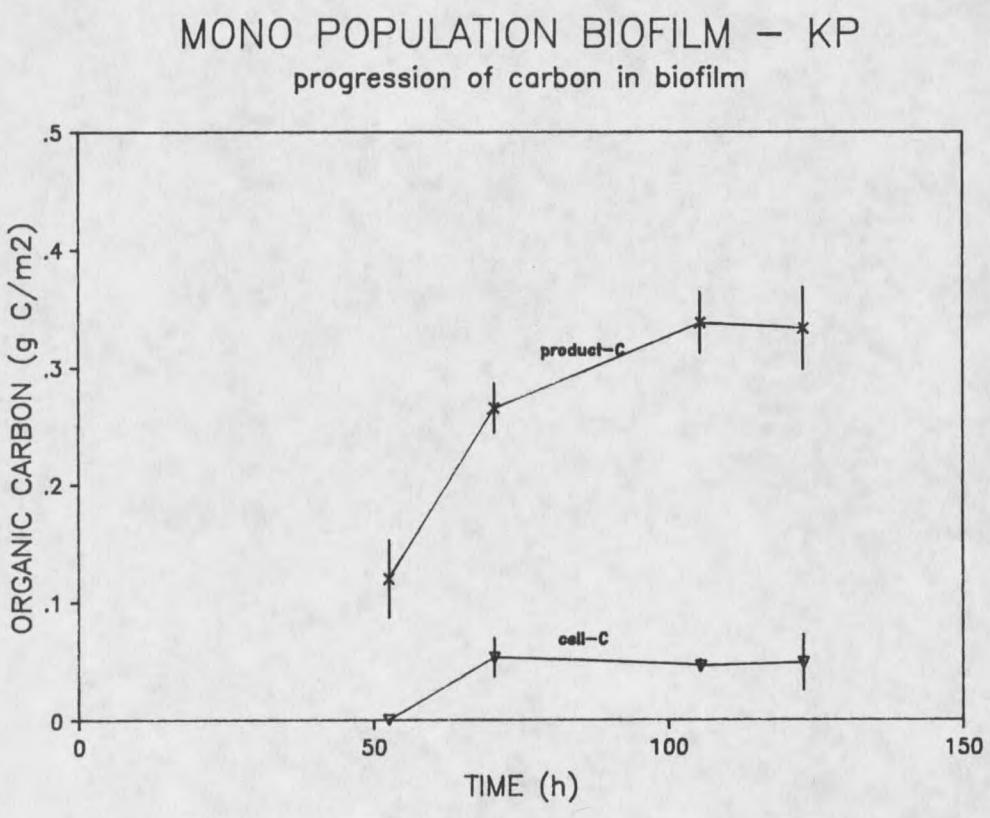

Figure 15. Typical progression of organic carbon in a P. aeruginosa biofilm. Length of bars is two times the standard error.

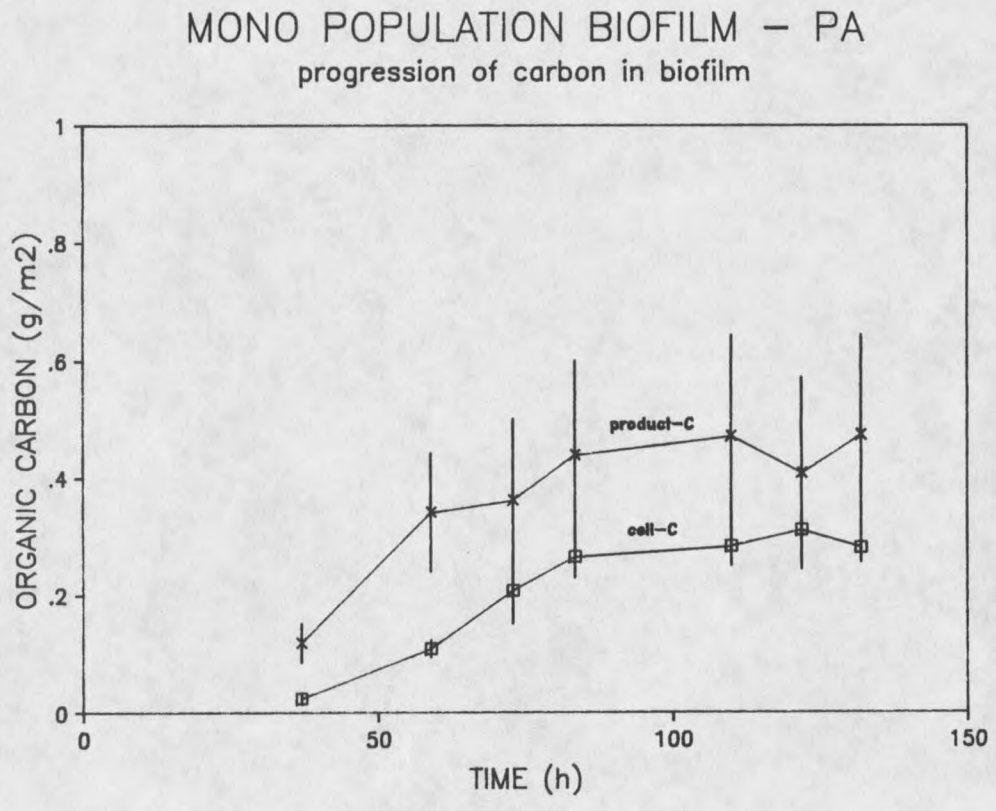

Figure 16. Typical progression of organic carbon in a binary population biofilm. Length of bars is two times the standard error.

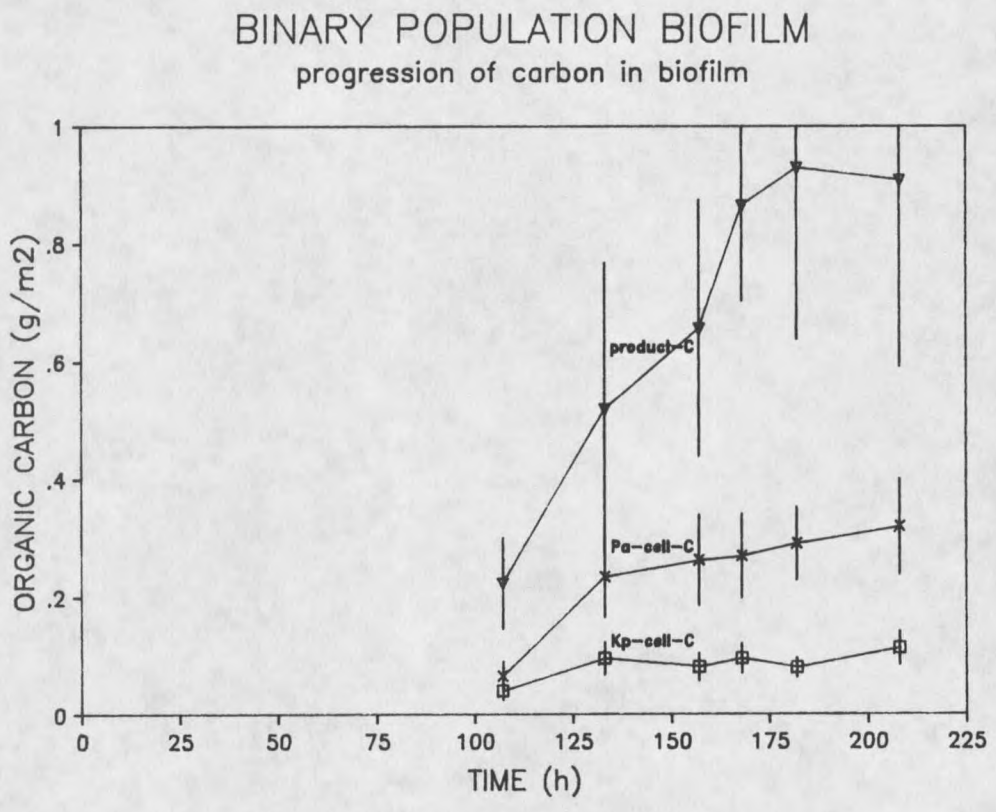

Figure 17. Comparison of organic carbon components in steady state biofilms of K. pneumoniae, P. aeruginosa and binary populations (L = grown on low glucose carbon concentration, 10 g $C.m^{-3}$, H = grown on high glucose carbon concentration, 20 g $C.m^{-3}$).

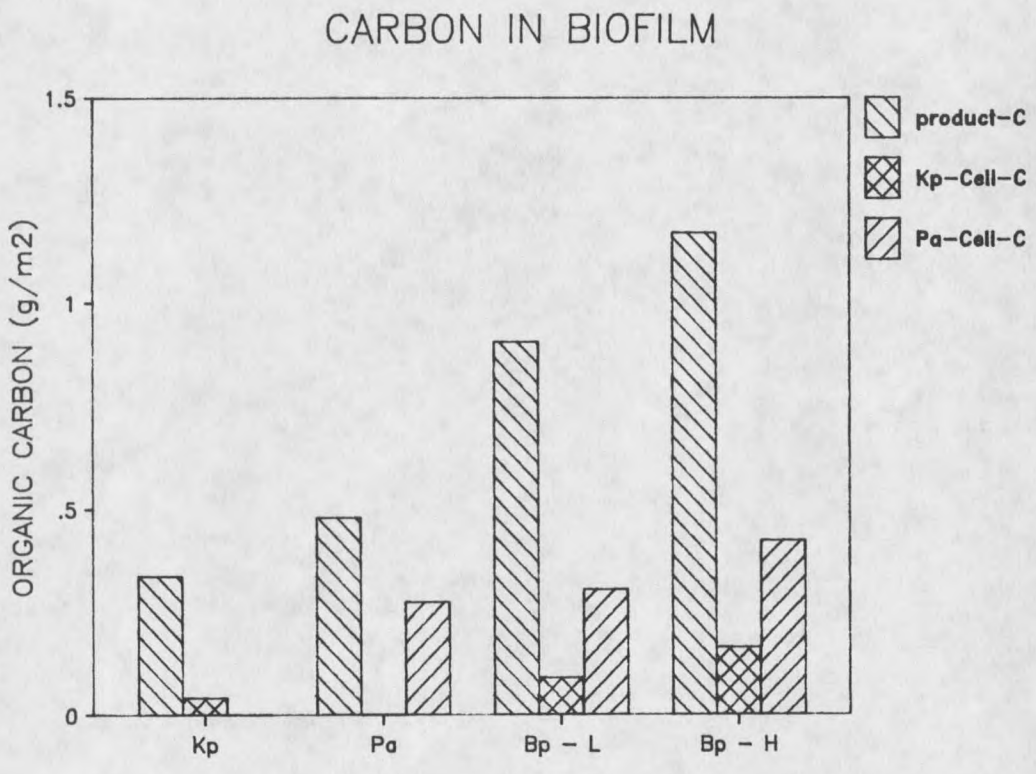

Specific Cellular Detachment Rate. The specific cellular detachment rate (r_{dM}) is obtained from the balance of liquid phase cell carbon (Eq. 2).

$$r_{Md} = \frac{\frac{dX_{Ml}}{dt} - D.-X_{Ml} - X_{Ml}.\mu}{X_{Mf}.\frac{A}{V}} \qquad (24)$$

Biofilm Specific Cellular Growth Rate. Rewriting the mass balance of biofilm cell carbon (Eq. 5) by dividing by X_{Mf},

$$\frac{1}{X_{Mf}}.\frac{dX_{Mf}}{dt} = - r_{Md} + \mu_f \qquad (25)$$

permits the calculation of the biofilm specific cellular growth rate.

Specific Product Detachment Rate. The specific rate of product detachment may be determined from the liquid phase product balance (Eq. 3):

$$r_{Pd} = \frac{\frac{dS_{Pl}}{dt} - D.-S_{Pl} - X_{Ml}.r_{Pl}}{S_{Pf}.\frac{A}{V}} \qquad (26)$$

When assuming that the liquid phase cell concentration X_{Ml} is negligible (liquid detention time in Rototorque is 10 minutes), Eq. 26 reduces to:

$$r_{dP} = \frac{\frac{dS_{Pl}}{dt} - D.-S_{Pl}}{S_{Pf}.\frac{A}{V}} \qquad (27)$$

Biofilm Specific Product Formation Rate. Biofilm specific product formation rate is determined by dividing the biofilm product mass balance (Eq. 6) by the biofilm cell mass X_{Mf}:

$$\frac{dS_{Pf}}{X_{Mf}.dt} = -\frac{S_{Pf}}{X_{Mf}}.r_{Pd} + r_{Pf} \qquad (28)$$

Specific biofilm cellular growth and biofilm product formation rates for steady state conditions are summarized for K. pneumoniae, P. aeruginosa and the binary populations with low (10 g $C.m^{-3}$) and high (20 g $C.m^{-3}$) substrate influent concentration (Figure 18).

Product Formation Coefficients

Product formation coefficients (Eq. 8) can be evaluated for biofilm conditions according to Luedeking and Piret (1959):

$$r_{Pf} = k_{Pg}.\mu_f + k_{Pn} \qquad (29)$$

by performing linear regression (MSUSTAT, 1986) of r_{Pf} versus μ_f (Figures 19, 20 and 21 for K. pneumoniae, P. aeruginosa and for binary populations). Table 8 summarizes values for k_{Pg} and k_{Pn}.

Figure 18. Comparison of specific biofilm cellular growth rate (hatched) and biofilm product formation rate (cross-hatched) in steady state biofilms of K. pneumoniae, P. aeruginosa and binary populations (L = grown on low glucose carbon concentration, 10 g $C.m^{-3}$, H = grown on high glucose carbon concetration, 20 g $C.m^{-3}$).

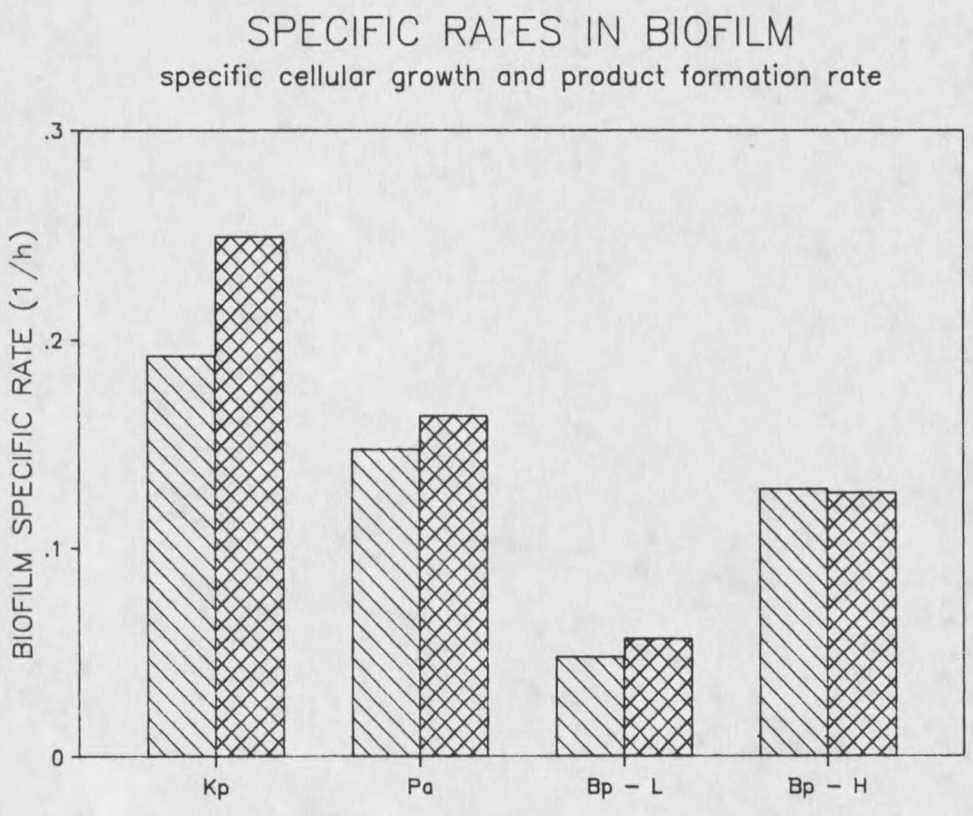

Figure 19. Biofilm specific product formation rate vs. biofilm specific cellular growth rate for K. pneumoniae. Continuous line is regression model (R^2=0.74).

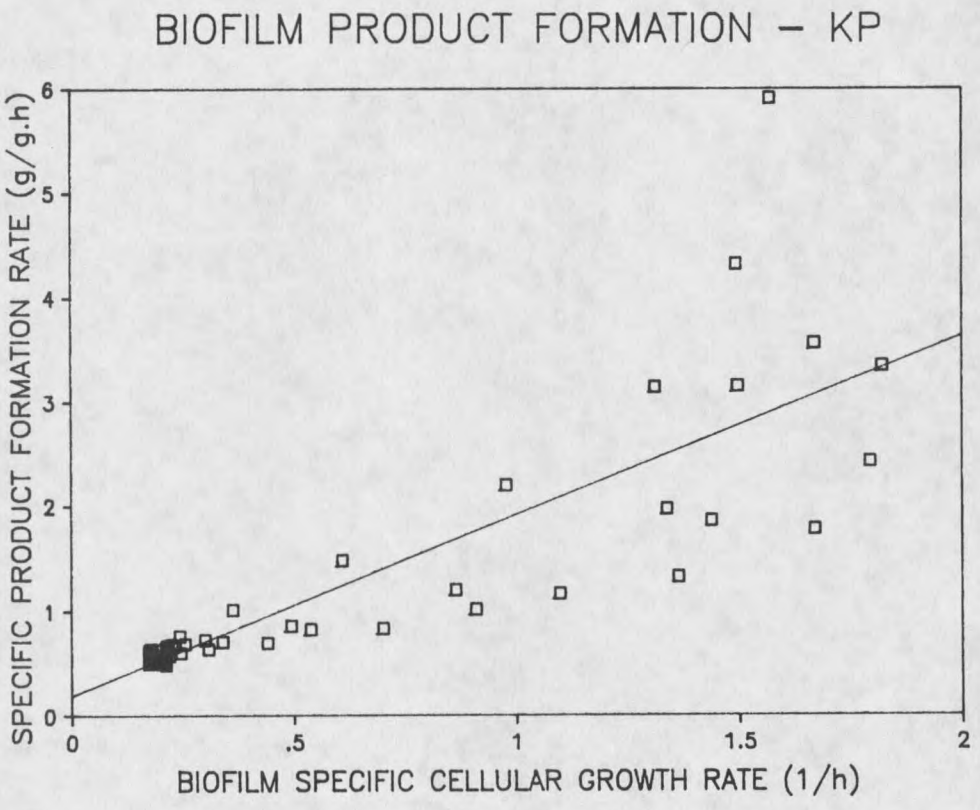

Figure 20. Biofilm specific product formation rate vs. biofilm specific cellular growth rate for P. aeruginosa. Continuous line is regression model (R^2=0.31).

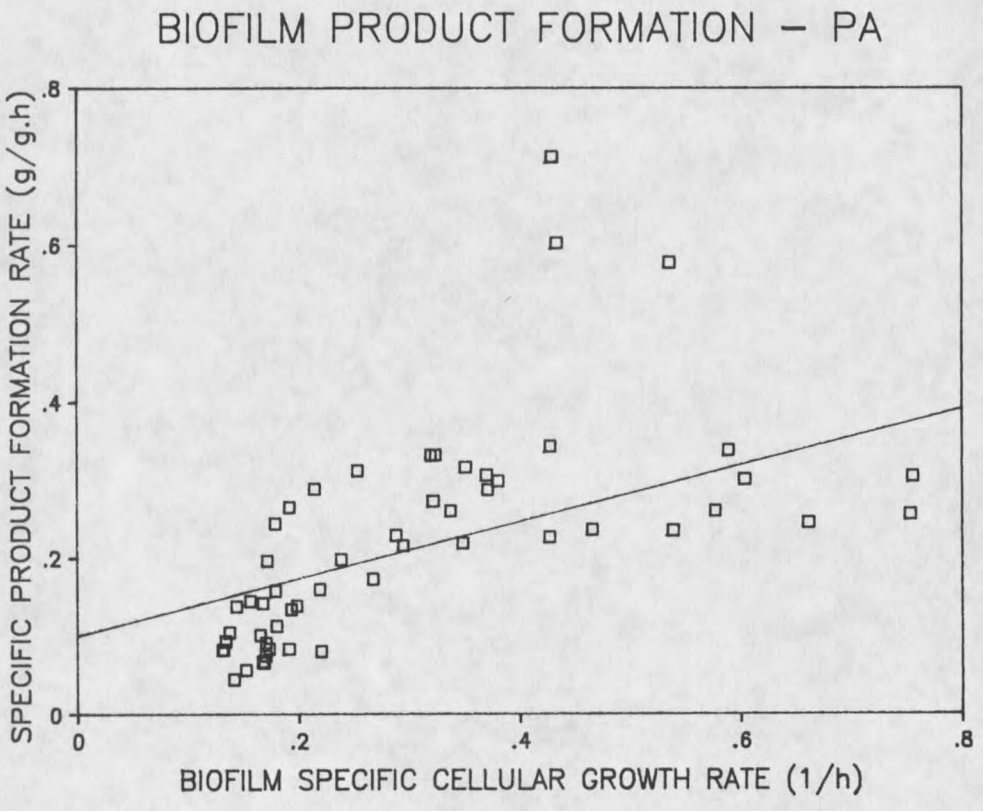

Figure 21. Biofilm specific product formation rate vs. biofilm specific cellular growth rate for binary population. Continuous line is regression model (R^2=0.90).

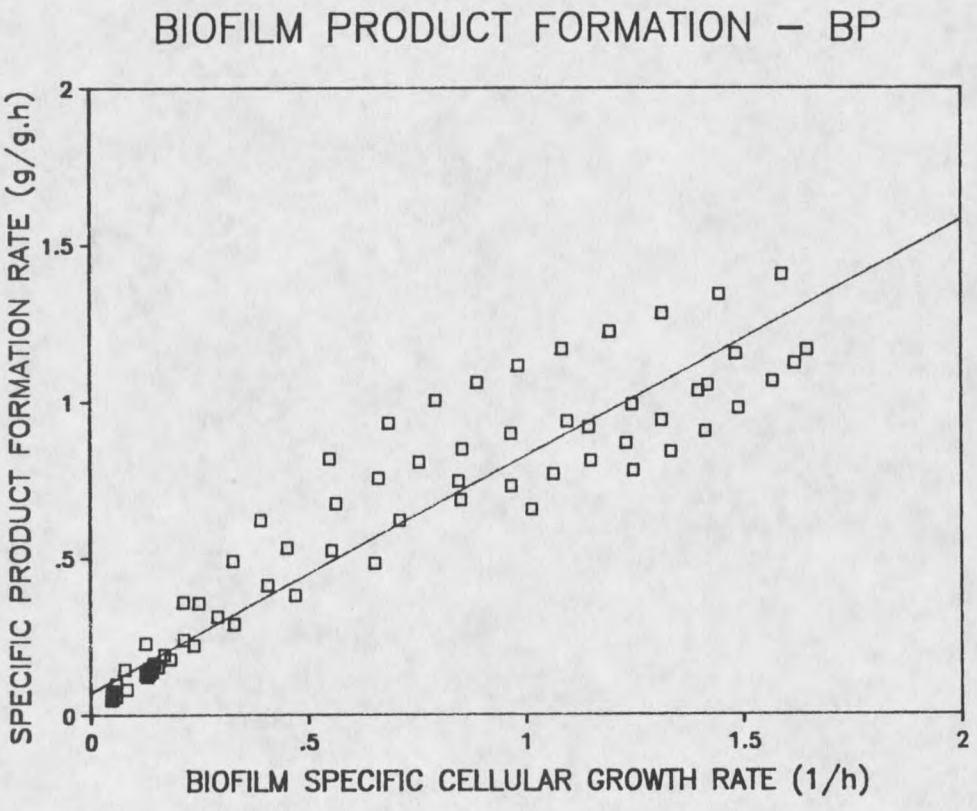

Table 8. Specific growth- and non-growth associated product formation coefficients in the biofilm for K. pneumoniae, P. aeruginosa and binary population.

		K. pneumoniae	P. aeruginosa	binary population
k_{Pg}	($g.g^{-1}$)	1.72 ± 0.11	0.36 ± 0.07	0.75 ± 0.03
k_{Pn}	($g.g^{-1}h^{-1}$)	0.20 ± 0.04[1]	0.10 ± 0.07[1]	0.08 ± 0.02[1]

[1] Values for k_{Pn} are different from zero at the 5% level of significance.

Biofilm Specific Substrate Uptake Rate

Biofilm specific substrate uptake rate can be evaluated from the material balance for biofilm phase substrate (Eq. 4). When assuming that there is no substrate in the biofilm, substituting μ_f for the product of f_D and μ, $k_{Pg}.\mu_f + k_{Pn}$ for the product of f_D and r_{Pl}, and after dividing by the concentration of biofilm cell carbon, X_{Mf}, Eq. 14 changes to

$$r_S = \frac{\mu_f}{Y_{MS}} + \frac{r_{Pf}}{Y_{PS}} = \mu_f \cdot \underbrace{\left[\frac{1}{Y_{MS}} + \frac{k_{Pg}}{Y_{PS}}\right]}_{(A)} + \underbrace{\left[\frac{k_{Pn}}{Y_{PS}}\right]}_{(B)} \qquad (30)$$

in which r_S is defined as the biofilm specific substrate uptake rate.

r_S can be determined from the liquid phase substrate balance (Eq. 1) when assuming that liquid phase cell mass is negligible:

$$r_S = \frac{D(S_{Si}-S_{Sl}) - \frac{dS_{Sl}}{dt}}{X_{Mf} \cdot \frac{A}{V}} \qquad (31)$$

Using linear regression of r_S versus μ_f (Figures 22, 23 and 24 for K. pneumoniae, for P. aeruginosa and binary populations) allows the evaluation of the biofilm specific substrate uptake rate expressed in a growth (A in Eq. 30) and a non-growth (B in Eq. 30) associated term (Table 9).

Table 9. Values for the growth- (A) and the non-growth (B) associated term in Eq. 30 of specific substrate uptake rate in the biofilm for K. pneumoniae, P. aeruginosa and binary population.

		K. pneumoniae	P. aeruginosa	binary population
(A)	($g.g^{-1}$)	16.30 ± 1.07	0.10 ± 0.60	6.61 ± 0.10
(B)	($g.g^{-1}h^{-1}$)	0.41 ± 0.76[1]	0.25 ± 0.191	0.20 ± 0.07[1]

[1] Values for the intercept are different from zero at the 5% level of significance.

Biofilm Cell and Product Yield Coefficients

Y_{MS} and Y_{PS} can now be calculated from Eq. 30 (Table 10).

Figure 22. Biofilm specific substrate uptake rate vs. biofilm specific cellular growth rate for K. pneumoniae. Continuous line is regression model (R^2=0.72).

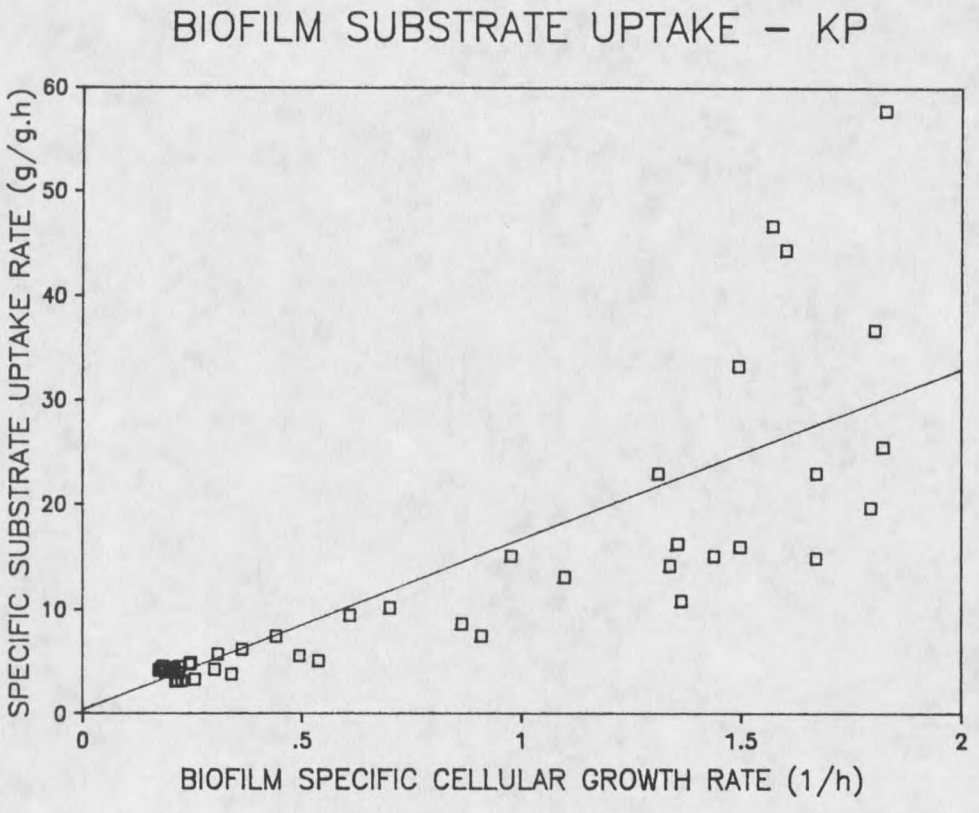

Figure 23. Biofilm specific substrate uptake rate vs. biofilm specific cellular growth rate for P. aeruginosa. Continuous line is regression model (R^2=0.57).

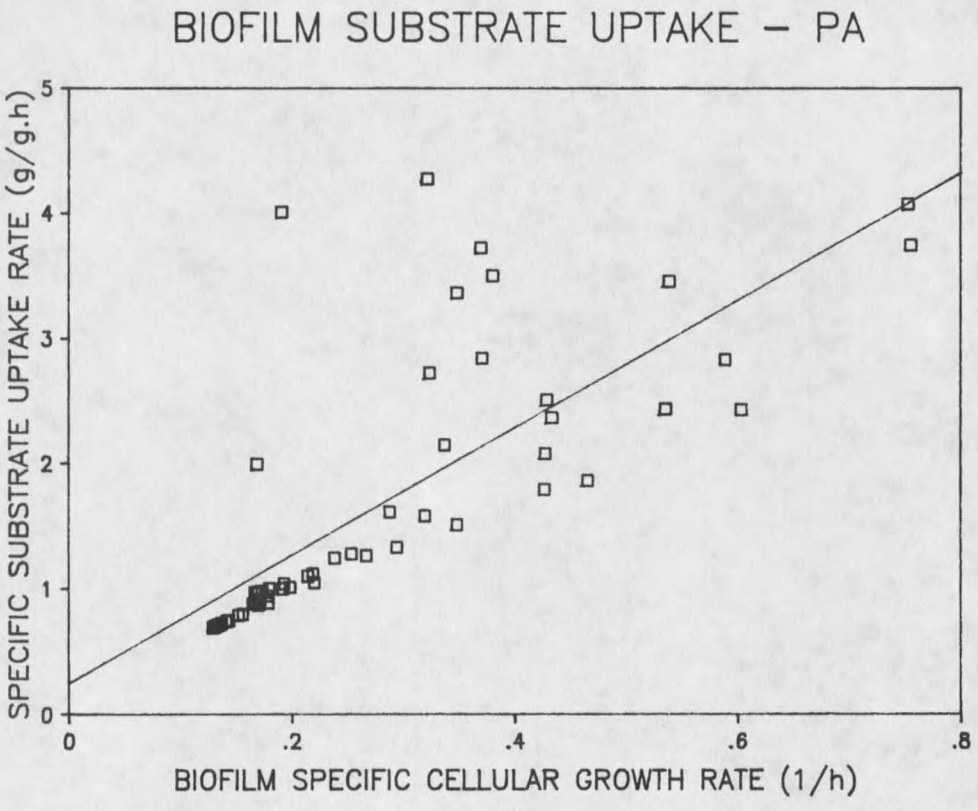

Figure 24. Biofilm specific substrate uptake rate vs. biofilm specific cellular growth rate for binary population. Continuous line is regression model (R^2=0.98).

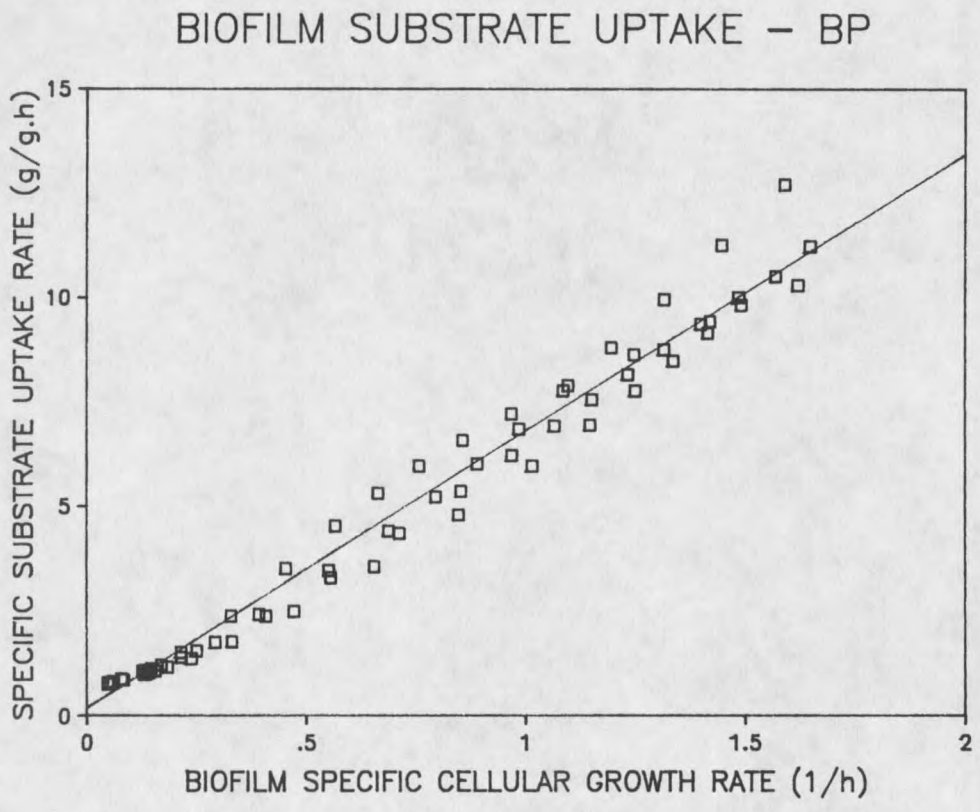

Table 10. Yield coefficients Y_{MS} and Y_{PS} in the biofilm for K. pneumoniae, P. aeruginosa and binary population.

	K. pneumoniae	P. aeruginosa	binary population
Y_{MS} $(g.g^{-1})$	0.08 ± 0.04	0.24 ± 0.06	0.22 ± 0.05
Y_{PS} $(g.g^{-1})$	0.48 ± 0.90	0.41 ± 0.41	0.38 ± 0.43

Biofilm Glucose-Oxygen Stoichiometric Ratio

The ratio of oxygen consumed and glucose consumed (Ω_S) can be evaluated by comparing the specific uptake rates of oxygen and glucose. The specific glucose uptake rate is given by Eq. 31. The specific oxygen uptake rate can be derived from Eq A-4 (Appendix A) by assuming liquid phase activity negligible, defining r_O as

$$r_O = \frac{\mu_f}{Y_{MO}} + \frac{r_{Pf}}{Y_{PO}} \qquad (32)$$

and rearranging:

$$r_O = \frac{(D+k_c).(S_{Os}-S_{Ol}) - \frac{dS_{Ol}}{dt}}{S_{Mf}.\frac{A}{V}} \qquad (33)$$

Using linear regression of r_S versus r_O (Figures 25, 26 and 27 for K. pneumoniae, for P. aeruginosa and binary populations) allows the evaluation of the glucose-oxygen stoichiometric ratio. Table 11 summarizes results.

Figure 25. Biofilm specific glucose uptake rate vs. biofilm specific oxygen uptake rate for K. pneumoniae. Continuous line is regression model (R^2=0.93).

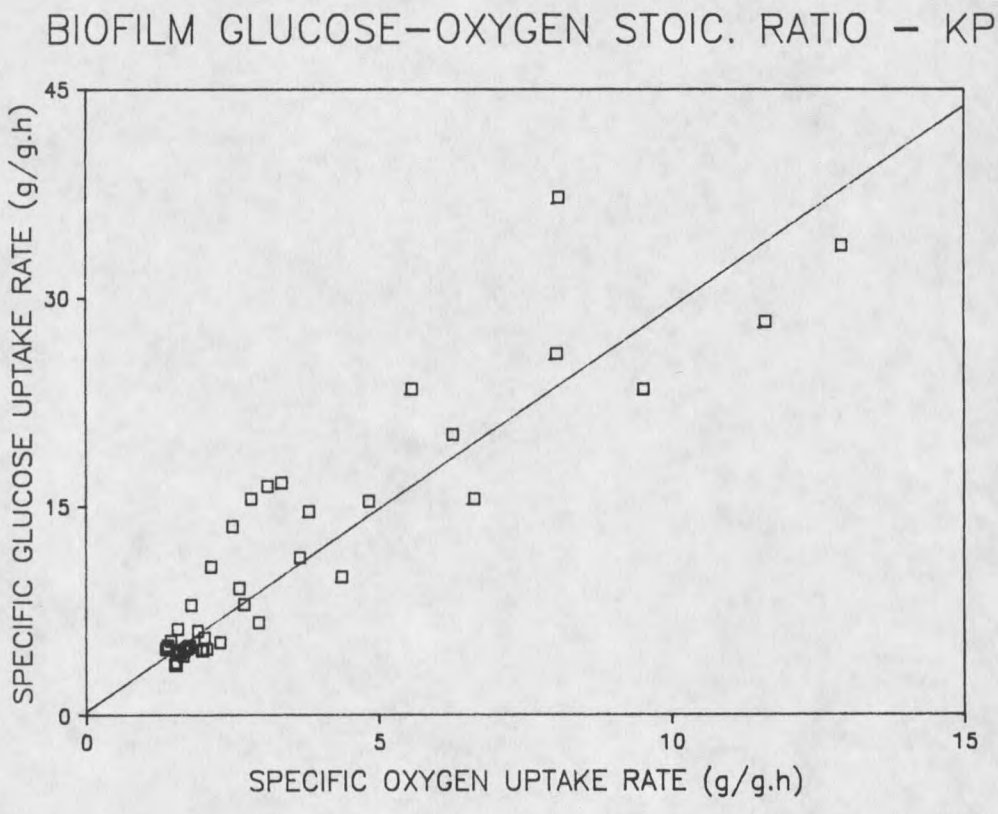

Figure 26. Biofilm specific glucose uptake rate vs. biofilm specific oxygen uptake rate for P. aeruginosa. Continuous line is regression model (R^2=0.34).

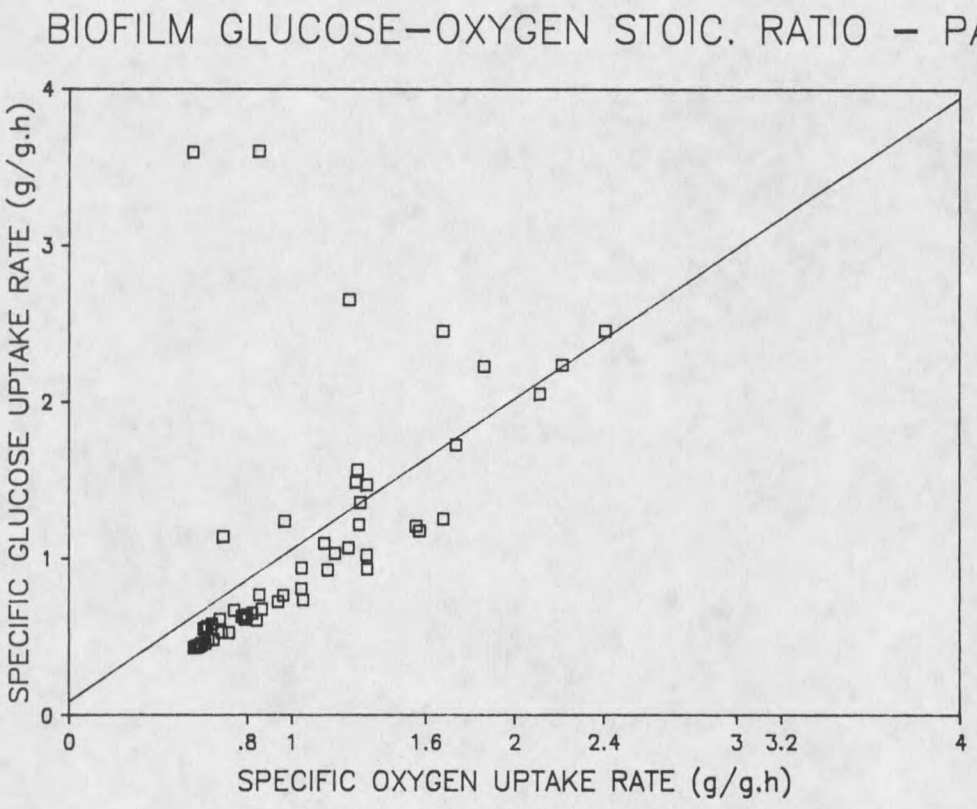

Figure 27. Biofilm specific glucose uptake rate vs. biofilm specific oxygen uptake rate for binary population. Continuous line is regression model (R^2=0.94).

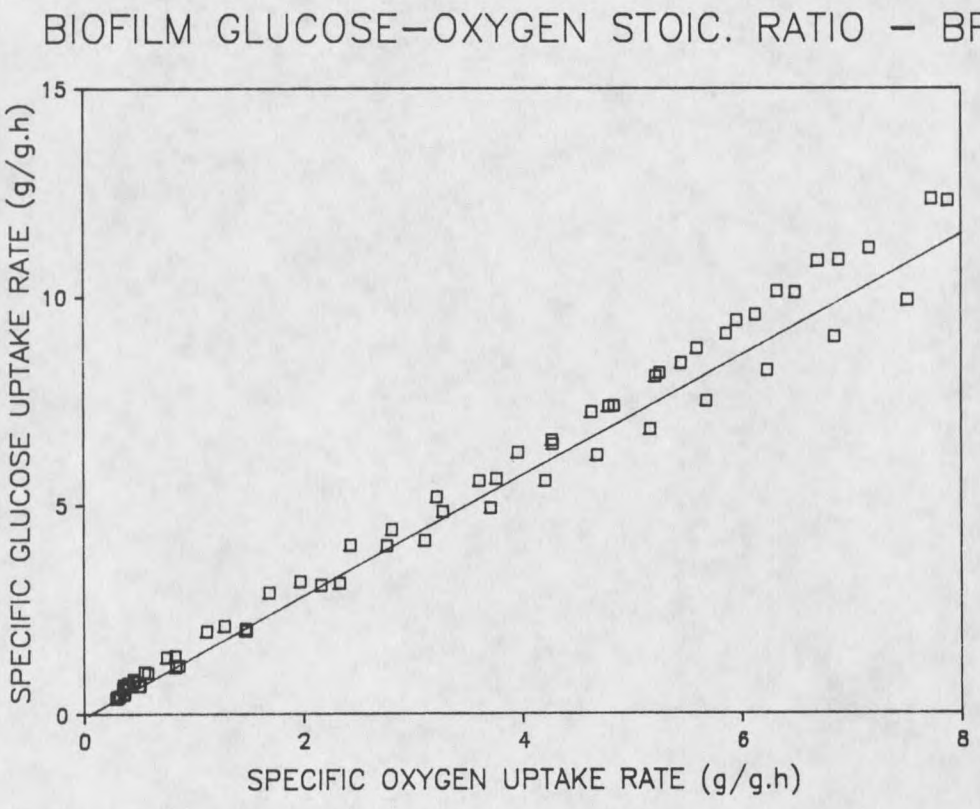

Table 11. Glucose-oxygen stoichiometric ratio in the biofilm for K. pneumoniae, P. aeruginosa and binary population.

		K. pneumoniae	P. aeruginosa	binary population
Ω_S	$(g.g^{-1})$	2.90 ± 0.08	0.96 ± 0.18	1.46 ± 0.04
I	$(g.g^{-1}h^{-1})$	0.33 ± 0.37[1]	0.07 ± 0.20[1]	0.19 ± 0.13[1]

[1] The intercepts (I) are different from zero at the 5% level of significance.

Biofilm Thickness

Biofilm thickness was determined by measuring thickness at 8 locations on the biofilm slide. The mean value for the 8 data points represents the average biofilm thickness at that point and time. The variation in values is indicative of the roughness of the biofilm. Individual measuring points per sampling time and time smoothed curves (LOGIT, 1986) through the means of the points and through the means + or - the standard deviation have been combined for K. pneumoniae, P. aeruginosa and binary population (Figures 28, 29 and 30).

Individual measuring points for K. pneumoniae cover a wide range of thicknesses, indicative of a rough biofilm surface. This contrasts with the P. aeruginosa biofilm where the range of thicknesses, especially past the 100 hours mark, is relatively narrow. The binary population biofilm is relatively smooth in the period around 100 hours and widens after that. Comparison of the variation in biofilm thickness is facilitated (Figure 31) by contrasting the relative mean biofilm thickness and standard deviation at steady state for the three populations.

Figure 28. Progression of biofilm thickness for K. pneumoniae. Continuous line represents time smoothed means and means plus or minus the standard deviation of the means.

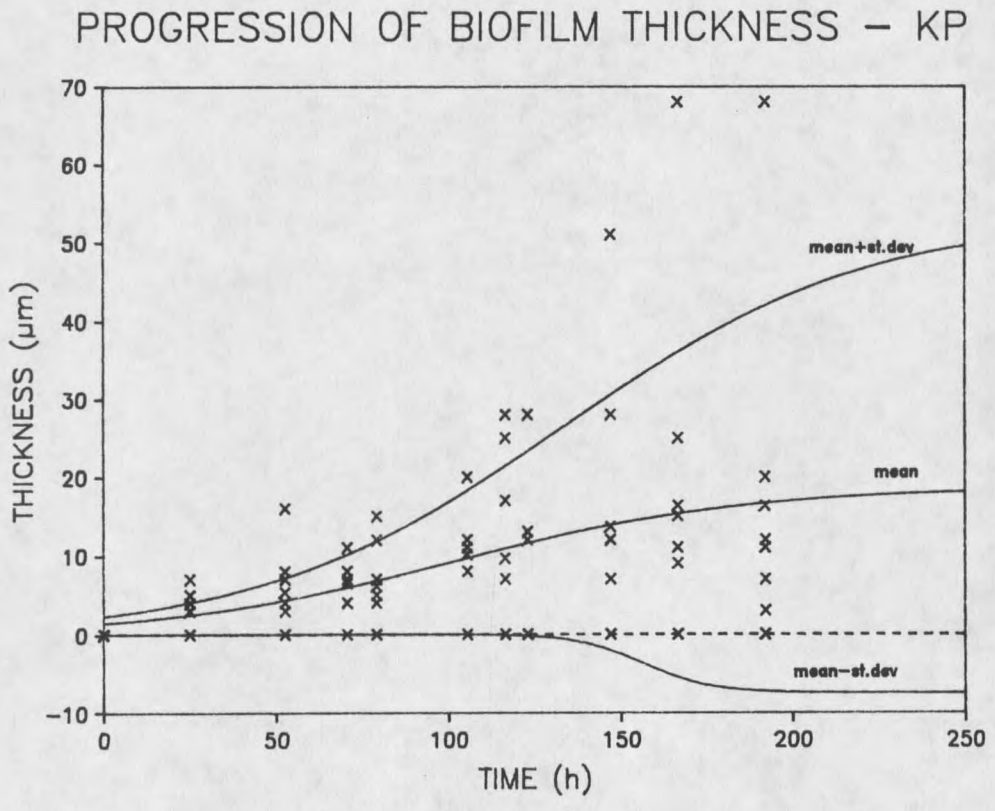

Figure 29. Progression of biofilm thickness for P. aeruginosa. Continuous line represents time smoothed means and means plus or minus the standard deviation of the means.

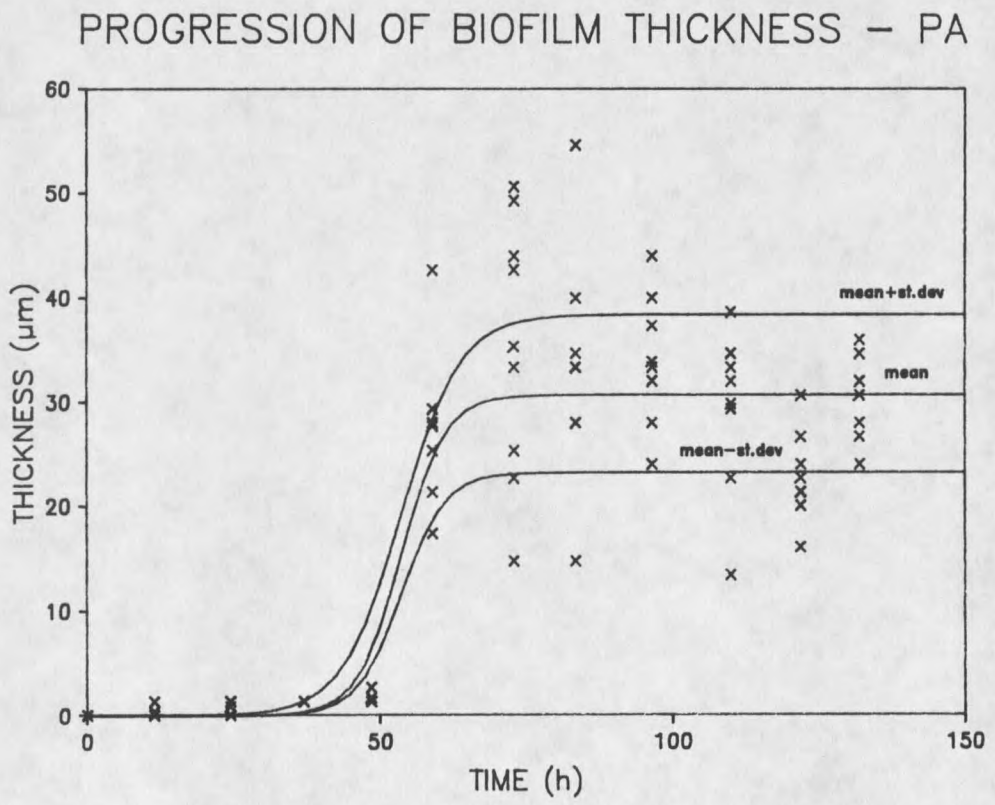

Figure 30. Progression of biofilm thickness for binary population. Continuous line represents time smoothed means and means plus or minus the standard deviation of the means.

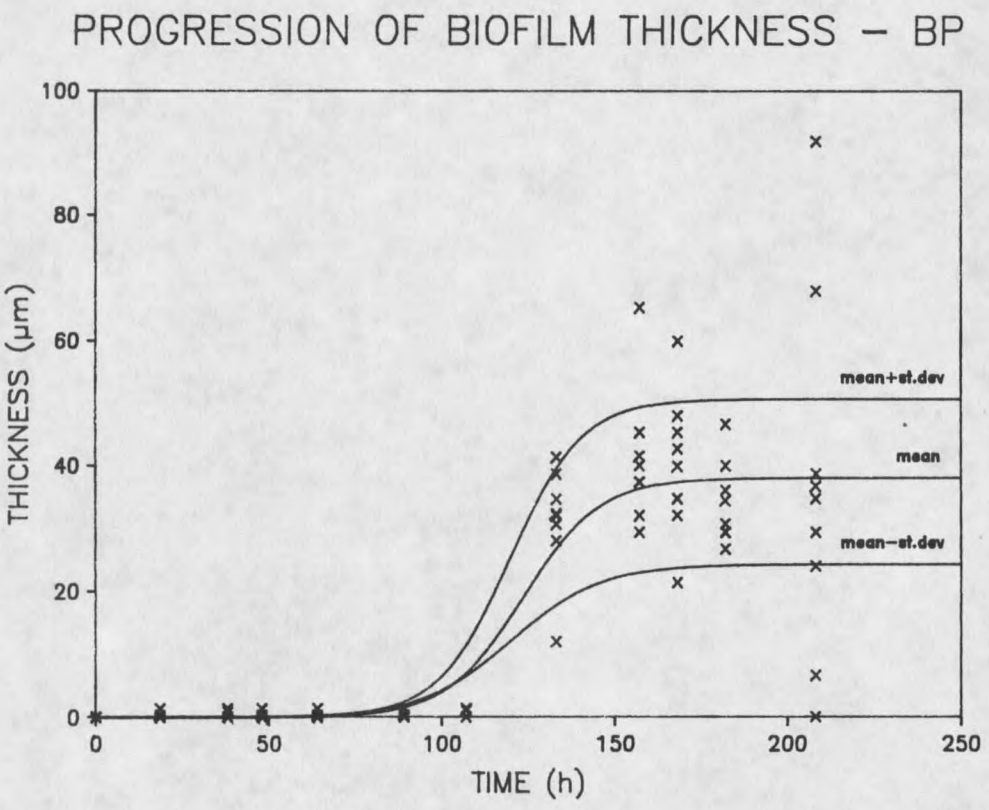

Figure 31. Comparison of relative thickness of steady state biofilms of K. pneumoniae, P. aeruginosa and binary population.

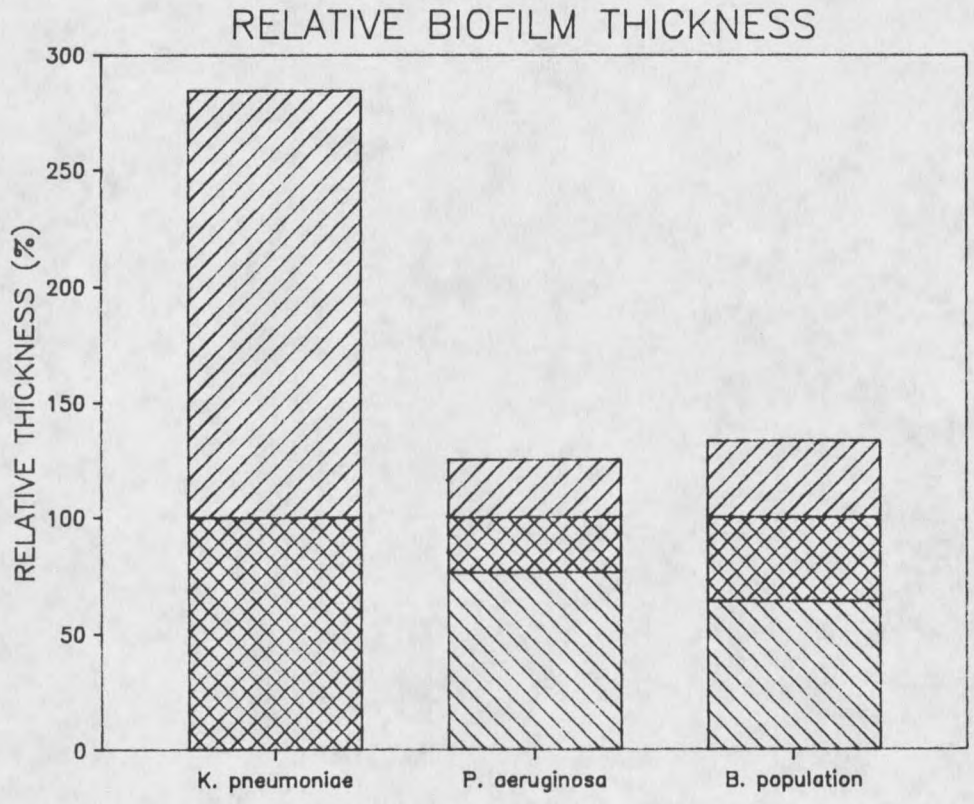

The extent of accumulation, the length of the period preceding accumulation and the rate at which accumulation takes place are compared in terms of biofilm thickness in Figure 32. K. pneumoniae accumulates to a lesser extent than P. aeruginosa (approx. 15 vs. 30 μm at steady state) or the binary population (approx. 40 μm). Biofilm accumulation for K. pneumoniae starts in a very early stage of the experiment relative to accumulation for P. aeruginosa (starting at 50 hours) and the binary population (starting at 100 hours). The last two have clearly distinguishable periods in which no accumulation takes place. The maximum rate of increase of biofilm thickness for P. aeruginosa (8 $\mu m.h^{-1}$) is twice as high as that of the binary population (4 $\mu m.h^{-1}$). Maximum rate of thickness increase for K. pneumoniae is only a fraction of that (0.4 $\mu m.h^{-1}$).

Species Distribution

Distribution of K. pneumoniae and P. aeruginosa in the biofilm is of importance in the evaluation of properties of the binary population biofilm. Data points and time smoothed curves (LOGIT, 1986) for the means and the means + or - the standard deviation of K. pneumoniae cell mass fraction in the biofilm have been combined (Figure 33). Starting the experiments with both species having the same cell mass, steady state conditions show that K. pneumoniae cell mass occupies 26% of the biofilm.

Photographic Illustrations

Transmission Electron Micrographs were made from the binary population. In addition, Nomarsky Photo Micrographs (NPM's) were made of the dried surface of the K. pneumoniae, P. aeruginosa and the binary population biofilm. The differences between the three populations in

Figure 32. Comparison of biofilm thickness models for K. pneumoniae, P. aeruginosa and binary population. Note differences between duration of 'lag phase', slope of 'log phase' and level of 'plateau'.

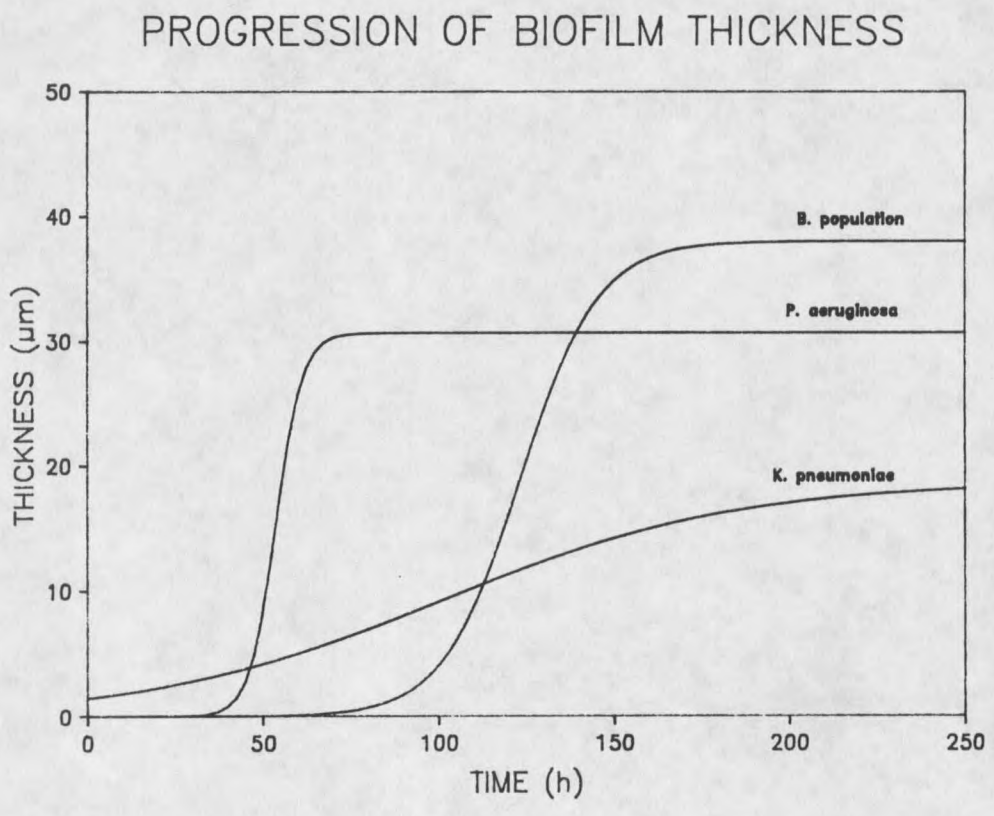

Figure 33. Progression of biofilm cell mass ratio for binary population biofilms. Continuous line represents time smoothed means and means plus or minus the standard deviation of the means.

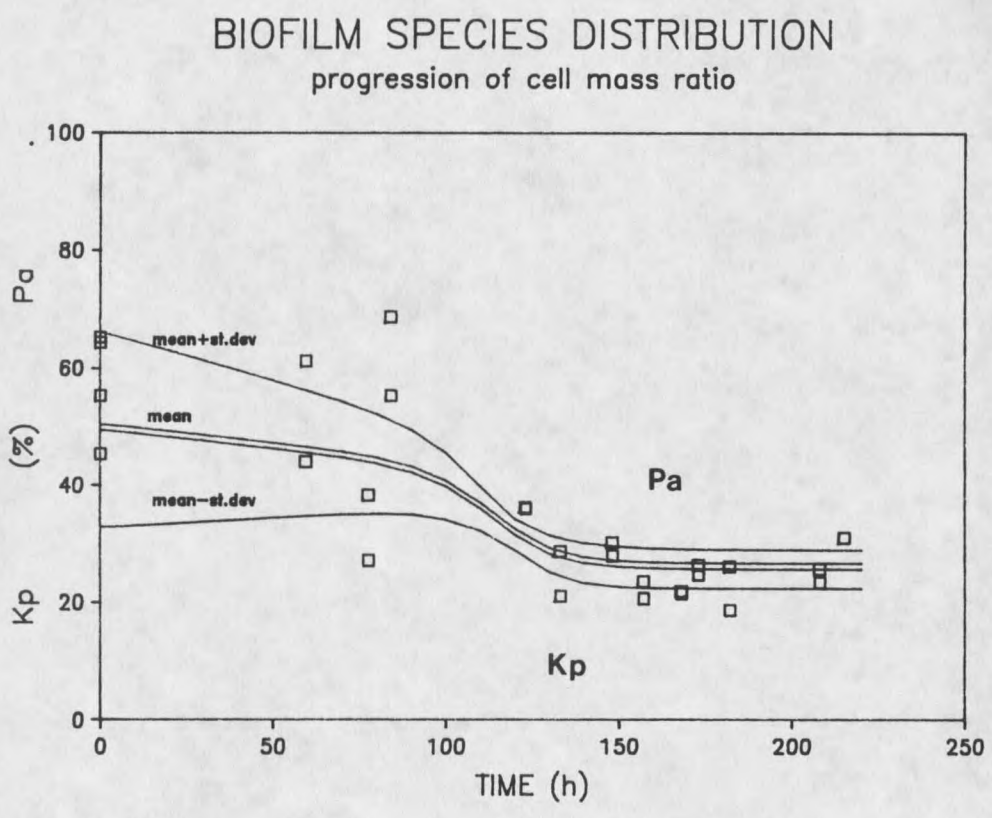

biofilm accumulation can be illustrated with Figures 34 through 40.

K. pneumoniae accumulates in little, well spaced clusters of cells (Figure 34) which rapidly multiply. Cells appear to stay together enlarging the cluster. This results in expansion parallel and perpendicular to the substratum (Figure 35) resulting in the formation of "microtowers" (Figure 36) which can reach a height of 60 μm and more with bare substratum between the towers. Only gradually is the space between clusters being filled up.

P. aeruginosa colonizes the substratum in a relatively equal distribution (Figure 37). Cells grow and multiply, reducing intercellular distance. Gradually, a smooth biofilm builds up (Figure 38).

A binary population biofilm consists of a relatively smooth surface with peaks sticking out (Figure 39). Gradually, surface roughness increases (Figure 40).

Figure 34. Accumulation of K. pneumoniae on polycarbonate substratum (Nomarsky microscopic picture, taken 50 hours after inoculation, magnification 625 times).

Figure 35. Accumulation of K. pneumoniae on polycarbonate substratum (Nomarsky microscopic picture, taken 100 hours after inoculation, magnification 500 times). Cell clusters expand but uncolonized space between clusters still exists.

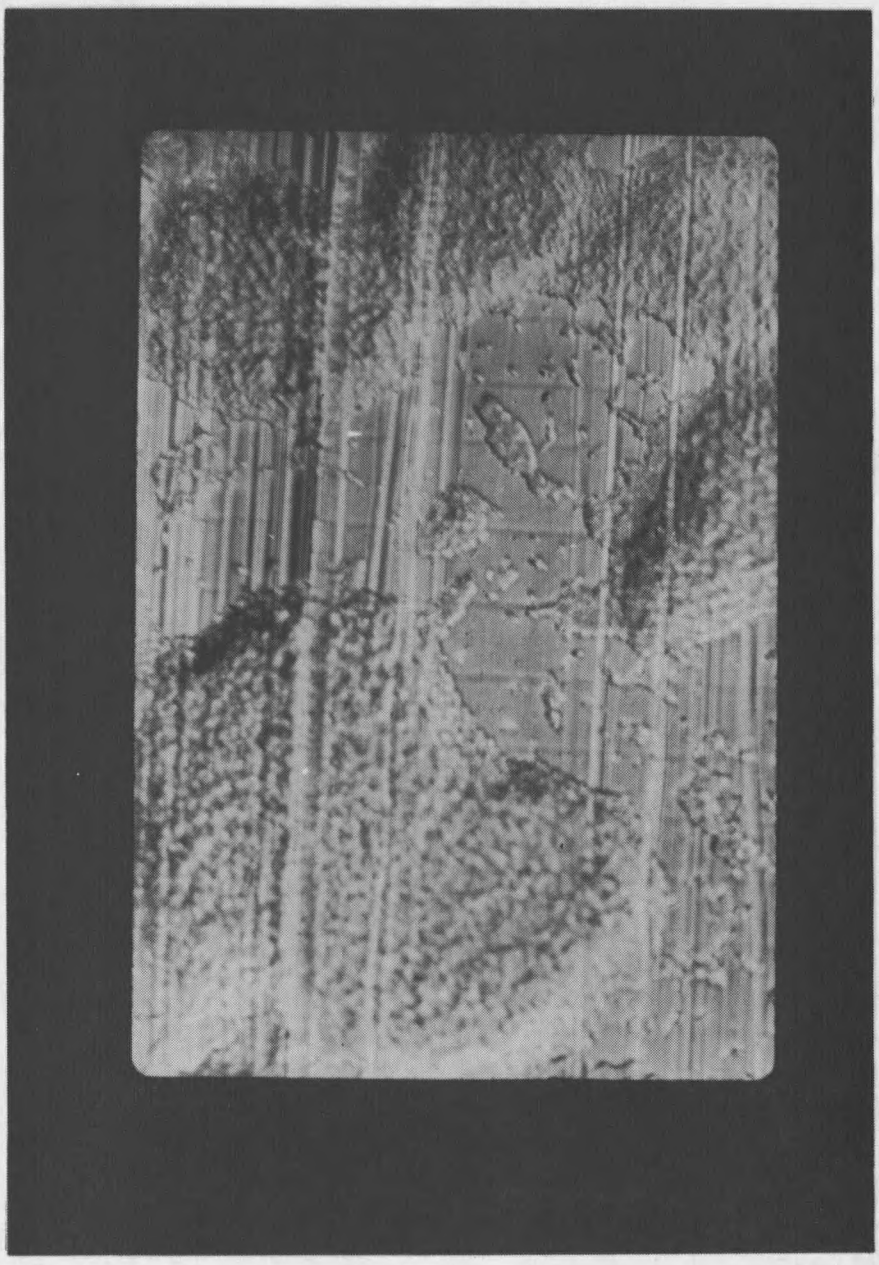

Figure 36. Accumulation of K. pneumoniae on polycarbonate substratum (Nomarsky microscopic picture, taken 125 hours after inoculation, magnification 625 times). The colored rings indicate different elevations.

Figure 37. Accumulation of P. aeruginosa on polycarbonate substratum (Nomarsky microscopic picture, taken 50 hours after inoculation, magnification 625 times). Cells are more or less regularly distributed at the substratum.

Figure 38. Accumulation of *P. aeruginosa* on polycarbonate substratum (Nomarsky microscopic picture, taken 65 hours after inoculation, magnification 625 times). Mono layer of closely packed cells.

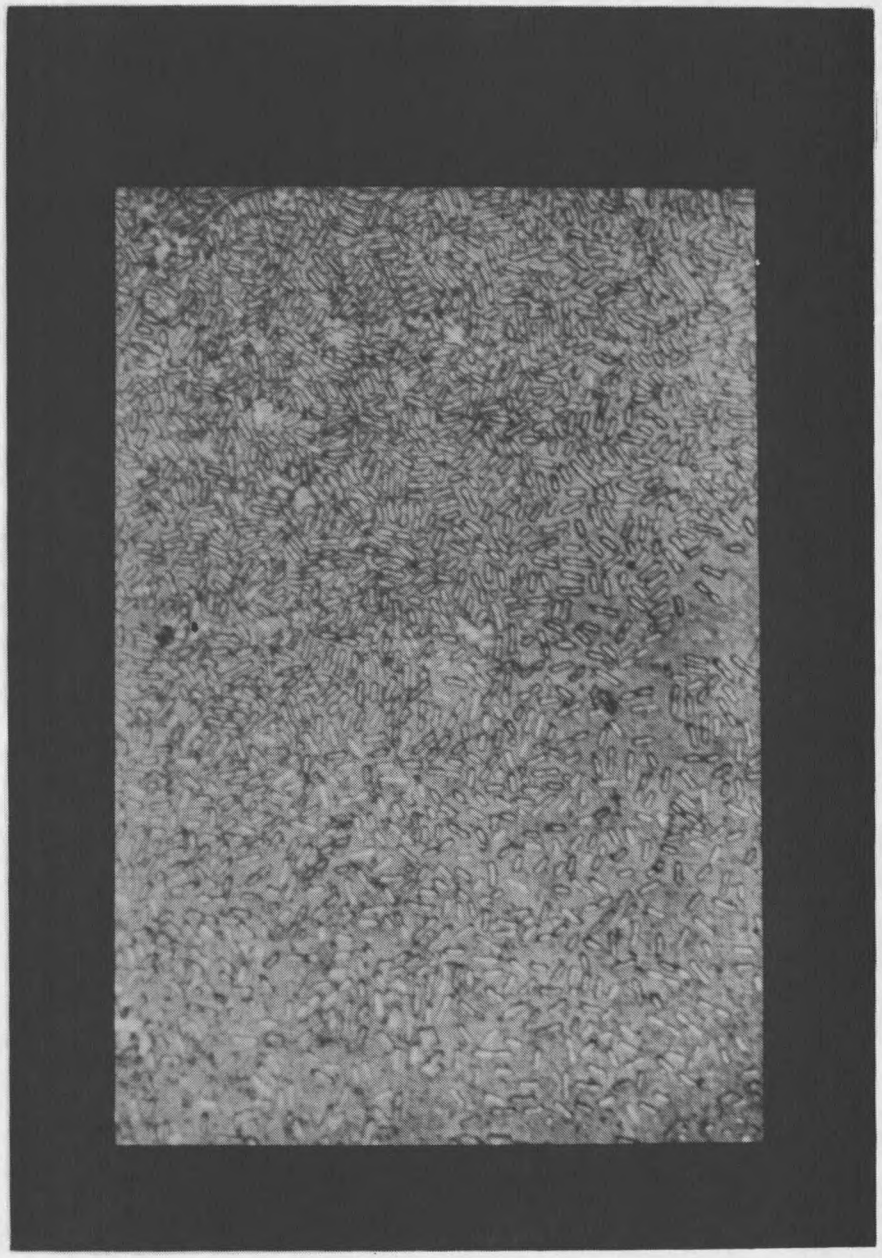

Figure 39. Accumulation of a binary population biofilm on polycarbonate substratum (Nomarsky microscopic picture, taken 123 hours after inoculation, magnification 500 times). A relatively smooth surface with peaks sticking out.

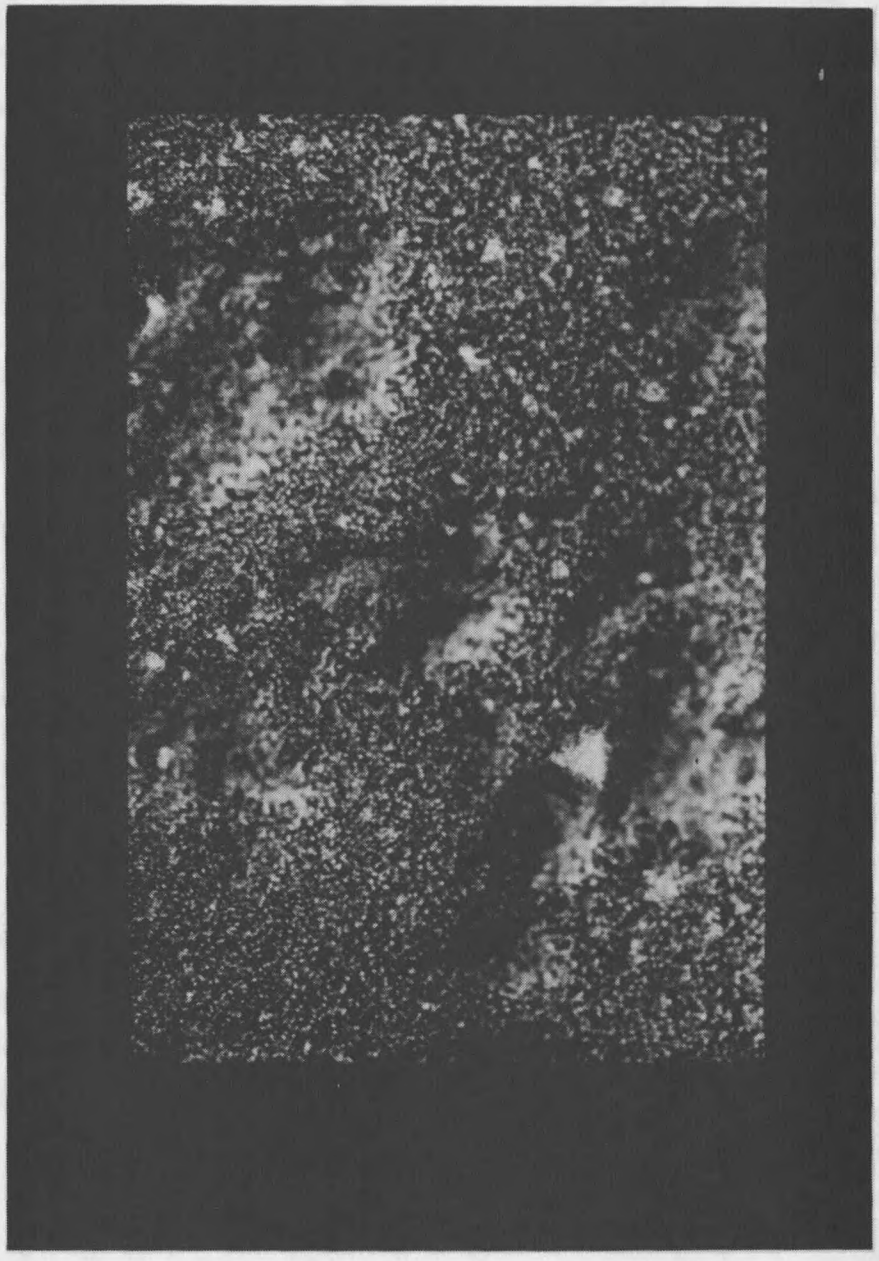

Figure 40. Accumulation of a binary population biofilm on polycarbonate substratum (Nomarsky microscopic picture, taken 208 hours after inoculation, magnification 500 times). Surface roughness increases when binary population biofilms get older.

DISCUSSION

Processes in mixed population biofilms of K. pneumoniae and P. aeruginosa have been observed. The results will be discussed in terms of observations in mono population biofilms.

Product Formation

Both K. pneumoniae and P. aeruginosa form extracellular products. Erbing et al. (1976) found that K. pneumoniae produced D-glucose, L-fucose, D-glucuronic and pyruvic acid in equal ratios. Neijssel and Tempest (1975) emphasized the effect of the limiting nutrient in the excretion of products. Yields of polysaccharide of almost 40% simultaneous with yields of various acids (appr. 30%) occurred with chemostat growth under nitrogen limitation. The range of products and the relative quantities in which they are produced is determined by the qualitative and quantitative composition of the nutrient solution (Neijssel and Tempest, 1975). P. aeruginosa produces extracellular material in both batch and chemostat growth. In chemostat studies, P. aeruginosa produced mannuronic and guluronic acid in a ratio of 4:1 (Mian et al. 1978).

Growth- and non-growth associated product formation coefficients are summarized in Table 12. Nutrient limitation other than carbon, appears to increase the specific rate of growth-associated product formation (Mian et al. 1978). In this study, specific rates of product formation by both K. pneumoniae and P. aeruginosa are a function of the specific cellular growth rate, both in suspended and in attached growth (Figure 41).

Figure 41. Comparison of product kinetic models for mono population biofilms of K. pneumoniae and P. aeruginosa and of binary population biofilms. Single lines represent attached, double lines represent suspended growth models.

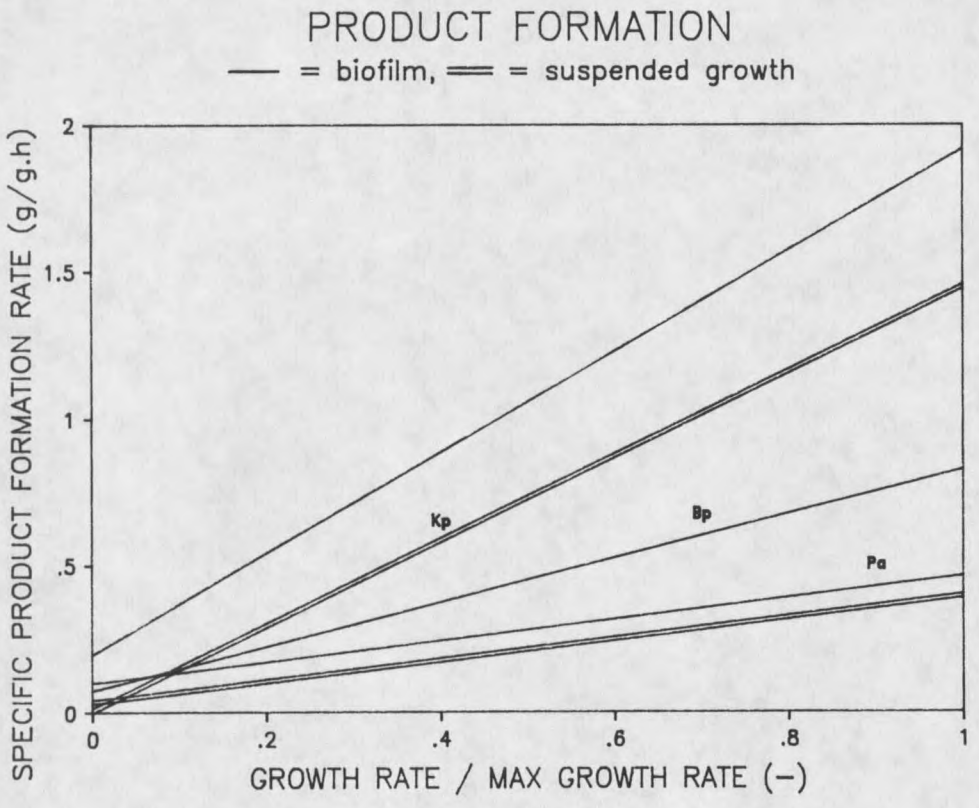

Product Formation in Suspension

Specific product formation rates in suspension for K. pneumoniae (C-limited) are considerably higher than those measured by Trulear (1983) for P. aeruginosa (C-limited) but in the same range as those measured by Mian et al. (1978) for P. aeruginosa (N-limited). Neijssel and Tempest (1975), studying chemostat growth of K. aerogenes under carbon, sulphate, ammonia or phosphate limitations for four different carbon sources (glucose, glycerol, mannitol and lactate) found a wide range of specific product formation rates. Under carbon limitation, the specific product formation rate of K. aerogenes (product concentration determined according to Herbert et al., 1971) was zero, but excess carbon (carbon in excess of the stoichiometric required amount) invariably resulted in excretion of 'overflow' metabolites. The specific growth-associated product formation coefficients for K. aerogenes grown in suspension on glucose under limitations other than carbon are in the range of 2.2 - 3.5 g product C.(g cell C)$^{-1}$ (Neijssel and Tempest (1975). Specific growth-associated product formation coefficients found in this research are 1.4 g product C.(g cell C)$^{-1}$ for suspended growth of K. pneumoniae (Table 12). This suggests that growth under non-carbon limitation could be responsible for the high specific product formation rates found in this research. Comparison of the glucose mineral salts medium used in this study for the growth of K. pneumoniae and P. aeruginosa with the one used by Neijssel and Tempest (1975, specified by Evans et al., 1970, Appendix E) indicates that the glucose mineral salts medium contains an excess of all nutrients but one, cobalt, required at 0.2 $\mu g.m^{-3}$. Batch and chemostat experiments were conducted using distilled water, the Rototorque experiments used specially treated water (Bozeman city tap water followed by softening and

reverse osmosis). Both water sources may contain cobalt in insufficient concentrations, leaving growth media cobalt limited.

It should be noted that in this study and in the study by Trulear (1983) product formation in suspension included soluble product and product adsorbed to the cell while Neijssel and Tempest (1975) measured only soluble product.

Product Formation in the Biofilm

For the binary population biofilms, the growth-associated product formation coefficient is 0.75 ± 0.02 g product C.(g cell C)$^{-1}$. Based on a biofilm composed of 74% P. aeruginosa and 26% K. pneumoniae and assuming no interaction between species, the specific growth-associated product formation coefficient in the binary population biofilm can be predicted by summing the products of the growth-associated product formation coefficient for each species found in the mono population biofilm experiments and the cell mass fraction in the binary population biofilm. The specific growth-associated product formation coefficient, based on species distribution is 0.72 ± 0.11 g product C.(g cell C)$^{-1}$. At the 5% level of significance, there is no difference between the growth-associated product formation coefficient in the binary population biofilm determined experimentally and that predicted on the basis of species composition. Consequently, in the binary population biofilm, the specific product formation rate of K. pneumoniae or P. aeruginosa appears not to be affected by the presence of the other species.

Table 12. Summary of specific growth- (k_{Pg}) and non-growth- (k_{Pn}) associated product formation coefficients.

Reactor	k_{Pg} ($g.g^{-1}$)	k_{Pn} ($g.g^{-1}h^{-1}$)	S_{Si} (g $C.m^{-3}$)	Reference
P. aeruginosa				
chemost.	3.29±0.53[1]	0.13±0.04	8000	Mian et al. (1978)
chemost.	0.36±0.44	0.03±0.10[2]	36.8±2.3	Trulear (1983)
biofilm[3]	1.0 ±0.86	0.25±0.36	3.8±1.1	Trulear (1983)
biofilm	0.01±0.14	0.09±0.04	9.6±0.1	Trulear (1983)
biofilm	0.02±0.13	0.01±0.03	16.7±0.3	Trulear (1983)
biofilm	0.36±0.07	0.10±0.07	9.8±0.3	This study
K. pneumoniae				
chemost.	0 [4]	-	10,000	Neijssel and
chemost.	2.2 [5]	-	30,000	Tempest (1975)
chemost.	3.4 [6]	-	30,000	Neijssel and
chemost.	3.5 [7]	-	30,000	Tempest (1975)
chemost.	1.44±0.06 [8]	0	36.4±0.9	This study
chemost.	2.29±0.17 [9]	0	36.4±0.9	This study
biofilm	1.72±0.11	0.20±0.04	10.8±0.1	This study
Binary population				
biofilm	0.75±0.03	0.08±.0.025	8.9/20.5	This study

1 Mean ± standard deviation, except if otherwise noted.

2 Not different from zero at 5% level of significance.

3 Expressed as mean ± 95% confidence interval.

4, 5, 6, 7 Determined under respectively carbon, sulphate, ammonia and phosphate limitations.

8 Product material in suspension (not attached to cells).

9 The sum of product material in suspension and attached to cells.

Glucose-Oxygen Stoichiometric Ratio

Conversion of glucose into biomass can be described stoichiometrically as follows (Busch, 1971):

$$C_6H_{12}O_6 + 2.46O_2 + 0.71NH_3 \rightarrow 0.71C_5H_7NO_2 + 2.46CO_2 + 0.46H_2O \quad (34)$$

Thus, 1 g of oxygen is required for the biochemical conversion of 0.92 g (= Y_{SO}) of glucose carbon into biomass. This equation was derived for the removal of glucose by an undefined mixed population in a batch reactor system, which was initially substrate saturated. Turakhia (1986) found Y_{SO} = 0.89 ± 0.06 g glucose carbon consumed.(g oxygen consumed)$^{-1}$ for batch growth of P. aeruginosa and Y_{SO} = 0.92 ± 0.02 g glucose carbon consumed.(g oxygen consumed)$^{-1}$ for P. aeruginosa biofilms. This study found a glucose-oxygen stoichiometric ratio of 0.96 ± 0.18 g glucose carbon consumed.(g oxygen consumed)$^{-1}$ for P. aeruginosa biofilm experiments (Figure 42), well in agreement with the theoretical value (Eq. 34) and the other investigations.

Glucose-Oxygen Stoichiometric Ratio for K. pneumoniae

In this study Y_{SO} = 0.90 ± 0.01 g glucose carbon consumed.(g oxygen consumed)$^{-1}$ in C-limited batch growth of K. pneumoniae. In contrast, Neijssel and Tempest (1975), studying chemostat growth of K. aerogenes, reported Y_{SO} varied between 2.8 (C-limited) and 4.5 (N-limited) g glucose carbon consumed.(g oxygen consumed)$^{-1}$ (Figure 43).

For the mono population biofilms of K. pneumoniae, Y_{SO} = 2.90 ± 0.08 g glucose carbon consumed.(g oxygen consumed)$^{-1}$ (Figure 42). This is the same value as found by

Figure 42. Comparison of glucose-oxygen stoichiometric ratio for mono population biofilms of K. pneumoniae and P. aeruginosa and for binary population biofilms. Curved lines represent 95% confidence interval.

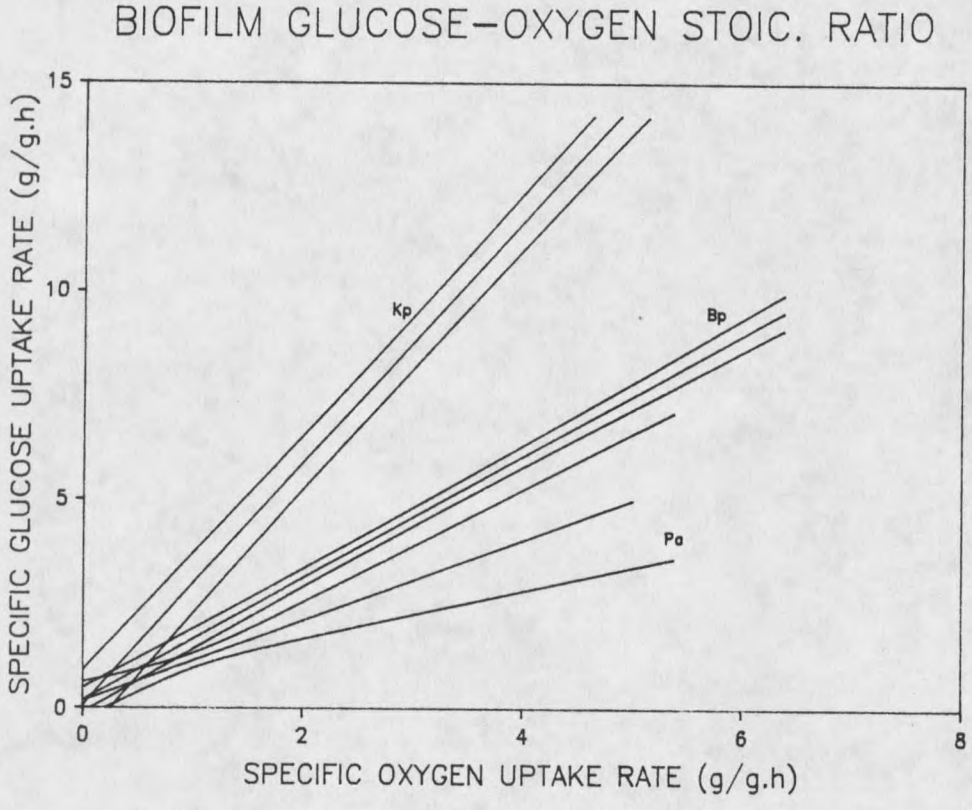

Figure 43. Glucose-oxygen stoichiometric ratio for K. aerogenes grown in a chemostat under various nutrient limitations (Neijssel and Tempest, 1975). Bars indicate Y_{SO} for growth on glucose carbon under resp. phosphorus, nitrogen, sulfur and carbon limitation.

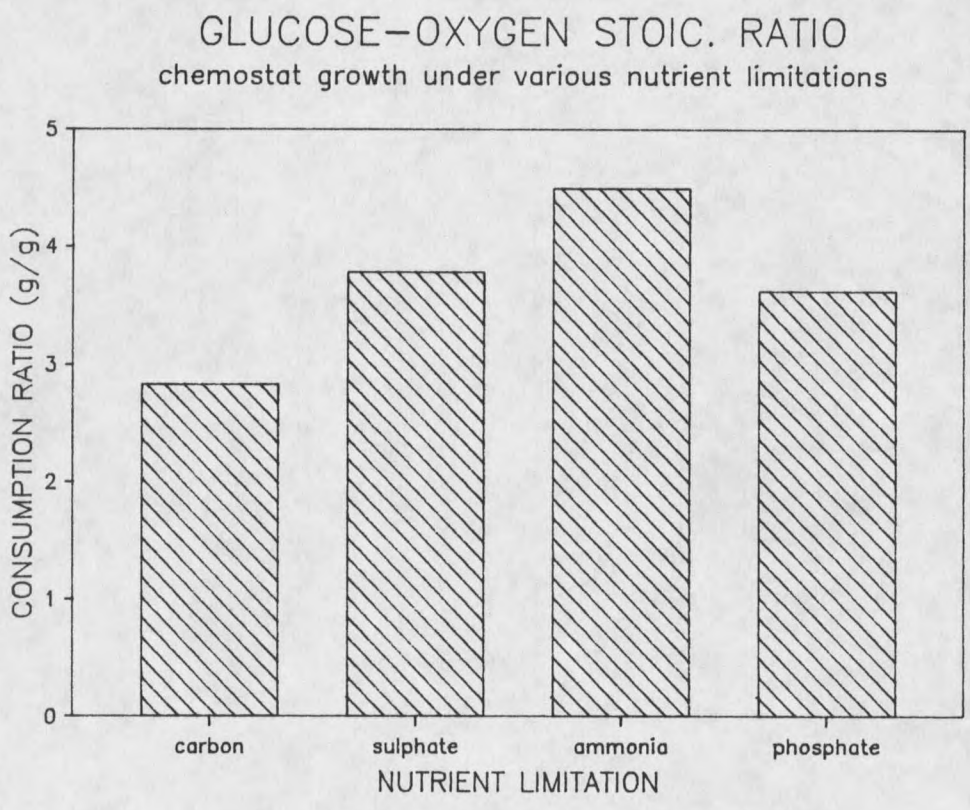

Neijssel and Tempest (1975) for suspended growth of K. aerogenes under glucose carbon limitation.

Y_{SO} for Binary Population Biofilms

The glucose-oxygen stoichiometric ratio, Y_{SO}, in the binary population biofilm can be determined by summing the products of the glucose-oxygen stoichiometric ratio for each species found in the mono population biofilms and the cell mass fraction in the binary population biofilm. This results in a glucose-oxygen stoichiometric ratio, based on species distribution, of 1.47 ± 0.20 g glucose carbon consumed.(g oxygen consumed)$^{-1}$. Y_{SO} determined experimentally equals 1.44 ± 0.02 g glucose carbon consumed.(g oxygen consumed)$^{-1}$. At the 5% level of significance, there is no difference between Y_{SO} in the binary population biofilm determined experimentally and Y_{SO} determined on the basis of species composition. Consequently, in the binary population biofilm, the glucose-oxygen stoichiometric ratio of K. pneumoniae or P. aeruginosa appears not to be affected by the presence of the other species.

Binary population biofilm experiments were conducted at substrate carbon concentrations of 10 and 20 g C.m^{-3}. The extent of biofilm accumulation for the 20 g C.m^{-3} experiments is approximately twice the accumulation for the 10 g C.m^{-3}. Nevertheless, the glucose-oxygen stoichiometric ratio is the same for both experiments. This implies that both the glucose consumption rate and the oxygen consumption rate for the 20 g C.m^{-3} is double that rate for the 10 g C.m^{-3} experiments. This is consistent with the observation of DO concentrations in the effluent of the 20 g C.m^{-3} experiments which are lower than those in the 10 g C.m^{-3}. Lower DO concentrations in the effluent mean lower DO concentrations in the biofilm. Hence, anaerobic

microenvironments in the aggregates may more likely occur in the 20 g $C.m^{-3}$ than in the 10 g $C.m^{-3}$ experiments. As mono population biofilm experiments of K. pneumoniae may be substrate diffusion limited, diffusion limitation is also likely to occur in the binary population biofilm experiments. Consequently, microbial activity of both species is reduced in the deeper layers of the biofilm. This is consistent with the observation that the species distribution in the 20 g $C.m^{-3}$ experiments was not different from the one in the 10 g $C.m^{-3}$.

Influence of Diffusional Resistance on Y_{SO}

The difference in glucose-oxygen stoichiometric ratio between P. aeruginosa and K. pneumoniae may be related to the respective physiology of the organisms or to differences in diffusional resistance within the respective biofilms. K. pneumoniae has a high specific growth rate and a high specific rate of product formation. In addition, this organism is non-motile. As a result, K. pneumoniae biofilm cells aggregate to a high degree relative to P. aeruginosa. The aggregates can reach a height of 60 μm or more with a base width of approximately 30 μm. Cohesive forces between the cells in the aggregates are sufficient to resist the hydraulic pressure at the aggregates in a direction parallel to the substratum. Extracellular product (Figure 44) and cell density may impose a considerable diffusional resistance for transport of dissolved compounds to and from the biofilm cells. A comparison of the effectiveness factor for diffusion of substrate into

Figure 44. Transmission Electron Micrograph of a microbial cell in a binary population biofilm. Comparison with a TEM of K. pneumoniae by Roth (1977) indicates that this picture probably shows a K. pneumoniae cell.

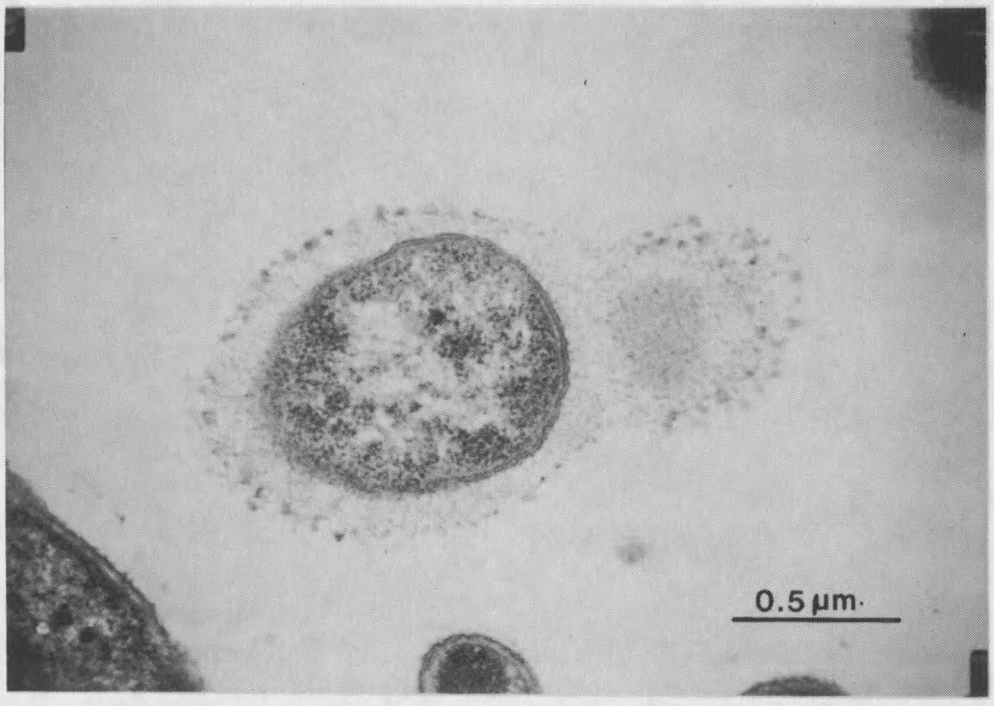

biofilms which differ only in the microbial species that has accumulated. K. pneumoniae and P. aeruginosa (Appendix K), suggests that this is indeed the case (Table 13).

Table 13. Relation between steady state biofilm thickness and diffusion effectiveness factor ϵ for K. pneumoniae and P. aeruginosa.

thickness (μm)	K. pneumoniae	P. aeruginosa
10	64%	-
15	45%	92%
30	23%	78%

Resistance against substrate diffusion in a biofilm of 30 μm thickness, built up of K. pneumoniae, is 3 times as high as in a similar biofilm of P. aeruginosa. Diffusional resistance in aggregates of K. pneumoniae with a base width of 30 μm or more is, therefore, certain to affect substrate concentrations in the core of the aggregate significantly.

Factors affecting Initial Adsorption

Initial adsorption at the substratum is considerably different for the two organisms (Figures 34 through 40). Various factors influence adsorption including the nature of the wetted substratum (material of construction and surface roughness), the deposition of conditioning film, and the characteristics of the adsorbing cells.

Cell suspensions pumped into the Rototorque were observed microscopically for aggregation as this could affect both the rate of particle diffusion through the laminar sublayer and subsequent adsorption and growth. Aggregation was not observed for either K. pneumoniae and P. aeruginosa.

The substratum in the biofilm studies was polycarbonate, a hydrophobic material. The cell wall of both organisms is hydrophobic at neutral pH (Buchanan and Gibbons, 1974) but the extent of hydrophobicity may be different. Also, both organisms produce product, some of which is immediately released into the environment, possibly more so for P. aeruginosa than for K. pneumoniae. Observation of the dried substratum showed that in the early stages of the experiment polymeric material was deposited in mono population biofilm experiments of both organisms. Drying of the substratum resulted in cracking (microscopically observed) of the P. aeruginosa deposit but not of that of K. pneumoniae. This could indicate that the former deposit is thicker than the latter. Product deposited at the substratum or adsorbed to the cell may obscure the effects of hydrophobicity and, therefore, may affect cell adsorption.

Specific Cellular Glucose Uptake Ratio

The specific cellular glucose uptake rate is proportional to the specific cellular growth rate. The proportionality coefficient (Π_S) is the inverse of the observed yield coefficient Y_{obs} and can be approximated by:

$$\Pi_S = \frac{1}{Y_{obs}} = \frac{1}{Y_{MS}} + \frac{k_{Pg}}{Y_{PS}} \qquad (35)$$

Specific cellular glucose uptake ratios (Π_S) for suspended and attached growth of K. pneumoniae and P. aeruginosa are summarized in Table 14. Π_{Sf} for P. aeruginosa biofilms in this study and in Trulear's (1983) are not different at the 5% level of significance. But Π_{Sl} for the suspended growth is significantly different from the one for biofilms. Also, Π_S for K. pneumoniae is considerably higher than for P. aeruginosa (Figure 45). The main reason for Π_S being higher in attached than in suspended growth is that the cellular growth yield is higher in suspension than in biofilms (Eq. 35). This is true for both K. pneumoniae and for P. aeruginosa (Table 15).

Figure 45. Comparison of biofilm specific glucose uptake rate models for K. pneumoniae, P. aeruginosa and binary population biofilms. Curved lines represent 95% confidence interval.

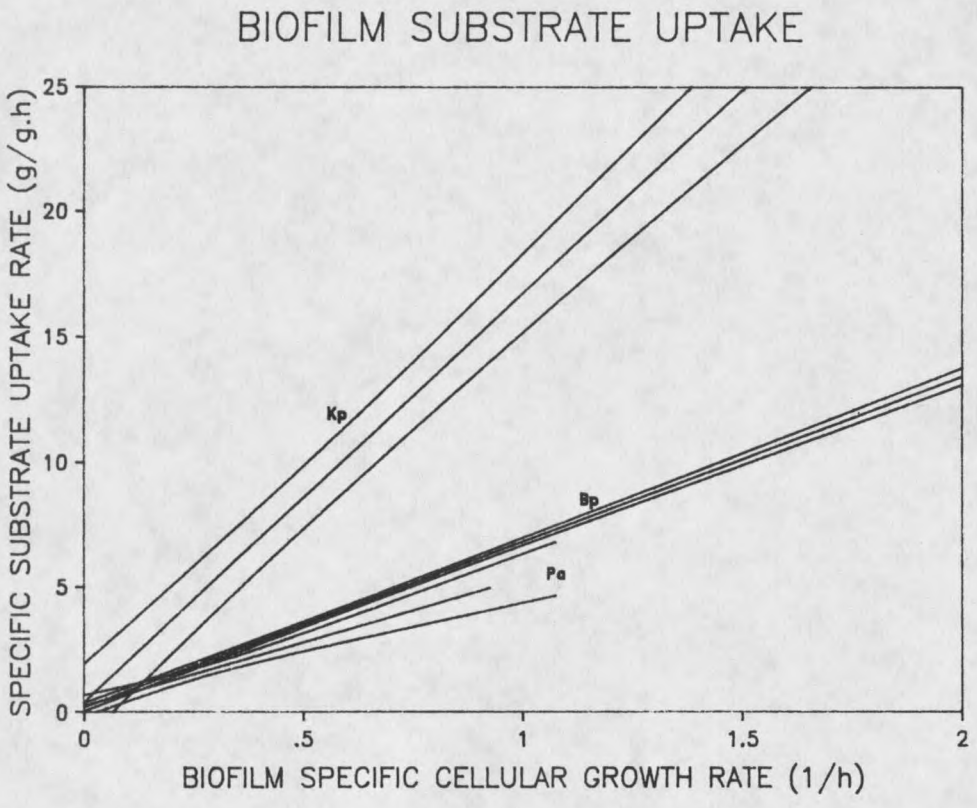

Table 14. Comparison of specific cellular glucose uptake ratios (Ω_S) for K. pneumoniae and P. aeruginosa in suspension and in biofilm.

	suspended growth	attached growth	Reference
P. aeruginosa	3.5 ± 0.2[1]	4.6 ± 1.3	Trulear (1983)
		5.1 ± 0.6	This study
K. pneumoniae	11.6 ± 1.7	16.3 ± 1.1	This study

1 Mean ± standard deviation.

Table 15. Comparison of growth and product yield coefficients for K. pneumoniae and P. aeruginosa.

	suspended growth	attached growth	Reference
P. aeruginosa			
Y_{MS} ($g.g^{-1}$)	0.36±0.38[1]	0.25±0.13[2]	Trulear (1983)
Y_{PS} ($g.g^{-1}$)	0.50±1.94	0.43±0.72[2]	
Y_{MS} ($g.g^{-1}$)		0.24±0.06	This study
Y_{PS} ($g.g^{-1}$)		0.41±0.41	
K. pneumoniae			
Y_{MS} ($g.g^{-1}$)	0.19±0.05	0.08±0.04	This study
Y_{PS} ($g.g^{-1}$)	0.27±0.04	0.48±0.90	

1 Mean ± standard deviation.

2 Mean of three values for Y_{MS} and Y_{PS}.

For the binary population biofilm, the experimental $\cap_{Sf}$ is 6.6 ± 0.1 glucose carbon.(g cell C)$^{-1}$ (Figure 45). Based on cell mass distribution and assuming no interaction, the theoretical $\cap_{Sf}$ equals 8.0 ± 1.0 glucose carbon.(g cell C)$^{-1}$. The values for the theoretical and the experimental specific cellular glucose uptake ratio are different at the 5% level of significance. An experimental $\cap_{Sf}$ which is less than $\cap_{Sf}$ determined on the basis of species distribution would suggest species interaction. This contradicts earlier findings. Therefore, the specific cellular glucose uptake ratio, $\cap_{Sf}$, for the binary population biofilm appears to be underestimated.

Growth Kinetics

Suspended Growth

The saturation kinetic (Monod) model describes the relation between substrate concentration and microbial growth rate in suspended growth systems. Robinson et al. (1984) report growth kinetic coefficients for *P. aeruginosa*: μ_{max} = 0.40 ± 0.01 h^{-1} and K_S = 2.0 ± 0.5 g glucose carbon.m^{-3}. In this study, growth kinetic coefficients for *K. pneumoniae* were: μ_{max} = 2.0 ± 0.3 h^{-1} and K_S = 1.4 ± 0.5 g glucose carbon.m^{-3}. A comparison of chemostat growth kinetics (Figure 46) emphasizes the large difference in maximum specific growth rate between *K. pneumoniae* and *P. aeruginosa*.

Mono Population Biofilms

Saturation kinetics also apply to *P. aeruginosa* biofilms (Bakke et al., 1984). In this study, biofilm specific cellular growth rate of mono population biofilms of *P. aeruginosa* can also be described by the saturation equation (Figure 47).

The dependence of biofilm specific cellular growth rate on substrate concentration in *K. pneumoniae* biofilms can not be described by saturation kinetics (Figure 48). The observed behavior may be explained by diffusion limitation (Appendix K). Specific cellular growth rate for *K. pneumoniae* biofilm decreases rapidly during substratum colonization. The rapid formation of "microtowers" by this organism results in diffusional resistance so that most of the nutrients are consumed by the cells in the outer layer of the aggregate. Consequently, only a fraction of the cells is exposed to the liquid phase substrate concentration. The majority of the cells 'see' a much lower

Figure 46. Comparison of growth kinetic models for K. pneumoniae and P. aeruginosa.

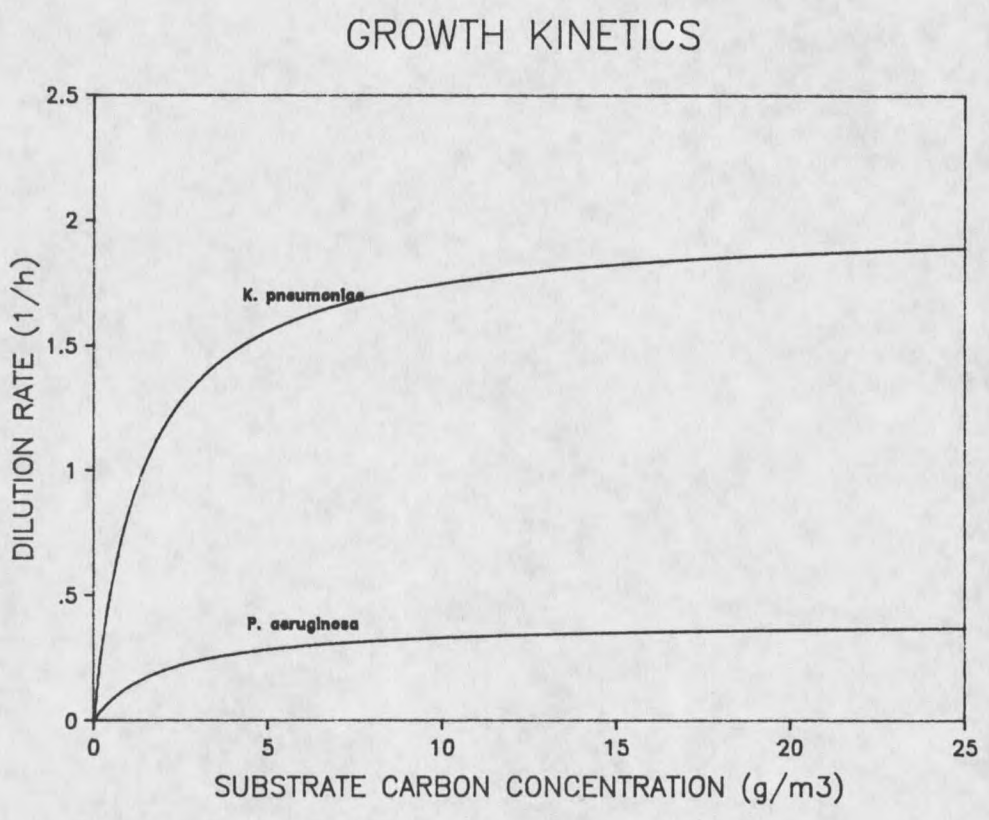

Figure 47. Comparison of specific cellular growth rate vs. substrate concentration for P. aeruginosa mono population biofilms (data points) with specific cellular growth rate vs. substrate concentration for suspended growth (continuous line) for P. aeruginosa.

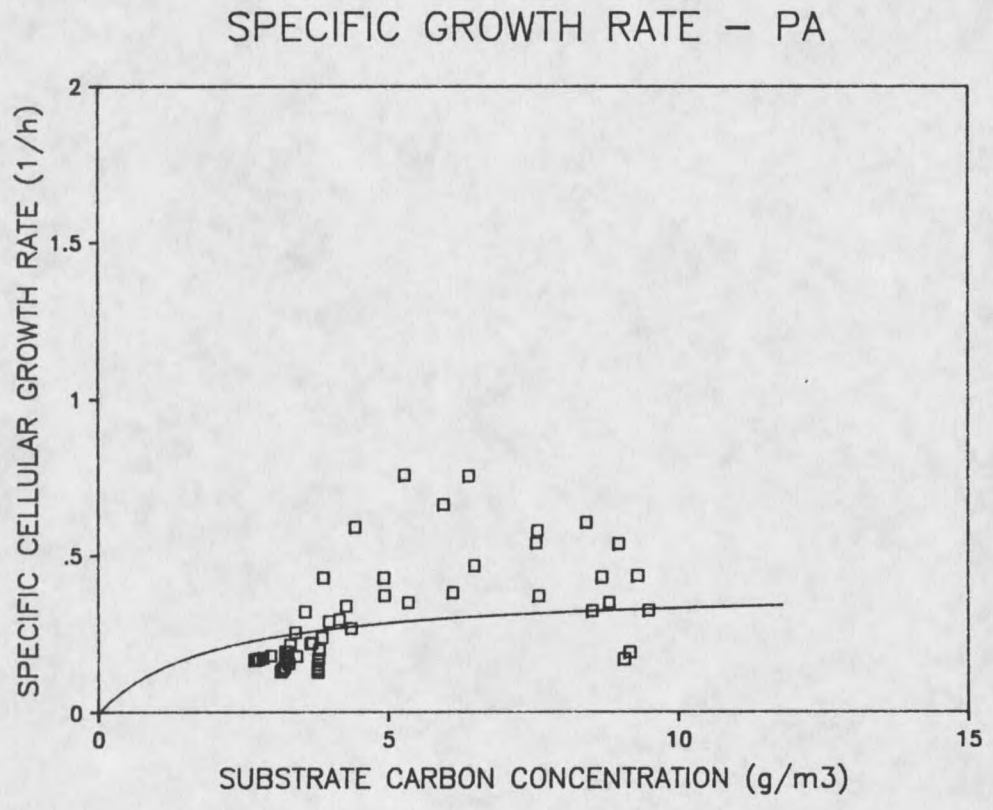

Figure 48. Comparison of specific cellular growth rate vs. substrate concentration for K. pneumoniae mono population biofilms (data points) with specific cellular growth rate vs. substrate concentration for suspended growth (continuous line) for K. pneumoniae.

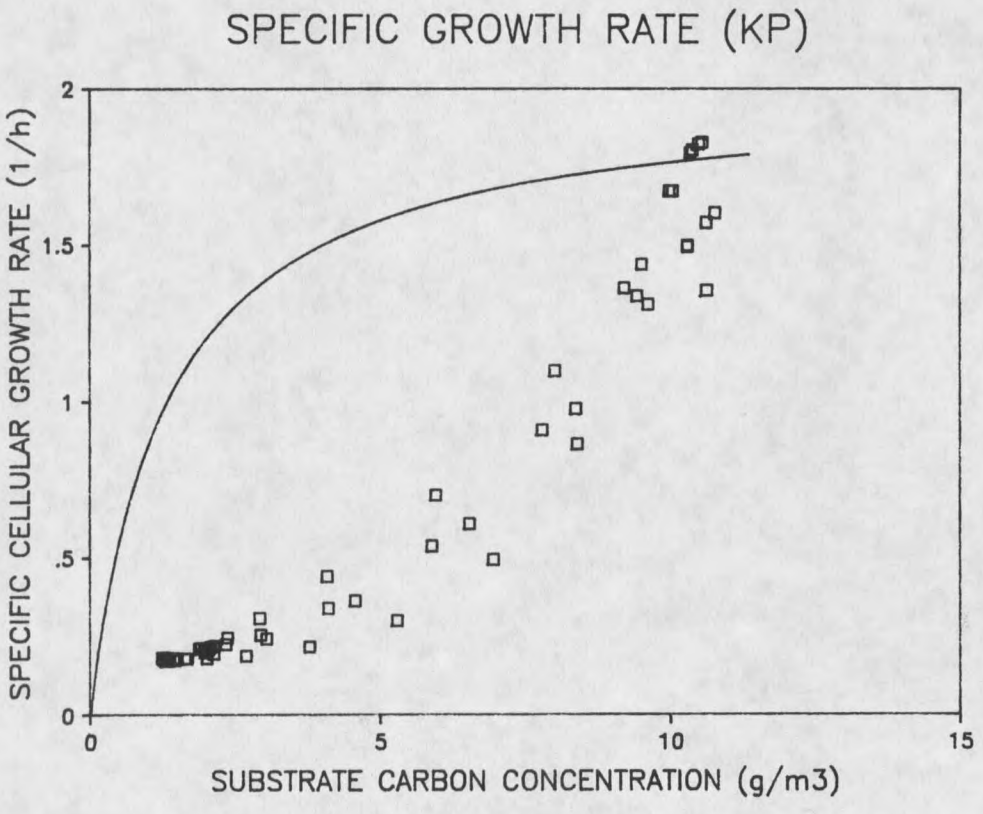

substrate concentration and exhibit a much lower specific cellular growth rate. With the increase of both size and number of aggregates, the specific biofilm cellular growth rate decreases with the bulk liquid substrate concentration.

Binary Population Biofilms

Progression of biofilm specific cellular growth rate vs. reactor substrate concentration for a binary population biofilm (Figure 49) shows that at high reactor substrate concentration biofilm specific cellular growth rate decreases almost independently of reactor substrate concentration. With accumulation of biofilm, the decrease of specific cellular growth rate follows the decrease in liquid phase substrate concentration. The change of specific biofilm cellular growth rate from almost independent, to proportional to liquid phase substrate concentration coincides with the change in biofilm species composition, ie., from a biofilm composed of equal amounts of cell mass of each species to a biofilm dominated by P. aeruginosa.

Comparison with the corresponding figure for K. pneumoniae (Figure 48) suggests that biofilm specific cellular growth rate is initially determined by cells in the rapidly growing aggregates of K. pneumoniae. When biofilm cell mass becomes dominated by P. aeruginosa, the specific biofilm cellular growth rate reflects the combined effect of growth of a P. aeruginosa biofilm and growth of a K. pneumoniae biofilm.

It should be noted that K. pneumoniae is the dominant species in the effluent. This finding is in agreement with the fact that, due to its high specific cellular growth rate, K. pneumoniae will rapidly produce cells in the

Figure 49. Comparison of specific cellular growth rate vs. substrate concentration for binary population biofilms (squares for 10 g $C.m^{-3}$ experiments, crosses for 20 g $C.m^{-3}$ experiments) with specific cellular growth rate vs. substrate concentration for suspended growth of *K. pneumoniae* and *P. aeruginosa*.

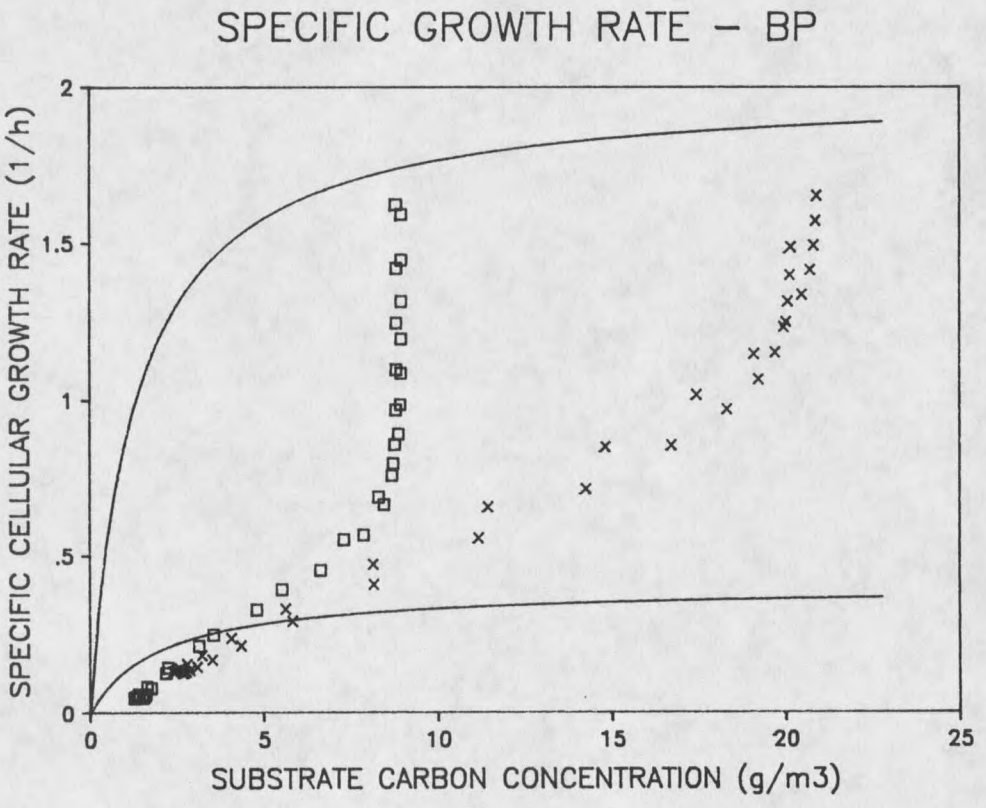

biofilm. Consequently, more K. pneumoniae cells will detach. P. aeruginosa nevertheless dominates the biofilm cell mass because the rate of (re-)attachment is higher for P. aeruginosa than for K. pneumoniae (Appendix J). In addition, forces between cells which permit the formation of aggregates, suggest that detachment of K. pneumoniae is likely to occur in "lumps" of cells rather than by single cells. Diffusion of these lumps through the laminar sublayer is considerably less than diffusion of individual cells of K. pneumoniae. Therefore, reattachment of K. pneumoniae is small compared to reattachment of P. aeruginosa.

Accumulation of a Binary Population Biofilm: a Conceptual Description

This section is intended to provide an overall picture of the sequence of events in initial adsorption and subsequent accumulation of a binary population biofilm.

Binary population biofilm accumulation is the net result of the following events:

1. Transport to the substratum from the liquid phase through the laminar sublayer: K. pneumoniae is not motile, P. aeruginosa is a motile organism. Rate of transport of single cells of P. aeruginosa through the laminar sublayer could be as high as 250 times the rate of transport of K. pneumoniae cells. Assuming an equal number of cells of both species in the liquid phase, 250 times more cells of P. aeruginosa could reach the substratum as compared to K. pneumoniae cells.
2. Net adsorption (= adsorption to and desorption from the substratum): Probability of adsorption to the substratum is often related to extracellular product

formation (Marshall et al. 1971). After initial contact in which stage cells are assumed to remain at close proximity of the substratum only (reversible adsorption), cells either desorb or bridge the distance to the substratum by means of extracellular material (irreversible adsorption). The specific rate of product formation by K. pneumoniae is almost 5 times the specific rate of product formation by P. aeruginosa. Consequently, probability that K. pneumoniae will remain at the substratum could be almost 5 times that of P. aeruginosa.

Following desorption, cells of P. aeruginosa are 250 times as likely to return to the substratum as cells of K. pneumoniae.

3. Motility: Daughter cells of K. pneumoniae will remain close to the parent cells and form cellular aggregates which expand both horizontally and vertically (microtowers) resulting in a patchy structure. The relationship between motility, high specific product formation rate, and formation of aggregates has been related by Costerton et al. (1985) by proposing that 'daughter cells are trapped in a juxtaposition that results in the formation of microcolonies'. P. aeruginosa, a motile organism, has the ability to move over the substratum (Marshall, personal communication). P. aeruginosa will form a relatively smooth layer of cells (Figure 50).

4. Growth rate: Maximum specific growth rate of K. pneumoniae is 5 times the maximum specific growth rate of P. aeruginosa. Therefore, the mass of K. pneumoniae will increase as much as 5 times as fast as that of P. aeruginosa. However, the high specific growth rate together with the high specific rate of product

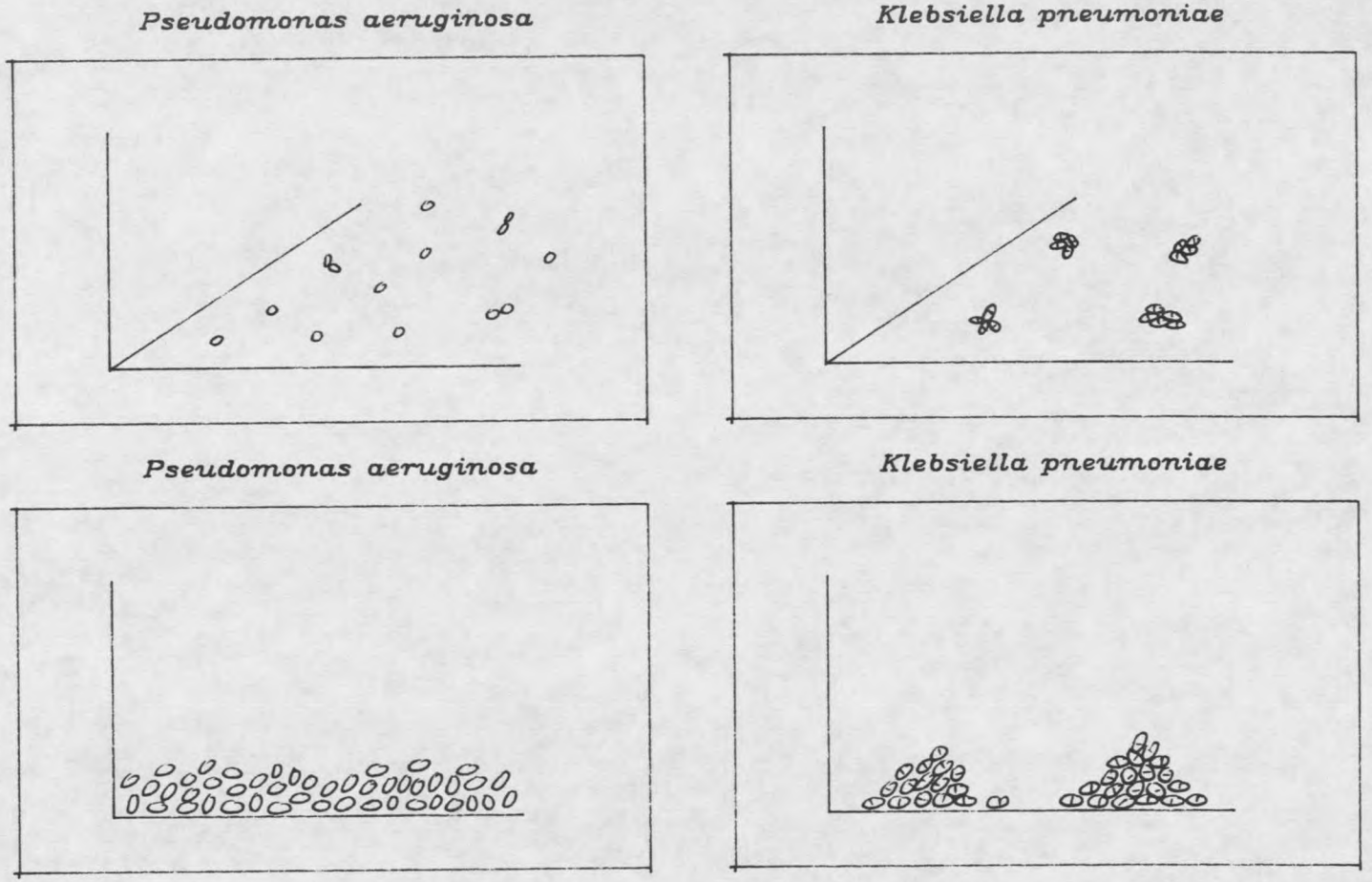

Figure 50. Schematic representation of accumulation of mono population biofilms of K. pneumoniae and P. aeruginosa.

formation may result in nutrient (oxygen, carbon) depletion in the core of the aggregate, significantly reducing (overall) biofilm specific cellular growth rate. With P. aeruginosa spreading out over the substratum, depletion of nutrients may occur only in a later stage of biofilm accumulation.

5. Detachment: Considering the adhesive cell-substratum and the cohesive cell-cell forces necessary to resist the hydraulic pressure at the aggregate in the flow system, detachment may occur in "lumps" rather than by single cells. The likelihood of lumps reattaching may be small since particle diffusion rate through the laminar sublayer is inversely proportional to particle diameter. Detachment might also occur when oxygen concentration in the core of the aggregate approaches zero. In fact, anaerobic conditions in the core environment may initiate detachment. Detachment of cells of P. aeruginosa has been shown to occur as lumps (sloughing) and as single cells (Bakke, 1986).

6. Accumulation: The two species form a biofilm, apparently unaware of the presence of the other species. K. pneumoniae forms aggregates in which a P. aeruginosa cell may become incorporated by attachment. P. aeruginosa forms a smooth layer of cells. In time, both species expand, P. aeruginosa taking up space between the aggregates, K. pneumoniae aggregates towering above the relatively smooth P. aeruginosa film. With the surrounding structural support of the P. aeruginosa biofilm, K. pneumoniae cell aggregates may develop to a greater height before detachment occurs than if this support were not present (Figure 51).

Summarizing, the accumulation of a binary population biofilm of K. pneumoniae and P. aeruginosa is the net

result of cellular transport, growth, product formation and motility properties. The proliferation of species in this binary population biofilm is, therefore, determined by the physiology of the species present.

Figure 51. Schematic representation of accumulation of a binary population biofilm consisting of K. pneumoniae and P. aeruginosa cells.

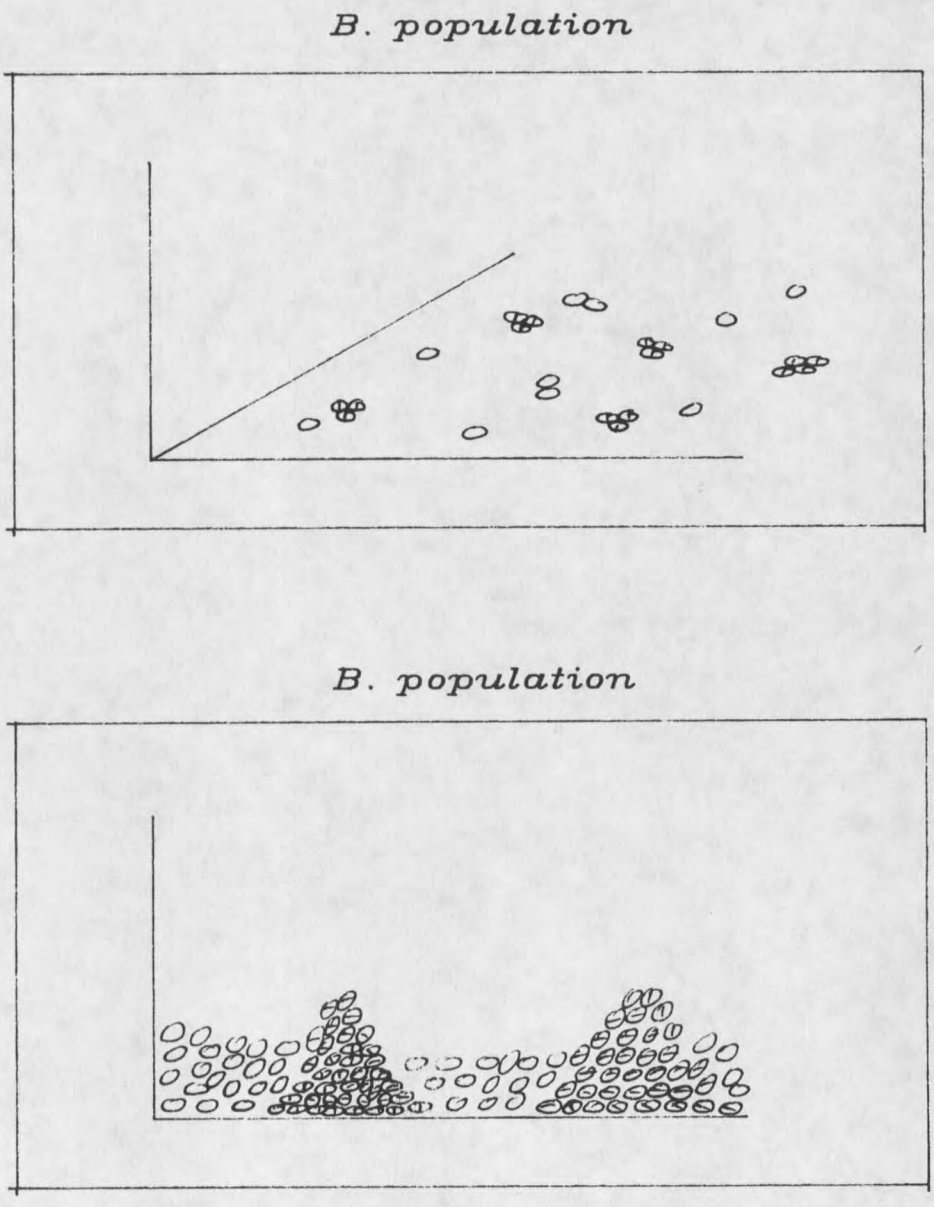

CONCLUSIONS

The following conclusions, valid within the range of experimental conditions tested, can be drawn from this study with K. pneumoniae and P. aeruginosa in binary population biofilms:

1. Specific product formation rate of K. pneumoniae or P. aeruginosa in the binary population biofilm is not affected by the presence of the other species.
2. Specific product formation rate in suspended growth and in the biofilm for K. pneumoniae is 5 times the specific product formation rate in suspended growth and in the biofilm for P. aeruginosa.
3. Specific product formation rate for K. pneumoniae and P. aeruginosa is linearly related to specific cellular growth rate. The slope of the linear relation, the growth associated product formation coefficient, is the same for suspended and for attached growth for each species.
4. Glucose-oxygen uptake ratio of K. pneumoniae or P. aeruginosa in the binary population biofilm is not affected by the presence of the other species.
5. The ratio of specific biofilm cellular glucose uptake rate and specific biofilm cellular oxygen uptake rate for K. pneumoniae is 3 times that for P. aeruginosa.
6. Specific growth rate for both K. pneumoniae and P. aeruginosa in suspended growth is described by saturation (Monod) kinetics. The maximum specific growth rate for K. pneumoniae is 5 times the maximum specific growth rate for P. aeruginosa.

7. Growth kinetics of P. aeruginosa in the biofilm have been described by the saturation model (Bakke, 1984). Growth kinetics of K. pneumoniae in the biofilm follow an exponential model.
8. The ratio of specific biofilm cellular glucose uptake rate vs. specific biofilm cellular growth rate for K. pneumoniae is 3 times that for P. aeruginosa.

REFERENCES

REFERENCES

Atkinson, B and Davies, I.J. 1974. The overall rate of substrate uptake (reaction) by microbial films. Part I - A biological rate equation. Trans. Instn. Chem. Engrs. Vol 52: 248-259.

Bakke, R., M.G. Trulear, J.A. Robinson and W.G. Characklis. 1984. Activity of Pseudomonas aeruginosa in Biofilms: Steady State. Biotech. Bioeng. 26:1418-1424.

Bakke, R. 1986. Biofilm Detachment. Ph.D. thesis, Montana State University, Bozeman, Mt.

Bakke, R. and P.Q. Ollsen. 1986. Biofilm thickness measurements by light microscopy. J. Microb. Met.5:1-6.

Bakken, L.R. and R.A. Olsen. 1983. Buoyant densities and dry-matter contents of microorganisms: conversion of a measured biovolume into biomass. Appl. Environ. Microbiol. 45:1188-1195.

Bevington, Ph. R. 1969. Data reduction and error analysis for the physical sciences. McGraw-Hill Book Company.

BMDP Statistical Software. 1983. W.J. Dixon. (Ed.). University of California Press, Berkeley, CA.

Brock, T.D. 1979. Biology of Microorganisms. Prentice-Hall. Inc.. Engelewood Cliffs, NJ.

Brown, C. and Seidler, R.J. 1973. Potential pathogens in the environment: K. pneumoniae, a taxonomic and ecological enigma. Appl. Microbiol. June:900-904.

Buchanan, R.E. and Gibbons, N.E. (Ed.'s). 1974. Bergey's manual of determinative bacteriology. The Williams and Wilkins Company, Baltimore, MD.

Campbell, L.M., Michaels, G., Klein, R.D. and Roth, I.L. 1976. Isolation of K. pneumoniae from lake water. Can. J. Microbiol. 22:1762-1767.

Characklis, W.G., and K.E. Cooksey. 1983. Biofilms and microbial fouling. Adv. Appl. Microbiol. 29:93-138.

Characklis, W.G., Zelver, N. and Roe, F.L. 1986. Continuous on-line monitoring of microbial deposition on surfaces. In: Sixth international biodeterioration symposium. Barry, S. and Houghton, D.R. (Ed.'s).

Costerton, J.W., Marrie, T.J. and Cheng, K.-J. 1985. Phenomena in bacterial adhesion. 3-43. In: Bacterial adhesion. Savage, D.C. and Fletcher, M. (Ed.'s). Plenum Press, New York.

Crisp, D.J. 1981. Overview of research on marine invertebrate larvae, 1940-1980. 103-126. In: Marine biodeterioration: an interdisciplinary study. Costlow, J.D. and Tipper, R.C. (Ed.'s). Naval institute press. Annapolis, MD.

Davies, D.G. and McFeters, G.A. 198.. Growth and comparative physiology of Klebsiella oxytoca attached to GAC particles and in liquid media. Microbial Ecology. Approved for publication.

Dixon, W.J. and Massey, Jr., F.J. 1983. Introduction to statistical analysis. McGraw-Hill Book Company.

Doetsch, R.N. and T.M. Cook. 1973. Introduction to bacteria and their ecobiology. University Park Press. Baltimore, MD.

Erbing, C., Kenne, L., Lindberg, B. and Lönngren, J. 1976. Structural studies of the capsular polysaccharide from Klebsiella type I. Carbohydrate Research. 50:115-120.

Escher, A. and Characklis, W.G. 1982. Algal-bacterial interactions within aggregates. Biotech. Bioeng. 24:2283-2290.

Escher, A.R. (1986) Bacterial Colonization of a Smooth Surface: An analysis with an Image Analyzer. Ph.D.-thesis, Montana State University, Bozeman, Mt.

Evans, C.G.T., Herbert, D. and Tempest, D.W. 1970. The continuous cultivation of micro-organisms. 2. Construction of a chemostat. 277-327. In: Methods in microbiology. Vol. 2. Norris, J.R. and Ribbons, D.W. (Ed.'s).

Frederickson, A.G. 1977. Behavior of mixed cultures of microorganisms. Ann. Rev. Microbiol. 31:63-87.

Geldreich, E.E. and E.W. Rice. 1987. Occurrence, significance and detection of Klebsiella in water systems. J AWWA. May:74-80.

Grady, C.P. 1982. Modeling of biological fixed films - A state of the art review. 344-404. In: Proceedings First International Conference on Fixed-Film Biological Processes. April 20-23. Kings Island. Ohio. Wu. Y.C., Smith, E.D., Miller, R.D. and Patken, E.J.O. (Ed.'s).

Haack, T.K. and McFeters, G.A. 1982. Nutritional relationships among microorganisms in an epilithic biofilm community. Microb. Ecol. 8:115-126.

Herbert, D., Phipps, P.J. and Strange, R.E. 1971. Chemical analysis of microbial cells. 210-341. In: Methods in microbiology, Vol. 5B. Norris,J.R. and Ribbons, D.W. (Ed.'s).

Hobbie, J.E., R.J. Daley, and S. Jasper. 1977. Use of nuclepore filters for counting bacteria by fluorescence microscopy. Appl. Env. Microbiol. 35:858-862.

Holmes, P.E. 1986. Bacterial enhancement of vinyl fouling by algae. Appl. Env. Microbiol. Dec.:1391-1393.

Holt, H.G. 1977. The shorter Bergey's manual of determinative bacteriology. Eighth Edition. The Williams & Wilkins Company. Baltimore, MD.

Jang, L.K. and T.F. Yen. 1985. A theoretical model of convective diffusion of motile and non-motile bacteria toward solid surfaces. 226-246. In: Microbes and oil recovery, Vol. 1. Zajic, J.E. and Donaldson, E.C. (Ed.'s). International bioresources journal.

LOGIT. 1986. Logistic function data analysis program logit. Kirchhoff. W.H. Chemical Thermodynamics Division Center for Chemical Physics, National Bureau of Standards, Gaithersburg, MD 20899.

Kissel, J.C., P.L. McCarthy and R.L. Street. 1984. Numerical simulation of mixed-culture biofilm. J. Env. Eng. 110(2):393-411.

Knittel, M.D. 1975. Occurrence of K. pneumoniae in surface waters. Appl. Microbiol. May:595-597.

Luedeking, R. and E.L. Piret. 1959. A kinetic study of the lactic acid fermentation. Batch process at controlled pH. J. of Biochem. and Microbiol. Technology and Engrg. 1(4):393-412.

Marshall, K.C., Stout, R. and Mitchell, R. 1971. Mechanism of the initial events in the sorption of marine bacteria to surfaces. J. Gen. Microbiol. 68:337-348.

Matson, J.V. and Characklis, W.C. 1976. Diffusion into microbial aggregates. Water Res. 10:877-885.

Mian, F.A., Jarman, T.R. and Righelato, R.C. 1978. Biosynthesis of exopolysaccharide by Pseudomonas aeruginosa. J. Bacteriology. May: 418-422.

Mitchell, R. and Kirchman, D. 1981. The microbial ecology of marine surfaces. 49-56. In: Marine biodeterioration: an interdisciplinary study. Costlow, J.D. and Tipper, R.C. (Ed.'s). Naval institute press. Annapolis, MD.

Mizushina, T. 1971. The electrochemical method in transport phenomena. Adv. Heat Transfer. 7:87-161.

Monod, J. 1949. The growth of bacterial cultures. Annual Rev. of Microbiol. 3:371-394.

MSUSTAT - Statistical analysis package. 1986. Montana State University, Bozeman, MT.

Murray, R.E., Cooksey, K.E. and Priscu, J.C. 1986. Stimulation of bacterial DNA synthesis by algal exudates in attached algal-bacterial consortia. Appl. Env. Microbiol. Nov:1177-1182.

Neijssel, O.M. and Tempest, D.W. 1975. The regulation of carbohydrate metabolism in Klebsiella aerogenes NCTC418 organisms, growing in chemostat culture. Arch. Microbiol. 106:251-258.

Rittmann, B.E. and P.L. McCarty. P.L. 1980-a. Model of steady-state biofilm kinetics. Biotech. Bioeng. 22:2343-2357.

Rittmann, B.E. and P.L. McCarty. 1980-b. Evaluation of steady-state biofilm kinetics. Biotech. Bioeng. 22:2359-2373.

Robinson, J.A., Trulear, M.G. and Characklis. W.G. 1984. Cellular Reproduction and Extracellular Polymer Formation by Pseudomonas aeruginosa in Continuous Culture. Biotech. Bioeng. 26:1409-1417.

Roth, I.L. 1977. Physical structure of surface carbohydrates. 5-26. In: Surface carbohydrates of the prokaryotic cell. Sutherland, I. (Ed.). Academic Press.

London.

Sandbeck, K.A. and Ward, D.M. 1981. Fate of immediate methane precursors in low-sulfate, hotspring algal-bacterial mats. Appl. Env. Microbiol. Mar:775-782.

Schiefer, G.E. and Caldwell, D.E. 1982. Synergistic interaction between Anabaena and Zoogloea species in carbon dioxide-limited continuous culture. Appl. Env. Microbiol. Jul:84-87.

Slater, J.H. and Lovatt, D. 1984. Biodegradation and the significance of microbial communities. 439-485. In: Microbial degradation of organic compounds. Gibson, D.T. (Ed.). Dekker, New York, New York.

Snedecor, G.W. and Cochran, W.G. 1967. Statistical methods. The Iowa State University Press, Ames, Iowa.

Sutherland, I. 1977. Bacterial Exopolysaccharides - their nature and production. 27-96. In: Surface carbohydrates of the prokaryotic cell. Sutherland, I. (Ed.). Academic Press. London.

Sutherland, I. 1982. Biosynthesis of microbial exopolysaccharides. 79-150. In: Advances in Microbial Physiology. 23. Rose, A.H. and Morris, J.G. (Ed.'s).

Topiwala, H.H. and Hamer, G. 1971. Effect of wall growth on steady-state continuous culture. Biotech. Bioeng.13:919-922.

Trulear, M.G. 1983. Cellular reproduction and extracellular polymer formation in the development of biofilms. Ph.D.-thesis, Montana State University, Bozeman, MT.

Trulear, M.G. and W.G. Characklis. 1982. Dynamics of Biofilm Processes. J WPCF. 54(9):1288-1300.

Turakhia, M.H. 1986. The Influence of Calcium on Biofilm Processes. Ph.D.-thesis. Montana State University, Bozeman, Mt.

Vaituzis, Z. and Doetsch, R.N. 1969. Motility tracks: Technique for quantitative study of bacterial movement. Appl. Microbiol. 17(4):584-588.

Van Gemerden, H. 1974. Coexistence of organisms competing for the same substrate: an example among the purple sulfur bacteria. Microbial Ecology. 1:104-119.

NOMENCLATURE

NOMENCLATURE

A		substratum area $[L^{-2}]$
D		dilution rate $[t^{-1}]$
f_D		effectiveness factor for substrate diffusion [-]
k_c		dissolved oxygen specific carbon transfer rate $[t^{-1}]$
k_{Pg}	=	growth-associated product formation coefficient $[M_P M_M^{-1}]$
k_{Pn}	=	non-growth associated product formation coefficient $[M_P M_M^{-1} t^{-1}]$
K_S	=	half saturation concentration $[M_S L^{-3}]$
N_O		flux of dissolved oxygen into reactor system $[M_O L^{-2} t^{-}]$
r_{Md}		specific cell detachment rate $[t^{-1}]$
r_O		biofilm specific oxygen uptake rate $[M_O M_M^{-1} t^{-1}]$
r_{Pd}		specific rate of product detachment $[t^{-1}]$
r_{Pf}		specific rate of product formation in biofilm $[M_P M_M^{-1} t^{-1}]$
r_{Pl}		specific rate of product formation in suspension $[M_P M_M^{-1} t^{-1}]$
r_S		biofilm specific substrate uptake rate $[M_S M_M^{-1} t^{-1}]$
R_O		rate of oxygen generation $[M_O . L^{-3} . t^{-1}]$
S_{Oi}		concentration of oxygen in influent $[M_O L^{-3}]$
S_{Ol}		concentration of oxygen in liquid phase $[M_O L^{-3}]$
S_{Os}		oxygen saturation concentration in influent $[M_O L^{-3}]$
S_{Pf}		product carbon concentration in biofilm $[M_P L^{-2}]$
S_{Pi}		product carbon concentration in influent $[M_P L^{-3}]$
S_{Pl}		product carbon concentration in liquid phase $[M_P L^{-3}]$
S_{Pla}		adsorbed product carbon concentration in liquid phase $[M_P L^{-3}]$
S_{Plt}		total product carbon concentration in liquid phase $[M_P L^{-3}]$

S_{Sf}	substrate carbon concentration in biofilm $[M_S L^{-2}]$
S_{Si}	substrate carbon concentration in influent $[M_S L^{-3}]$
S_{Sl}	substrate carbon concentration in liquid phase $[M_S L^{-3}]$
S_{TOCl}	concentration of total organic carbon in liquid phase $[M_C L^{-3}]$
S_{SOCl}	concentration of soluble organic carbon in liquid phase $[M_C L^{-3}]$
S_{TOCf}	concentration of total organic carbon in biofilm $[M_C L^{-3}]$
t	time [t]
V	Volume $[L^{-3}]$
X_{Mf}	cell carbon concentration in film $[M_M L^{-2}]$
X_{Mi}	cell carbon concentration in influent $[M_M L^{-3}]$
X_{Ml}	cell carbon concentration in liquid phase $[M_M L^{-3}]$
Y_{MS}	yield of cell carbon from substrate carbon $[M_M M_S^{-1}]$
Y_{MO}	yield of cell carbon from oxygen $[M_M M_O^{-1}]$
Y_{obs}	observed yield coefficient $[M_M M_S^{-1}]$
Y_{PS}	yield of product carbon from substrate carbon $[M_M M_P^{-1}]$
Y_{PSl}	Yield of soluble product carbon from substrate carbon $[M_M M_P^{-1}]$
Y_{PSt}	Yield of total product carbon from substrate carbon $[M_M M_P^{-1}]$
Y_{PO}	yield of product carbon from oxygen $[M_M M_P^{-1}]$
Y_{SO}	glucose-oxygen stoichiometric ratio $[M_S M_O^{-1}]$

Greek letters

δ_f	biofilm thickness [L]
ϵ	effectiveness factor [-]
τ_{Mf}	cell carbon density in biofilm [$M_M L^{-3}$]
Ω_S	specific cellular glucose uptake ratio [$M_S M_M^{-1}$]
μ	specific cellular growth rate [t^{-1}]
μ_m	maximum specific cellular growth rate [t^{-1}]

subscripts

a	adsorption, attachment
d	desorption, detachment
i	influent
f	biofilm phase
l	liquid phase
s	saturation
M	Microbial cell
O	Oxygen
P	Product
S	Substrate

APPENDICES

APPENDIX A: Oxygen Diffusion Study

Objective of this study was the determination of the mass transfer coefficient of dissolved oxygen (DO) for the Rototorques.

Diffusion of dissolved oxygen into the reactors can be determined by pumping dilution water of low dissolved oxygen concentration into the sterile reactors and monitoring the (DO) concentration in the effluent. The rate at which oxygen diffuses into the reactors is determined by a material balance across the reactor.

Dissolved oxygen concentration in the influent was varied by purging the dilution water mixing tank with nitrogen gas. Varying the nitrogen gas flow rate for a constant flow rate of dilution water ($0.06*10^{-3}$ $m^3.min^{-1}$) resulted in different concentrations of dissolved oxygen entering the reactors. The reactors were pretreated as described in Experimental Approach. Rotational speed was 200 rpm. After changing the nitrogen gas flow, dissolved oxygen concentration in the effluent was monitored continuously to determine steady state DO concentration. DO concentration was measured with a YSI model-54 oxygen meter.

A DO mass balance (Eq. 7 without DO consumption terms) was used to quantify the oxygen transfer rate in the reactor:

$$\frac{dS_{Ol}}{dt} = D.(S_{Oi}-S_{Ol}) + N_O.\frac{A}{V} \qquad (A-1)$$

where:

S_{Ol} = dissolved oxygen concentration in effluent $[M_O L^{-3}]$

S_{Oi} = dissolved oxygen concentration in influent $[M_O L^{-3}]$

D = dilution rate $[t^{-1}]$

N_O =flux of dissolved oxygen into the system $[M_O L^{-2} t^{-1}]$

The dissolved oxygen flux into the reactor is defined by:

$$N_O = k_c . (S_{Os} - S_{Ol}) . \frac{V}{A} \qquad (A-2)$$

where:

k_c = DO specific mass transfer rate $[t^{-1}]$

S_{Os} = DO saturation concentration $[M_O L^{-3}]$

Substituting Eq. A-2 into Eq. A-1 and assuming steady state conditions results in:

$$k_c = D . \frac{S_{Oi} - S_{Ol}}{S_{Ol} - S_{Os}} \qquad (A-3)$$

The specific DO mass transfer rate for the experimental reactors was determined from 14 independent measurements (Table 16). The means and standard deviations are:
$k_{c1} = 9.30 \pm 1.06\ h^{-1}$, $k_{c2} = 9.44 \pm 0.95\ h^{-1}$.

Biofilm experiments were designed such that dilution water was DO saturated in a mixing chamber prior to entering the reactor. Therefore, mass transfer of DO into the reactors could be accounted for in the DO material balance as follows:

$$\frac{dS_O}{dt} = D(S_{Os} - S_{Ol}) + N_O \frac{A}{V} - X_{Mf}\left[\frac{\mu_f}{Y_{MO}} + \frac{r_{Pf}}{Y_{PO}}\right] . \frac{A}{V}$$

$$- X_{Ml}\left[\frac{\mu}{Y_{MO}} + \frac{r_P}{Y_{PO}}\right] \qquad (7)$$

Influent		Effluent Reactor 1			Effluent Reactor 2		
temp. (°C)	DO ($g.m^{-3}$)	temp. (°C)	DO ($g.m^{-3}$)	k_{c1} (h^{-1})	temp. (°C)	DO ($g.m^{-3}$)	k_{c2} (h^{-1})
20.8	.75	20.5	4.70	9.77	20.3	4.75	10.07
20.7	.46	20.5	4.35	8.55	20.3	4.45	9.06
20.7	.40	20.4	4.65	10.32	20.3	4.68	10.51
20.8	.41	20.5	4.73	10.80	20.3	4.62	10.12
20.5	.42	20.5	4.65	10.28	20.3	4.55	9.69
20.5	.45	20.3	4.70	10.51	20.3	4.80	11.15
20.5	1.65	20.3	4.75	7.80	20.3	4.80	8.08
20.5	2.05	20.3	5.08	8.67	20.5	5.13	9.00
20.7	1.50	20.5	4.95	9.37	20.4	4.85	8.75
20.7	1.35	20.5	4.92	9.58	20.3	4.95	9.77
20.7	2.62	20.5	5.35	8.79	20.4	5.30	8.43
20.5	4.50	20.4	6.10	7.91	20.3	6.10	7.91
20.5	6.44	20.3	7.00	7.75	20.3	7.05	9.38
20.2	6.71	20.5	7.18	10.17	20.5	7.18	10.17

Table 16. Experimental data from oxygen diffusion study.

With the time constant for microbial oxygen consumption greater than for the oxygen diffusion, the value for the specific oxygen mass transfer rate, derived for steady state conditions, can be used to describe oxygen diffusion in non-steady state conditions. This results in:

$$\frac{dS_O}{dt} = (D+k_c).(S_{Os}-S_{Ol}) - X_{Mf}\left[\frac{\mu_f}{Y_{MO}} + \frac{r_{Pf}}{Y_{PO}}\right].\frac{A}{V}$$

$$- X_{Ml}\left[\frac{\mu}{Y_{MO}} + \frac{r_P}{Y_{PO}}\right] \qquad (A-4)$$

APPENDIX B: Characteristics of the Rototorque

Inner cylinder:		
- wetted height	177	mm
- diameter	102	mm
- wetted surface area (vertical)	56700	mm^2
- wetted surface area (horizontal)	16300	mm^2
- total inner cylinder wetted surface area	73100	mm^2
Draft tubes:		
- number	4	
- diameter	10	mm
- length	180	mm
- angle of inclination	80	°
- surface area	23100	mm^2
Outer cylinder:		
- wetted height	220	mm
- diameter	113	mm
- wetted surface area (vertical)	78100	mm^2
- wetted surface area (horizontal)	20100	mm^2
- total outer cylinder wetted surface area	98200	mm^2
- number of slides	12	
Slides:		
- number	12	
- thickness	0.5	mm
- width	15	mm
- wetted length	220	mm
- wetted slide surface area	3300	mm^2
- volume of 1 slide	1650	mm^3
- volume of 12 slides	20000	mm^3
Reactor:		
- wetted surface area (excl. tubes)	0.17	m^2
- slide surface area (excl. tubes)	42	%
- total wetted surface area (incl. tubes)	0.19	m^2
- slide surface area (incl. tubes)	37	%
- liquid volume (at 200 rpm)	$0.52*10^{-3}$	m^3
- surface/volume ratio (excl. tubes)	0.29	mm^{-1}
- surface/volume ratio (incl. tubes)	0.33	mm^{-1}
- liquid residence time (at 1 $ml.s^{-1}$ dilution water flow rate, at 200 rpm)	594 s (9.9 min)	
- recycle flow rate[1] (at 200 rpm)	500	$mm^3.s^{-1}$
- width of annular gap	5.5	mm

[1] Flow rate through draft tubes as a result of inner cylinder rotation.

APPENDIX C: Raw Data Batch Experiments

Oxygen consumption

Time	Experiment		
(h)	I	II	III
	dissolved oxygen concentration ($g.m^{-3}$)		
.0	.0	.0	.0
1.0	.0	.0	.0
2.0	.0	.0	.0
3.0	.0	.0	.0
4.0	.0	.0	.0
5.0	.0	.0	.0
6.0	.0	.0	.0
7.0	.0	.0	.0
8.0	1.3	.0	.6
9.0	2.2	.8	.6
10.0	2.9	2.3	1.3
11.0	5.1	6.3	2.7
12.0	10.0	12.2	5.8
13.0	15.8	16.2	10.9
13.9	18.1	18.4	15.5
14.0	18.7	18.4	15.5
14.2	18.7	18.7	16.1
14.5	19.5	19.4	17.4
14.9	21.1	20.7	18.6
15.0	21.1	20.7	18.8
15.3	21.8	21.3	19.4
15.5	21.8	22.0	20.0
15.8	22.5	22.8	20.7
16.0	23.1	23.5	21.4
16.3	23.7	24.2	22.0
16.5	24.6	25.0	22.7
16.8	25.3	25.8	23.3
17.0	25.8	26.5	23.9
17.3	26.5	27.2	24.6
17.5	27.2	27.2	25.2
17.8	27.8	28.0	25.9
18.0	28.5	28.6	26.4
18.3	29.1	28.6	27.1
18.5	29.8	28.6	27.7
18.8	30.3	29.2	28.4

(continued)

Time	Experiment		
(h)	I	II	III
	dissolved oxygen concentration ($g.m^{-3}$)		
19.0	31.0	29.2	28.9
19.3	31.4	29.2	29.5
19.5	31.5	29.8	30.1
19.8	32.2	29.8	30.7
20.0	32.2	29.8	31.3
20.3	32.2	30.5	31.9
20.5	32.0	30.5	31.9
20.8	32.8	30.5	31.9
21.0	33.4	30.5	32.5
22.0	34.0	31.2	33.1
23.0	34.7	32.6	34.3
24.0	35.4	33.3	34.8
25.0	36.2	34.1	35.4
26.0	36.8	34.8	36.0
27.0	37.4	35.4	36.6
28.0	37.4	35.4	37.2
29.0	38.2	36.1	37.8
30.0	38.2	36.7	37.8
31.0	38.8	37.3	38.4
32.0	39.6	38.0	39.0
33.0	39.6	38.0	39.0
34.0	40.3	38.7	39.7
35.0	41.1	39.4	40.3
35.7	41.1	40.0	40.9
36.0	41.7	40.8	40.9
36.5	41.7	40.8	41.6
37.0	41.7	40.8	41.6
37.2	41.7	40.8	41.6
37.7	41.7	40.8	41.6
38.0	41.7	40.8	41.6
38.5	41.7	40.8	41.6
39.0	41.7	40.8	41.6
39.5	41.7	40.8	41.6
40.0	41.7	40.8	41.6
41.0	41.7	40.8	41.6
42.0	41.7	40.8	41.6
43.0	41.7	40.8	41.6
44.0	41.7	40.8	41.6
45.0	41.7	40.8	41.6

Results of analysis

Reactor #	S_{Si}	S_{Sl}	S_{TOCi}	S_{TOCl}	S_{SOCl}
	..... ($g\ C.m^{-3}$)				
I	38.5	0	39.1	21.5	10.7
II	38.5	0	39.1	23.6	11.3
III	38.5	0	39.1	21.4	9.0
MEANS	38.5	0	39.1	22.2	10.3
STD	.0	.0	.0	1.2	1.2

Reactor #	Cell# ($\#.m^{-3}$)	Length (μm)	Breadth (μm)	Roundness (-)
I	9.331e13	1.20	.85	1500
II	9.453e13	1.25	.86	1489
III	8.037e13	1.32	.93	1485
MEANS	8.940e13	1.26	.88	1491
STD	7.845e12	.06	.04	8

Reactor #	Oxygen consumed ($g\ O_2.m^{-3}$)	Mass ($g.m^{-3}$)
I	42.7	31.5
II	42.3	31.1
III	42.6	38.8
MEANS	42.6	33.8
STD	.2	4.3

APPENDIX D: Raw Data Chemostat Experiments

Dilution rate ($l.h^{-1}$)	S_{Si}	S_{Sl}	S_{TOCi}	S_{TOCl}	S_{SOCl}
	..... ($g\ C.m^{-3}$)				
.10	37.4	.32	38.1	17.4	9.4
.13	37.3	.29	38.1	19.9	9.9
.27	37.1	.66	39.3	23.0	9.2
.27	37.1	.35	39.3	22.4	8.9
.40	37.0	.60	38.4	23.5	9.5
.40	37.0	.17	38.4	23.8	9.5
.50	36.5	.54	37.9	23.8	10.9
.50	36.5	1.28	37.9	24.6	12.3
.56	35.4	.23	37.8	24.2	11.6
.56	35.4	.61	37.8	24.6	11.9
.67	34.5	.23	37.2	26.2	11.4
.67	34.5	.04	37.2	23.9	11.3
.80	35.9	.41	36.5	25.0	10.5
.80	35.9	.41	36.5	22.1	10.0
1.07	37.1	.79	36.9	22.0	10.9
1.07	37.1	1.04	36.9	22.9	10.0
1.60	36.7	6.05	39.4	25.9	14.5
1.87	36.7	17.79	39.4	31.6	21.3

Dilution rate ($l.h^{-1}$)	Mass ($g.m^{-3}$)	Cell # ($\#.m^{-3}$)	Length (μm)	Breadth (μm)	Roundness (-)
.10	47.0	1.047e14	1.11	.75	1684
.13	76.5	1.276e14	1.22	.76	1745
.27	50.0	1.176e14	1.43	.71	2155
.27	31.5	9.732e13	1.24	.76	2053
.40	30.5	1.023e14	1.51	.73	2121
.40	36.0	9.615e13	1.65	.77	2068
.50	24.5	7.145e13	1.54	.78	2043
.50	29.5	5.498e13	1.91	.89	1995
.56	53.0	4.852e13	2.11	.84	2186
.56	30.5	6.910e13	2.28	.90	1834
.67	59.0	3.659e13	2.45	.89	2200
.67	54.5	5.293e13	2.27	.89	1945
.80	61.0	3.661e13	1.96	.82	2211
.80	50.0	5.072e13	2.24	.86	2114
1.07	57.5	9.203e13	1.45	.75	1934
1.07	50.5	6.528e13	1.98	.83	2073
1.60	37.5	5.440e13	1.47	.79	1993
1.87	23.5	2.382e13	1.09	.73	2101

APPENDIX E: Comparison of Nutrient Compositions

	Evans et al. (1970)		This study
	original	based on 10 g.C m^{-3}	
Carbon (g C.m^{-3})	3000	10	10
Phosphorus (g.m^{-3})	310	0.10	92.40
Nitrogen (g.m^{-3})	1400	0.47	1.88
Sulphur (g.m^{-3})	64	0.02	0.31
Magnesium (g.m^{-3})	30.4	0.01	0.20
Molybdenum (g.m^{-3})	0.0096	3.2e-6	4.7e-4
Iron (g.m^{-3})	5.59	0.002	0.023
Cobalt (g.m^{-3})	0.59	0.0002	-
Copper (g.m^{-3})	0.32	0.0001	0.0005
Manganese (g.m^{-3})	2.78	0.0009	0.0026
Zinc (g.m^{-3})	0.33	0.0001	0.0228
Boron (g.m^{-3})	0.043	0.00001	0.00011

APPENDIX F: Sample Preparation Procedure

Transmission Electron Microscopy (TEM)

1. Fix sample with 2.5% (v/v) glutaraldehyde in millonig's phosphate buffer (pH 7.2) for 6-8 hours (or overnight).
2. If necessary, store at 4°C in millonig's phosphate buffer (pH 7.2) till sample preparation - change weekly.
3. Wash 3 times in millonig's phosphate buffer (pH 7.2) for 20 minutes each.
4. Postfix in 1% (w/v) osmium tetroxide (OsO_4) for 1 hour
5. Wash 3 times in millonig's phosphate buffer (pH 7.2) for 20 minutes each.
6. Dehydrate in ethanol:
   - 15 minutes in 50% ethanol
   - 15 minutes in 70% ethanol; sample may be stored in 70% ethanol overnight if needed
   - 15 minutes in 95% ethanol
   - 3 times for 15 minutes each in 100% ethanol
7. Embed in Spurr's (1969)[1] epoxy resin:
   - 1 hour in mixture of (v/v) 2 (100% ethanol) : 1 (epoxy resin)
   - 1 hour in mixture of (v/v) 1 (100% ethanol) : 1 (epoxy resin)
   - 8 hours or overnight in pure epoxy resin.
8. Polymerize in 70°C oven for 14 hours in a capsule.

---

[1] Spurr, A.R. 1969. Low-viscosity epoxy resin embedding medium for electron microscopy. J. of Ultra Structure Research. 25:31-43.

Scanning Electron Microscopy (SEM)

1. Fix with 2.5% (v/v) glutaraldehyde in millonig's phosphate buffer (pH 7.2) for 6-8 hours (or overnight).
2. If necessary, store at 4°C in millonig's phosphate buffer (pH 7.2) till sample preparation - change weekly.
3. Wash 3 times in phosphate buffer (pH 7.2) for 20 minutes each.
4. Dehydrate in ethanol:
   - 15 minutes in 30% ethanol
   - 15 minutes in 50% ethanol
   - 15 minutes in 70% ethanol
   - 15 minutes in 90% ethanol
   - twice for 10 minutes each in 100 ethanol.
6. Critical point dry.
7. Mount on sample holder with colloidal graphite.
8. Sputter coat with gold (or other good electron conductor).

APPENDIX G: Raw Data and Parameters Logistic Equation

Mono Population Biofilm - K. pneumoniae

Notation

DO = Dissolved Oxygen concentration [$g.m^{-3}$]
gluc = glucose carbon concentration [$g\ C.m^{-3}$]
TOC = Total Organic Carbon [$g\ C.m^{-3}$]
SOC = Soluble Organic Carbon [$g\ C.m^{-3}$]
mass = mass of suspended solids [$g.m^{-3}$]
Kp = *K. pneumoniae* cell concentration [$\#.m^{-3}$]
Pa = *P. aeruginosa* cell concentration [$\#.m^{-3}$]

A = pretransition region intercept
B = posttransition region asymptote
X_o = position of the transition region
D_o = width of the transition region
StDev = Standard deviation of overall fit

Mono population biofilm - K. pneumoniae

Experiment 1 - liquid phase

Raw data

time (h)	DO ($g.m^{-3}$)	gluc	TOC ($g\ C.m^{-3}$)	SOC	mass ($g.m^{-3}$)	Kp ($\#.m^{-3}$)	Pa
.0	7.0	10.1	14.6	13.5	.0	0	
24.5	6.9	9.7	13.4	13.3	.0	3.8e9	
50.0	6.4	6.6	12.0	12.5	3.6	3.1e12	
72.0	5.5	2.9	11.0	9.4	4.0	6.9e11	
96.5	5.2	.0	9.7	6.8	6.4	5.2e12	
148.0	5.3	1.0	9.5	5.4	8.2	4.5e12	

time (h)	length (μm)	breadth (μm)	area (μm^2)
.0	.00	.00	.00
24.5	1.23	.72	.56
50.0	1.35	.87	.88
72.0	1.61	.91	1.08
96.5	1.51	.98	1.03
148.0	1.06	.64	.45

Parameters

	DO	gluc	TOC	SOC	mass	Kp	Pa
A	6.9	10.9	14.3	14.3	.0	1e0	
B	5.1	1.3	9.4	9.4	8.3	4.7e12	
X0	51.0	52.2	56.0	63.3	71.8	41.6	
D0	11.0	11.8	14.0	14.4	19.3	8.7	
StDev	.23	.94	.40	.67	.53	.17	

Mono population biofilm - K. pneumoniae

Experiment 1 - biofilm phase

Raw data

time (h)	TOC (g C.m^{-2})	thickness (µm)	mass (g.m^{-2})	Kp ..... (#.m^{-2})	Pa ..
.0	.00	.00		0	
25.0					
52.5	.12	4.99		8.9e9	
70.5	.32	6.98		6.1e11	
79.0					
105.5	.38	12.64		5.3e11	
116.5					
123.0	.38	12.30		5.6e11	
147.0					
166.0					
192.0					

time (h)	length (µm)	breadth (µm)	area (µm^2)
.0	.00	.00	.00
25.0			
52.5	1.51	.75	.81
70.5	1.54	.81	.83
79.0			
105.5	1.21	.88	.92
116.5			
123.0	1.44	.87	.90
147.0			
166.0			
192.0			

Parameters

	TOC	thickness	mass	Kp	Pa
A	.00	.00		1e0	
B	.39	13.30		5e11	
X0	55.20	65.20		61.20	
D0	16.70	18.80		8.68	
StDev		.84			

Mono population biofilm - K. pneumoniae

Experiment 2 - liquid phase

Raw data

time	DO	gluc	TOC	SOC	mass	Kp	Pa
(h)	($g.m^{-3}$)	....	(g $C.m^{-3}$)	.....	($g.m^{-3}$)	.	(#.m^{-3}) .
.0	7.0	10.5	14.3	14.2	.0	0	
24.5	6.9	9.2	13.9	13.2	.0	9.6e9	
50.0	6.0	6.1	12.5	11.7	4.0	5.9e12	
72.0	5.6	2.8	9.2	8.3	4.8	5.9e12	
96.5	5.2	2.2	7.9	5.3	7.2	7.2e12	
148.0	5.6	1.9	8.7	5.4	6.6	7.0e12	

time	length	breadth	area
(h)	(µm)	(µm)	(μm^2)
.0	.00	.00	.00
24.5	1.38	.85	.80
50.0	1.52	.96	1.02
72.0	1.70	.91	1.14
96.5	1.50	.90	.99
148.0	2.15	1.23	1.88

Parameters

	TOC	thickn	mass	Kp	Pa
A	.00	.00		1e0	
B	.37	18.70		6e11	
X0	60.00	102.00		55.20	
D0	16.70	4201.00		8.70	
StDev	.02	.81		.43	

Mono population biofilm - K. pneumoniae

Experiment 2 - biofilm phase

Raw data

time (h)	TOC (g C.m^{-2})	thickness (µm)	mass (g.m^{-2})	Kp ..... (#.m^{-2})	Pa ..
.0	.00	.00		0	
25.0		3.49			
52.5	.14	5.32		3.6e11	
70.5	.20	6.48		6.4e11	
79.0		6.15			
105.5	.28	10.14		6.2e11	
116.5		9.64			
123.0	.39	11.97		6.3e11	

time (h)	length (µm)	breadth (µm)	area (µm^2)
.0	.00	.00	.00
25.0			
52.5	1.60	.84	.88
70.5	1.49	.91	.93
79.0			
105.5	1.15	.89	.92
116.5			
123.0	1.34	.97	.96

Parameters

	TOC	thickn	mass	Kp	Pa
A	.00	.00		1e0	
B	.37	18.70		6e11	
X0	60.00	102.00		55.20	
D0	16.70	42.10		8.70	
StDev		.81			

Mono population biofilm - K. pneumoniae

Experiment 3 - liquid phase

Raw data

time (h)	DO ($g.m^{-3}$)	gluc	TOC ($g\ C.m^{-3}$)	SOC	mass ($g.m^{-3}$)	Kp ($\#.m^{-3}$)	Pa
.0	7.0	11.3	11.6	11.9	.0	0	
12.5	7.0	10.3	11.1	10.3	4.0	8.8e11	
27.0	7.0	7.7	10.4	10.5	4.2	1.2e12	
50.5	6.5	3.8	9.3	9.1	4.4	1.5e12	
75.5	5.5	2.7	7.1	6.4	10.2	4.1e12	
95.0	5.6	1.3	6.6	7.6	7.8	4.5e12	
118.5	5.7	1.9	5.1	5.3	8.4	5.2e12	
142.5	6.1	2.0	5.2	5.9	8.0	4.1e12	

time (h)	length (μm)	breadth (μm)	area (μm^2)
.0	.00	.00	.00
12.5	1.15	.73	.55
27.0	1.18	.78	.64
50.5	1.17	.73	.59
75.5	1.18	.74	.63
95.0	1.42	.92	.96
118.5	1.85	1.28	1.63
142.5	2.03	1.42	2.16

Parameters

	DO	gluc	TOC	SOC	mass	Kp	Pa
A	7.0	10.7	12.9	13.1	.0	1e0	
B	5.6	1.2	8.8	6.0	7.0	4.6e12	
X0	57.5	55.8	58.2	61.0	37.2	34.8	
D0	12.7	14.1	9.8	17.2	7.3	8.6	
StDev	.09	.55	1.89	.60	2.29	.25	

Mono population biofilm - K. pneumoniae

Experiment 3 - biofilm phase

Raw data

time (h)	TOC (g C.m^{-2})	thickness (µm)	mass (g.m^{-2})	Kp ..... (#.m^{-2})	Pa ..
.0	.00	.0		0	
27.0		1.3			
77.0	.22	6.5		3.9e11	
97.5	.35	10.1		4.6e11	
106.5		13.5			
119.0	.46	9.3		5.3e11	
132.5		12.3			

time (h)	length (µm)	breadth (µm)	area (µm^2)
.0	.00	.00	.00
27.0			
77.0	1.60	.84	.88
97.5	1.45	.92	.94
106.5			
119.0	1.15	.89	.92
132.5			

Parameters

	TOC	thickness	mass	Kp	Pa
A	.00	.00		1e0	
B	.42	12.70		5e11	
X0	63.00	61.80		56.20	
D0	29.00	17.30		8.75	
StDev	2.31	5.16		.28	

Mono population biofilm - K. pneumoniae

Experiment 4 - liquid phase

Raw data

time (h)	DO ($g.m^{-3}$)	gluc	TOC ($g\ C.m^{-3}$)	SOC	mass ($g.m^{-3}$)	Kp ($\#.m^{-3}$)	Pa
.0	7.0	10.3	11.9	12.0	.0	.0	
12.5	7.0	10.3	11.7	10.9	.2	2.0e11	
27.0	7.0	8.8	10.4	10.6	1.6	1.6e12	
50.5	6.8	4.2	8.3	10.3	2.8	1.8e12	
75.5	5.5	1.8	7.0	6.9	6.0	3.9e12	
95.0	5.6	1.8	6.4	5.4	11.4	6.0e12	
118.5	5.5	2.1	5.2	5.6	4.2	5.2e12	
142.5	5.9	.7	5.4	6.0	8.7	8.5e11	

time (h)	length (μm)	breadth (μm)	area (μm^2)
.0	.00	.00	.00
12.5	1.15	.73	.55
27.0	1.26	.77	.66
50.5	1.09	.68	.51
75.5	1.25	.85	.73
95.0	1.26	.75	.76
118.5	1.54	1.10	1.33
142.5	1.45	.94	.94

Parameters

	DO	gluc	TOC	SOC	mass	Kp	Pa
A	7.00	10.86	12.3	12.29	0	1e0	
B	5.92	1.98	5.1	5.70	8.20	5.1e12	
X0	45.00	37.80	57.0	53.50	63.00	25.43	
D0	11.30	10.40	26.0	15.70	12.50	8.7	
StDev	.05	.56	.3	1.62	2.51	.408	

Mono population biofilm - K. pneumoniae

Experiment 4 - biofilm phase

Raw data

time (h)	TOC (g C.m^{-2})	thickness (µm)	mass (g.m^{-2})	Kp ..... (#.m^{-2})	Pa ..
.0	0	.0		0	
27.0		4.2			
77.0	.21	5.5		3.6e11	
97.5	.31	9.8		4.4e11	
106.5		12.3			
119.0	.28	14.8		3.5e11	
132.5		8.1			

time (h)	length (µm)	breadth (µm)	area (µm^2)
.0	.00	.00	.00
27.0			
77.0	1.46	.84	.87
97.5	1.21	.86	.91
106.5			
119.0	1.41	.81	.88
132.5			

Parameters

	TOC	thickness	mass	Kp	Pa
A	.00	.00		1e0	
B	.35	16.10		4e11	
X0	33.70	73.80		51.60	
D0	31.00	17.30		10.60	
StDev	.98	7.45		.64	

APPENDIX H: Raw Data and Parameters Logistic Equation

Mono Population Biofilm - P. aeruginosa

Notation

DO = Dissolved Oxygen concentration [$g.m^{-3}$]
gluc = glucose carbon concentration [g $C.m^{-3}$]
TOC = Total Organic Carbon [g $C.m^{-3}$]
SOC = Soluble Organic Carbon [g $C.m^{-3}$]
mass = Mass of suspended solids [$g.m^{-3}$]
Kp = *K. pneumoniae* cell concentration [$\#.m^{-3}$]
Pa = *P. aeruginosa* cell concentration [$\#.m^{-3}$]

A = pretransition region intercept
B = posttransition region asymptote
X_o = position of the transition region
D_o = width of the transition region
StDev = Standard deviation of overall fit

Mono population biofilm - P. aeruginosa

Experiment 1 - liquid phase

Raw data

time	DO	gluc	TOC	SOC	mass	Kp	Pa
(h)	($g.m^{-3}$)		($g\ C.m^{-2}$)		($g.m^{-3}$)	($\#.m^{-3}$)	
.0	7.0	10.0	14.5	14.5	.0		0
19.5	6.8	7.3	14.3	12.8	.4		1.3e9
35.5	6.6	5.6	13.3	12.6	7.8		6e12
59.5	3.7	4.1	11.9	9.6	11.8		2e13
92.5	3.6	3.9	11.3	7.1	4.9		6e13
112.0	3.4	3.5	9.7	7.4	5.2		1.3e13

time	length	breadth	area
(h)	(µm)	(µm)	(μm^2)
.0			
35.5	1.4	.87	.83
59.5	1.6	.71	.74
92.5	1.8	.82	1.03
112.0	1.5	.70	.74

Parameters

	DO	gluc	TOC	SOC	mass	Kp	Pa
A	6.89	10.0	14.2	14.5	0		1e0
B	3.54	3.8	10.8	6.9	5.3		2.7e13
X0	45.20	24.7	47.5	49.3	27.5		46.68
D0	7.97	10.30	12.00	16.40	8.00		13.50
StDev	.126	.426	.757	.668	1.820		.274

Mono population biofilm - P. aeruginosa

Experiment 1 - biofilm phase

Raw data

time (h)	TOC ($g.m^{-2}$)	thickness (µm)	mass ($g.m^{-2}$)	Kp ... ($\#.m^{-2}$)	Pa ...
.0	.00	.0	.0		1e0
62.5	.49	16.5	.4		1.6e12
93.5	.60	25.3	.7		3.5e12
116.0	.72	31.4	1.9		4.0e12
134.5	.76	33.4	1.5		4.3e12
137.5	.77	34.4	1.8		4.2e12

time (h)	length (µm)	breadth (µm)	area (μm^2)
.0	.00	.00	.00
62.5			
93.5	1.58	.69	.75
116.0	1.54	.73	.76
134.5	1.26	.58	.45
137.5	1.60	.77	.87

Parameters

	TOC	thickness	mass	Kp	Pa
A	.00	.00	.00		1e0
B	.81	35.50	1.83		4e12
X0	60.00	68.80	63.20		66.70
D0	27.00	23.10	26.80		16.50
StDev	.05	1.41	.27		.19

Mono population biofilm - P. aeruginosa

Experiment 2 - liquid phase

Raw data

time	DO	gluc	TOC	SOC	mass	Kp	Pa
(h)	($g.m^{-3}$)	.....	($g\ C.m^{-2}$)	....	($g.m^{-3}$)	..	($\#.m^{-3}$) ...
.0	7.0	10.0	14.0	14.0	.0		0
19.5	6.6	6.9	13.8	13.8	.2		4.9e9
35.5	5.8	5.9	12.2	12.5	5.6		8.4e12
59.5	3.6	4.3	10.5	8.9	16.6		2.1e13
92.5	3.7	2.9	10.6	7.5	4.9		3.7e13
112.0	3.8	3.3	9.6	7.9	5.2		2.7e13

time	length	breadth	area
(h)	(µm)	(µm)	(μm^2)
.0			
35.5	1.4	.84	.83
59.5	1.7	.75	.81
92.5	1.6	.77	.80
112.0	1.4	.65	.60

Parameters

	DO	gluc	TOC	SOC	mass	Kp	Pa
A	6.84	10.0	14.1	14.1	0		1e0
B	3.69	3.2	10.2	7.7	5.26		3e13
XO	38.80	28.1	36.6	45.9	27.5		31.96
DO	9.56	14.3	15.5	9.1	3.8		7.7
StDev	.17	.713	.425	.225	.283		.275

Mono population biofilm - P. aeruginosa

Experiment 2 - biofilm phase

Raw data

time (h)	TOC ($g.m^{-2}$)	thickness (µm)	mass ($g.m^{-2}$)	Kp ... ($\#.m^{-2}$)	Pa ...
.0	.00	.0	.0		1e0
62.5	.23	19.8	.4		-
93.5	.37	27.6	.6		2.7e12
116.0	.45	33.7	1.6		3.8e12
134.5	.65	34.7	1.6		4.7e12
137.5	.58	32.6	1.5		4.1e12

time (h)	length (µm)	breadth (µm)	area (μm^2)
.0	.00	.00	.00
62.5			
93.5	1.67	.70	.76
116.0	1.50	.69	.68
134.5	1.49	.72	.69
137.0	1.60	.74	.80

Parameters

coeff.	TOC	thickness	mass	Kp	Pa
A	.00	.00	.00		1e0
B	.84	34.20	1.66		4e12
X0	67.70	58.50	95.70		66.70
D0	35.00	19.00	23.80		16.80
StDev	.05	1.86	.20		.13

Mono population biofilm - P. aeruginosa

Experiment 3 - liquid phase

Raw data

time (h)	DO ($g.m^{-3}$)	gluc	TOC ($g\ C.m^{-3}$)	SOC	mass ($g.m^{-3}$)	Kp ($\#.m^{-3}$)	Pa
.0	7.0	9.5	14.4	14.5	.0		.0
13.5	6.8	7.9	14.4	14.5	.0		3.9e9
35.5	5.3	6.1	12.3	11.1	.0		2.4e13
58.5	3.9	4.4	10.1	8.4	3.4		2.9e13
82.0	3.4	3.1	10.6	6.6	5.3		2.5e13
108.0	3.5	3.2	10.1	6.3	5.6		2.6e13
131.5	3.4	2.8	9.4	6.0	5.6		3.1e13

time (h)	length (µm)	breadth (µm)	area (μm^2)
.0	0	.00	.00
13.5	1.33	.74	.65
35.5	1.31	.72	.61
58.5	1.58	.93	.94
82.0	1.38	.82	.74
108.0	-	.60	.46
131.5	-	.64	.45

Parameters

	DO	gluc	TOC	SOC	mass	Kp	Pa
A	7.0	9.5	14.4	14.4	.0		1e0
B	3.4	3.1	9.7	6.1	5.8		2.8e13
X0	37.3	36.7	51.9	50.1	47.0		21.31
D0	9.8	14.0	12.4	12.3	11.5		5.02
StDev	.11	.84	.64	.53	2.02		.19

Mono population biofilm - P. aeruginosa

Experiment 3 - biofilm phase

Raw data

time (h)	TOC ($g.m^{-2}$)	thickness (µm)	mass ($g.m^{-2}$)	...	Kp ($\#.m^{-2}$)	Pa ...
.0	.00	.0	.0			0
11.5		.3	.0			
24.5		.8	.0			
37.0	.14	1.3	.0			3.4e11
48.5	.30	1.7	.0			
59.0	.45	27.6	.3			1.5e12
73.0	.56	35.2	.8			2.9e12
83.5	.70	33.3	.6			3.7e12
96.5	.78	33.7	.8			
110.0	.75	29.8	1.6			4.0e12
122.0	.72	22.6	1.6			4.4e12
132.0	.75	30.6	1.9			4.0e12

time (h)	length (µm)	breadth (µm)	area (μm^2)
.0	.00	.00	.00
37.0	1.46	.66	.62
48.5			
59.0	1.59	.76	.76
73.0	1.32	.68	.55
83.5	1.04	.58	.37
96.5			
110.0	1.22	.66	.53
122.0	1.15	.63	.47
132.0	1.32	.68	.20

Parameters

	TOC	thickn	mass	Kp	Pa
A	.0	.0	.0		1e0
B	.8	30.7	1.8		4.2e12
X0	56.1	53.8	63.6		60.31
D0	12.3	13.8	12.3		15.06
StDev	.1	3.1	.2		.177

Mono population biofilm - P. aeruginosa

Experiment 4 - liquid phase

Raw data

time (h)	DO ($g.m^{-3}$)	gluc	TOC ($g\ C.m^{-3}$)	SOC	mass ($g.m^{-3}$)	Kp ($\#.m^{-3}$)	Pa
.0	7	9.9	13.4	13.6	.0		.0
13.5	6.8	8.7	13.4	13.6	.0		2.6e9
35.5	5.3	6.7	11.3	10.3	.0		1.4e13
58.5	3.6	4.6	11.7	9.9	1.8		2.9e13
82.0	3.3	3.5	10.4	8.4	6.0		2.5e13
108.0	3.4	2.4	9.2	7.6	9.8		2.8e13
131.5	3.4	2.8	9.4	6.0	6.2		2.6e13

time (h)	length (μm)	breadth (μm)	area (μm^2)
.0	.00	.00	.00
13.5	1.38	.80	.74
35.5	1.42	.90	.86
58.5	.13	.70	.58
82.0	1.27	.80	.69
108.0	1.27	.80	.67
131.5	.95	.61	.37

Parameters

	DO	gluc	TOC	SOC	mass	Kp	Pa
A	7.0	9.7	13.4	13.6	.0		1e0
B	3.4	2.7	9.6	6.7	6.6		2.7e13
X0	41.7	42.5	58.3	61.5	72.2		27.6
D0	13.1	15.1	16.2	19.9	12.1		9.5
StDev	.05	.77	.44	.74	.19		.13

Mono population biofilm - P. aeruginosa

Experiment 4 - biofilm phase

Raw data

time (h)	TOC ($g.m^{-2}$)	thickness (µm)	mass ($g.m^{-2}$)	...	Kp ($\#.m^{-2}$)	...	Pa
.0	.00	.00	.00				0
11.5							
24.5							
37.0							
48.5							
59.0	.51	16.3	.55		1.9e12		
73.0							
83.5	.62	19.3	.69		3.0e12		
96.5							
110.0	.78	29.9	1.02		3.2e12		
122.0							
132.0	.74	26.8	.48		2.9e12		

time (h)	length (µm)	breadth (µm)	area (μm^2)
.0			
48.5			
59.0	1.59	.70	.72
73.0			
96.5			
110.0	1.32	.73	.64
122.0			
132.0	1.33	.54	.44

Parameters

	TOC	thickn	mass	Kp	Pa
A	.0	.0	.0		1e0
B	.7	28.8	.7		3.2e12
X0	48.0	71.2	48.0		50.8
D0	11.0	17.3	11.0		13.7
StDev	.05	3.27	.18		.22

APPENDIX I: Raw Data and Parameters Logistic Equation

Binary Population Biofilm

Notation

DO = Dissolved Oxygen concentration [$g.m^{-3}$]
gluc = glucose carbon concentration [g $C.m^{-3}$]
TOC = Total Organic Carbon [g $C.m^{-3}$]
SOC = Soluble Organic Carbon [g $C.m^{-3}$]
mass = Mass of suspended solids [$g.m^{-3}$]
Kp = *K. pneumoniae* cell concentration [$\#.m^{-3}$]
Pa = *P. aeruginosa* cell concentration [$\#.m^{-3}$]

A = pretransition region intercept
B = posttransition region asymptote
X_o = position of the transition region
D_o = width of the transition region
StDev = Standard deviation of overall fit

Binary population biofilm

Experiment 1 - liquid phase

Raw data

time (h)	DO ($g.m^{-3}$)	gluc	TOC	SOC	mass ($g.m^{-3}$)	Kp ($\#.m^{-3}$)	Pa
			($g\ C.m^{-3}$)				
.0	7.0	9.7	9.8	8.8	.0	0	0
13.5		9.1	9.3	8.8	.6	1e7	1e7
35.0	7.0	9.5	8.9	8.9	3.8	2.8e10	2.6e10
48.5						6.8e10	4.97e9
63.0	6.7	8.4	7.7	8.9	3.8		1.9e10
95.0						1.2e12	2.3e10
107.5						1.9e12	6.0e10
110.0						1.0e12	1e11
117.5						2.3e12	6.6e11
131.0	5.3	2.0	5.7	4.2	4.0	7.8e11	7.8e11
140.0						9.8e12	2.0e12
155.0	4.9	.9	6.0	3.9	16.6	2.8e13	6.8e11
179.0	5.2	2.9	5.7	3.5	5.0	7.4e12	9.5e11
205.0	4.1	1.2	6.2	3.5	14.0	1.9e13	6.2e11

time (h)	length (μm)	breadth (μm)	area (μm^2)
.0			
35.0	1.34	.79	.80
131.0	2.08	1.07	1.57
155.0	1.86	1.23	1.64
179.0	1.61	.92	1.04
205.0	1.68	1.00	1.19

Parameters

	DO	gluc	TOC	SOC	mass	Kp	Pa
A	7.0	8.9	9.5	8.7	.0	1e0	1e0
B	4.6	1.3	6.0	6.0	3.9	1.3e13	8.3e11
X0	102.5	97.0	71.5	71.5	98.5	99.7	96.2
D0	9.2	21.6	14.0	9.3	5.8	9.1	9.4
StDev	.10	.51	1.22	1.64	.09	.37	.57

Binary population biofilm

Experiment 1 - biofilm phase

Raw data

time (h)	TOC ($g\ C.m^{-2}$)	thickness (µm)	mass ($g.m^{-2}$)	Kp .... ($\#.m^{-2}$)	Pa ...
.0	.0	.0	.0	0	0
18.5		.3			
38.0		.8			
48.0		.3			
64.0		.3			
89.0		.3			
107.0	.2	1.0	.2	4.7e11	4.3e11
133.0	.5	22.0	1.3	1.1e12	3.3e12
157.0	1.0	31.4	1.6	9.3e11	3.7e12
168.0	1.4	22.3	1.5	1.1e12	2.9e12
182.0	1.3	25.4	1.2	9.2e11	4.1e12
208.0	1.3	19.8	1.9	1.3e12	4.5e12

time (h)	length (µm)	breadth (µm)	area (μm^2)
.0			
133.0	2.00	.91	1.18
157.0	1.58	.87	1.01
168.0	1.67	.84	.93
182.0	1.82	.77	.81
208.0	1.38	.76	.72

Parameters

	TOC	thickness	mass	Kp	Pa
A	.0	.0	.0	1e0	1e0
B	1.4	24.6	1.7	1.1e12	4e12
X0	97.5	120.0	125.3	114.0	122.5
D0	9.0	10.7	7.3	8.5	8.1
StDev	.01	2.80	.18	.18	.31

Binary population biofilm

Experiment 2 - liquid phase

Raw data

time (h)	DO ($g.m^{-3}$)	gluc	TOC ($g\ C.m^{-3}$)	SOC	mass ($g.m^{-3}$)	Kp ($\#.m^{-3}$)	Pa ..
.0	7.0	8.8	10.2	10.1	.0	1e0	1e0
13.5		8.5	9.8	9.9	1.6	1e7	2.0e7
35.0	7.0	8.6	9.9	9.4	1.8	7.9e7	5.1e8
48.5							3.2e9
63.0	6.9	8.3	9.7	8.9	2.4		2.0e11
95.0						1.1e12	3.0e10
107.5						1.9e12	1.1e11
110.0						1.0e12	2.3e11
114.5						1.5e12	6.9e11
131.0	5.0	2.1	6.3	5.0	3.2	1.8e13	8.1e11
140.0						8.6e12	4.2e12
155.0	4.8	1.6	6.5	3.9	10.4	2.6e13	8.1e11
179.0	5.2	1.5	6.3	4.0	6.2	8.1e12	3.6e12
205.0	4.2	1.5	6.2	4.3	3.4	1.4e13	1.1e12

time (h)	length (μm)	breadth (μm)	area (μm^2)
.0			
35.0	1.24	.79	.91
131.0	1.74	.84	.96
155.0	1.86	1.02	1.45
179.0	1.77	.95	1.16
205.0	1.61	.91	1.06

Parameters

	DO	gluc	TOC	SOC	mass	Kp	Pa
A	7.0	8.8	10.1	9.8	.0	1.0	1.0
B	4.7	1.5	6.4	4.3	3.3	1e13	1.4e12
X0	97.0	98.1	84.2	96.2	92.8	99.7	96.2
D0	9.5	9.5	10.8	9.7	13.1	10.1	8.4
StDev	.27	.14	1.04	1.42	.41	.23	.54

Binary population biofilm

Experiment 2 - biofilm phase

Raw data

time (h)	TOC ($g\ C.m^{-2}$)	thickness (μm)	mass ($g.m^{-2}$)	Kp .... ($\#.m^{-2}$)	Pa ...
.0	.0	.0	.0	0	0
18.5		.3			
38.0		.8			
48.0		.3			
64.0		.3			
89.0		.3			
107.0	.3	1.0	1.0	9.9e11	4.5e12
133.0	.9	32.3	1.2	8.0e11	3.7e12
157.0	1.3	41.4	1.5	9.9e11	4.7e12
168.0	1.1	39.7	1.1	9.0e11	4.1e12
182.0	1.3	34.3	1.6	8.3e11	4.5e12
208.0	1.2	36.6	1.2	9.5e11	3.9e12

time (h)	length (μm)	breadth (μm)	area (μm^2)
.0			
133.0	1.96	1.02	1.37
157.0	1.60	.80	.83
168.0	1.68	.81	.88
182.0	1.76	.79	.81
208.0	1.68	.83	.90

Parameters

	TOC	thickness	mass	Kp	Pa
A	.0	.0	.0	1e0	0
B	1.2	28.1	1.4	9e11	4e12
X0	129.8	123.1	122.5	112.0	120.0
D0	11.8	11.5	7.4	8.9	8.6
StDev	.05	1.93	.13	.24	.33

Binary population biofilm

Experiment 3 - liquid phase

Raw data

time (h)	DO ($g.m^{-3}$)	gluc	TOC ($g\ C.m^{-3}$)	SOC	mass ($g.m^{-3}$)	Kp ($\#.m^{-3}$)	Pa
.0	7.2	20.4	21.2	21.0	.0	1e6	1e6
24.0	7.0	20.1	22.7	21.5	.4	8e9	5e8
35.0						2.26e9	3e8
46.0	6.6	21.7	19.7	19.1	1.4	5.4e11	4.4e11
71.5	6.1	16.7	18.6	18.3	3.6	7.4e12	9.9e13
97.0	4.3	8.4	17.1	12.2	19.8	2.8e13	2.6e13
109.0	3.4						
128.0	1.6	2.8	15.3	10.3	42.0	1.8e13	1.6e13
171.0	3.1	3.0	16.8	10.9	11.4	8.5e13	2.9e13
190.5	2.4						
217.0	2.6	2.1	16.4	9.9	21.8	2.5e13	1.1e13

Parameters

	DO	gluc	TOC	SOC	mass	Kp	Pa
A	7.2	20.9	21.5	21.0	.0	1e0	1e0
B	2.7	2.4	16.7	10.1	21.7	3.5e13	2e13
X0	87.0	89.4	98.0	98.0	98.8	90.5	93.5
D0	2.2	12.3	12.8	14.0	12.8	12.9	13.2
StDev	.55	1.25	3.76	.87	10.70	1.18	.88

Binary population biofilm

Experiment 3 - biofilm phase

Raw data

time (h)	TOC ($g\ C.m^{-2}$)	thickness (µm)	mass ($g.m^{-2}$)	Kp .... ($\#.m^{-2}$)	Pa ...
.0	.0	.0	.0	0	0
26.5	.0	.0	.0		
48.0	.0	.0	.0		
59.5	.4	.0	.3	5.3e6	2.7e6
77.5	.6	.0	.5	2.7e9	5.3e9
84.0	.7	.3	.7	4.0e11	1.3e11
123.0	1.1	64.7	2.4	1.4e12	3.0e12
148.0	1.3	73.3	2.2	1.9e12	5.6e12
173.0	1.7	85.3	2.6	1.9e12	6.6e12
215.0	1.8	93.9	2.9	2.1e12	5.9e12

Parameters

	TOC	thickness	mass	Kp	Pa
A	.0	.0	.0	0	0
B	1.9	84.7	2.6	2.1e12	6e12
X0	104.0	117.0	104.0	114.0	118.0
D0	19.5	5.2	16.0	11.8	12.3
STDev	.44	5.28	.28	2.17	2.69

Binary population biofilm

Experiment 4 - liquid phase

Raw data

time	DO	gluc	TOC	SOC	mass	Kp	Pa
(h)	($g.m^{-3}$)	....	($g\ C.m^{-3}$)	...	($g.m^{-3}$)	. ($\#.m^{-3}$)	..
.0	7.3	20.2	21.1	21.0	.0	1e0	1e0
24.0	6.9	20.7	20.5	20.4	1.2	5.3e8	7.5e9
35.0						5.8e9	5.6e9
46.0	6.9	19.1	20.7	20.1	1.4	1.1e11	1.1e12
71.5	6.5	16.5	20.3	18.9	2.0	3.3e12	2.3e13
97.0	4.0	5.0	17.7	12.7	25.4	3e13	3.8e13
109.0	4.1						
124.0	3.5	3.8	16.8	9.1	19.4	2.5e13	2.5e13
171.0	3.2	3.0	17.1	10.4	17.4	1.3e13	3.5e13
190.5	3.0						
217.0	3.2	2.6	17.5	9.7	24.8	2.2e13	9.5e12

Parameters

	DO	gluc	TOC	SOC	mass	Kp	Pa
A	7.2	20.2	21.2	20.3	.0	1e0	1e0
B	3.3	2.7	17.4	9.9	21.4	2.2e13	2.5e13
X0	86.2	89.2	82.0	89.2	84.2	91.5	91.0
D0	13.7	13.3	15.5	12.2	12.8	13.1	13.3
StDev	.41	1.59	5.72	2.93	10.20	1.06	.87

Binary population biofilm

Experiment 4 - biofilm

Raw data

time (h)	TOC (g C.m^{-2})	thickness (μm)	mass (g.m^{-2})	Kp .... (#.m^{-2})	Pa ...
.0	.0	.0	.0	0	0
26.5	.0	.0	.0		
48.0	.0	.0	.0		
59.5	.2	.0	.3	8.4e6	1.3e7
77.5	.3	.0	.5	4.0e8	1.3e9
84.0	.3	.3	.9	4.0e11	4.9e11
123.0	.9	26.5	1.3	1.0e12	2.3e12
148.0	1.1	44.9	1.4	1.5e12	5.0e12
173.0	1.5	61.5	2.6	1.6e12	5.9e12
215.0	1.6	94.6	2.4	1.9e12	5.2e12

Parameters

	TOC	thickness	mass	Kp	Pa
A	.0	.0	.0	0	0
B	1.7	98.4	2.5	2.1e12	5e12
X0	111.0	127.0	82.2	108.0	117.0
D0	21.0	19.9	22.8	12.3	12.0
StDev	.23	6.05	.26	2.14	.40

APPENDIX J: Diffusion through the Laminar Sublayer

Microbial cells are transported through the laminar layer to the substratum by diffusion perpendicular to the direction of flow. As the size of microbial cells is in the range where diffusion contributes minimally to transport, motility may play an important role.

Diffusivity for non-motile spherical particulates is described by (Lister, 1981):

$$D_B = \frac{K_B\ T}{3\pi \emptyset d_M} \qquad (J1)$$

where:

D_B = (Brownian) Diffusivity $[L^2t^{-1}]$

K_B = Boltzmann constant $[13.807*10^{-24}\ JK^{-1} = 13.807\ kgm^2s^{-2}{}^\circ K^{-1}]$

T = absolute temperature [°K]

π = Pi [= 3.1416]

$\emptyset$ = dynamic viscosity $[ML^{-1}t^{-1}]$

d_M = diameter of Microbial cell [L]

Diffusivity, corrected for motility, can be calculated with (Jang and Yen, 1985):

$$D_m = \frac{v_M\ L_M}{3\ (1-\alpha)} \qquad (J2)$$

D_m = motility diffusivity $[L^2t^{-1}]$

v_M = velocity of motility $[Lt^{-1}]$

L_M =path length between tumblings [L]

α = mean sine of angle of turn [-]

For a temperature of 25 °C (298 °K), dynamic viscosity $\emptyset=0.90*10^{-3}$ $kgm^{-1}s^{-1}$. Assuming K. pneumoniae to be a spherical particle with $d_M=1.15$ μm, diffusivity for K. pneumoniae, $D_B = 4.3*10^{-13}$ m^2s^{-1}.
Assuming no chemotaxis, α equals zero. Maximum velocities of motility have been measured for P. aeruginosa at approx. 55 μms^{-1} (Brock, 1979). Path lengths between tumblings are in the range of 50 μm (Vaituzi and Doetsch, 1969). Using median values for both velocity and path length, diffusivity for P. aeruginosa, $D_M = 10^{-10}$ ms^{-1}.
This suggests that diffusivity for motile P. aeruginosa is approx. 250 times the diffusivity for non-motile K. pneumoniae.

APPENDIX K: Diffusion in the Biofilm

If microbial consumption of compounds (substrate, oxygen) in the biofilm is diffusion-limited, the rate of supply of compounds determines the rate at which compounds can be consumed. Consequently, the consumption rate is less than maximum. Diffusion limitation can be calculated on the basis of a diffusion-reaction model developed by Atkinson and Davies (1974).

According to the Atkinson model, the flux of substrate into a biofilm is described by:

$$N_S = \epsilon \frac{\tau_{Mf}\, \delta_f}{Y_{MS}} \left[\frac{\mu_m\, S_{Sl}}{K_S + S_{Sl}} \right] \qquad (K1)$$

where:

N_S = flux of substrate into the biofilm $[M_S L^{-2} t^{-1}]$
ϵ = effectiveness factor [-]
τ_{Mf} = cell carbon density in biofilm $[M_M L^{-3}]$ $(= X_{Mf}/\delta_f)$
μ_m = maximum specific cellular growth rate $[t^{-1}]$
δ_f = biofilm thickness [L]
S_{Sl} = substrate carbon concentration in liquid phase $[M_S L^{-3}]$
Y_{MS} = yield of cell carbon from substrate carbon $[M_M M_S^{-1}]$
K_S = half saturation concentration $[M_S L^{-3}]$

The effectiveness factor ϵ, the ratio of the actual substrate flux into the biofilm and the substrate flux if no diffusional-resistance would exist, is a measure of the importance of diffusional resistance in controlling the diffusion-reaction process. ϵ is defined using dimensionless variables:

1. for a predominantly reaction-controlled region (K2):

$$\epsilon = 1 - \left[\frac{\tanh(k_2.\delta_f)}{k_2.\delta_f} \cdot \left[\frac{\Phi}{\tanh(\Phi)} - 1 \right] \right] \quad \text{for } \Phi \leq 1$$

2. for a predominantly diffusion-controlled region (K3):

$$\epsilon = \frac{1}{\Phi} \left[\frac{\tanh(k_2.\delta_f)}{k_2.\delta_f} \cdot \left[\frac{1}{\tanh(\Phi)} - 1 \right] \right] \quad \text{for } \Phi \geq 1$$

where:

Φ = Thiele modulus [-], defined by:

$$\Phi = \left[\frac{(k_2\delta_f)\,(k_3 S_{S1})}{\sqrt{2}\,(1+k_3 S_{S1})} \right] \left[k_3 S_{S1} - \ln(1+k_3 S_{S1}) \right]^{-\frac{1}{2}} \qquad \text{(K4)}$$

with:

$k_2\delta_f$ = dimensionless thickness [-]

$$k_2 = \left[\frac{\mu_m \tau M_f}{K_S D_e} \frac{1}{Y_{obs}} \right]^{\frac{1}{2}} \qquad \text{(K5)}$$

D_e = effective diffusion coefficient within microbial mass [$L^2 t^{-1}$]

Y_{obs} = observed yield coefficient [$M_M M_S^{-1}$] defined as:

$$\frac{1}{Y_{obs}} = \left[\frac{1}{Y_{MS}} + \frac{k_{Pg}}{Y_{PS}} \right] + \frac{1}{\mu_m} \left[\frac{k_{Pn}}{Y_{PS}} \right] \qquad \text{(K6)}$$

Y_{PS} = yield of product carbon from substrate carbon $[M_M M_P^{-1}]$

k_{Pg} = growth associated product formation coefficient $[M_P M_M^{-1}]$

k_{Pn} = non-growth associated product formation coefficient $[M_P M_M^{-1} t^{-1}]$

$k_3 S_{S1}$ = dimensionless substrate concentration [-]

k_3 = K_S^{-1} $[L^3 M_S^{-1}]$

Substituting Eq. K6 into Eq. K5 results in

$$k_2 = \left[\left[\frac{\mu_m \tau_{Mf}}{K_S D_e} \right] \left[\frac{1}{Y_{MS}} + \frac{k_{Pg}}{Y_{PS}} + \frac{1}{\mu_m} \cdot \frac{k_{Pn}}{Y_{PS}} \right] \right]^{1/2} \qquad (K7)$$

Time progression of ϵ is determined for smooth biofilms of K. pneumoniae and P. aeruginosa of equal cellular carbon density and of 10 μm (Kp) and 15 and 30 μm (Kp and Pa) thickness. Table 17 presents the parameter values used for the simulation.

Table 17. Parameter values for determination of diffusion effectiveness factor.

		K. pneumoniae	P. aeruginosa
μm	$[h^{-1}]$	2.0	0.4
S_{S1}	$[g\ C.m^{-3}]$	10 - 1.5	10 - 1.5
Y_{MS}	$[g.g^{-1}]$	0.08	0.24
Y_{PS}	$[g.g^{-1}]$	0.48	0.41
K_S	$[g\ C.m^{-3}]$	1.43	2.0
k_{Pg}	$[g.g^{-1}]$	1.72	0.36
k_{Pn}	$[g.g^{-1}h^{-1}]$	0.20	0.10
k_3	$[g\ C.m^{-3}]$	0.70	0.50
τ_{Mf}	$[g\ C.m^{-3}]$	10.0	10.0

The effective diffusion coefficient of glucose into a mixed population biomass is taken from Matson and Characklis (1976) ($D_e = 0.6*10^{-9}\ m^2.s^{-1}$).

Results of the simulation (Figure K1) indicate that, under identical conditions, both biofilms are diffusion-limited. But the extent of the limitation is more severe for K. pneumoniae than for P. aeruginosa (Table 18).

Table 18. Relation between steady state biofilm thickness and diffusion effectiveness factor ϵ for K. pneumoniae and P. aeruginosa.

thickness (μm)	K. pneumoniae	P. aeruginosa
10	64%	-
15	45%	92%
30	23%	78%

Figure 52. Time progression of the diffusion effectiveness factor for various thicknesses of the biofilm of K. pneumoniae and P. aeruginosa.